NASA TECHNICAL MEMORANDUM

NASA TM X-2561

NASA TM X-2561

AERODYNAMIC CHARACTERISTICS OF A 60° SWEPT DELTA-WING SPACE SHUTTLE ORBITER AT MACH NUMBERS OF 2.50, 3.90, AND 4.60

by Ernald B. Graves

Langley Research Center
Hampton, Va. 23365

NATIONAL AERONAUTICS AND SPACE ADMINISTRATION • WASHINGTON, D. C. • MAY 1972

1. Report No. NASA TM X-2561	2. Government Accession No.	3. Recipient's Catalog No.
4. Title and Subtitle AERODYNAMIC CHARACTERISTICS OF A 60° SWEPT DELTA-WING SPACE SHUTTLE ORBITER AT MACH NUMBERS OF 2.50, 3.90, AND 4.60		5. Report Date May 1972 6. Performing Organization Code
7. Author(s) Ernald B. Graves		8. Performing Organization Report No. L-8243
9. Performing Organization Name and Address NASA Langley Research Center Hampton, Va. 23365		10. Work Unit No. 117-07-01-03 11. Contract or Grant No.
12. Sponsoring Agency Name and Address National Aeronautics and Space Administration Washington, D.C. 20546		13. Type of Report and Period Covered Technical Memorandum 14. Sponsoring Agency Code
15. Supplementary Notes		

16. Abstract

As part of the space shuttle systems study program, wind-tunnel tests have been performed to determine the static aerodynamic characteristics of a model of a 60° swept delta-wing space shuttle orbiter. Some control-effectiveness tests were also included. The tests were conducted in the Langley Unitary Plan wind tunnel at Mach numbers of 2.50, 3.90, and 4.60 and at a Reynolds number of 8.2×10^6 per meter (2.5×10^6 per foot).

17. Key Words (Suggested by Author(s))	18. Distribution Statement
Space shuttle orbiter Aerodynamic characteristics Delta-wing bodies	Unclassified – Unlimited

19. Security Classif. (of this report)	20. Security Classif. (of this page)	21. No. of Pages	22. Price*
Unclassified	Unclassified	114	$3.00

*For sale by the National Technical Information Service, Springfield, Virginia 22151

AERODYNAMIC CHARACTERISTICS OF A 60° SWEPT DELTA-WING SPACE SHUTTLE ORBITER AT MACH NUMBERS OF 2.50, 3.90, AND 4.60

By Ernald B. Graves
Langley Research Center

SUMMARY

Tests have been performed in the Langley Unitary Plan wind tunnel to determine the static aerodynamic characteristics of a 60° swept delta-wing space shuttle orbiter at Mach numbers of 2.50, 3.90, and 4.60. Various control-effectiveness tests were also included.

The results of the tests indicate that the elevons are effective in producing pitching moment but the trim angle of attack is limited to about 15° at a Mach number of 2.50 and to about 36° at Mach numbers of 3.90 and 4.60. The flared rudder is effective in producing drag at low angles of attack but became ineffective at high angles of attack. The rudder is effective in producing yawing moment; however, the effectiveness is considerably reduced at high angles of attack. Ventral fins provide somewhat less yaw-control effectiveness than the rudder at low angles of attack, but the effectiveness is maintained with increase in angles of attack. The basic model was directionally stable only at a Mach number of 2.50 and only to an angle of attack of about 10°. With the maximum-flared rudder, directional stability was maintained at all test Mach numbers but only to an angle of attack of about 13°. Modifications to the fuselage chine had essentially no effect on the model aerodynamic characteristics at the test Mach numbers.

INTRODUCTION

The National Aeronautics and Space Administration in conjunction with industry is currently involved in developmental studies of reusable space shuttle systems capable of placing large payloads in near-earth orbit. As part of these studies, wind-tunnel tests of a 60° swept delta-wing space shuttle orbiter have been performed in the Langley Unitary Plan wind tunnel.

The tests performed at Mach numbers of 2.50, 3.90, and 4.60 provided static aerodynamic data for the basic configuration and for model variations, such as the addition of ventral fins and changes in wing longitudinal location. Longitudinal-control effectiveness

of the elevators, as well as the lateral-control effectiveness of the ventral fins, rudder, and rudder flare, was investigated. The tests were conducted over an angle-of-attack range from -4^{o} to 42^{o} and over an angle-of-sideslip range from -4^{o} to 8^{o}.

SYMBOLS

Values are given in both SI and U.S. Customary Units. The measurements and calculations were made in U.S. Customary Units. Aerodynamic coefficients are referenced to the body-axis system except for lift and drag which are referenced to the stability-axis system. The moment reference was located 27.569 cm (10.854 in.) aft of the model nose (67.1 percent body length).

b	reference wing span, 27.574 cm (10.856 in.)
C_A	axial-force coefficient, $\frac{\text{Axial force}}{qS}$
C_D	drag coefficient, $\frac{\text{Drag}}{qS}$
$C_{D,b}$	base drag coefficient, $\frac{\text{Base drag}}{qS}$
$C_{D,c}$	chamber drag coefficient
$C_{D,o}$	drag coefficient at zero lift
C_L	lift coefficient, $\frac{\text{Lift}}{qS}$
C_{L_α}	lift-curve slope (near $\alpha = 0^{o}$)
C_l	rolling-moment coefficient, $\frac{\text{Rolling moment}}{qSb}$
C_{l_β}	effective dihedral parameter, $\left(\frac{\Delta C_l}{\Delta \beta}\right)_{\beta=0^{o},3^{o}}$, per degree
C_m	pitching-moment coefficient, $\frac{\text{Pitching moment}}{qS\bar{c}}$
$C_{m,o}$	pitching-moment coefficient at zero lift
C_{m_δ}	pitch-control parameter, $\frac{\Delta C_m}{\Delta \delta_e}$ at $\alpha = 0^{o}$, per degree

C_N normal-force coefficient, $\frac{\text{Normal force}}{qS}$

C_n yawing-moment coefficient, $\frac{\text{Yawing moment}}{qSb}$

C_{n_β} directional stability parameter, $\left(\frac{\Delta C_n}{\Delta \beta}\right)_{\beta=0^o,3^o}$, per degree

C_Y side-force coefficient, $\frac{\text{Side force}}{qS}$

C_{Y_β} side-force derivative, $\left(\frac{\Delta C_Y}{\Delta \beta}\right)_{\beta=0^o,3^o}$, per degree

$\bar{c}$ reference wing chord, 15.916 cm (6.266 in.)

L/D lift-drag ratio

$(L/D)_{max}$ maximum lift-drag ratio

M Mach number

q dynamic pressure

S reference area, 0.0329 m^2 (0.3542 ft^2)

$\frac{x_{ac}}{l}$ aerodynamic-center location, percent body length

α angle of attack, deg

β angle of sideslip, deg

δ_e elevon pitch deflection angle (positive when trailing edge is down), deg

δ_j rudder flare deflection half-angle, deg

δ_u ventral-fin deflection angle (positive when trailing edge is left), deg

δ_v rudder deflection angle (positive when trailing edge is left), deg

Model nomenclature:

B_0	basic fuselage
B_1	modified fuselage
W_0	basic wing position
W_1	wing in forward position
W_2	wing in aft position
V	vertical tail
U	ventral fins

APPARATUS AND METHODS

Model

Detailed drawings of the model are shown as figure 1, and a photograph of the model is shown as figure 2. The orbiter model consisted of a 60° swept delta-wing—body and a single center-line-mounted vertical tail. The low-mounted wing had -5.0° of aerodynamic twist about the trailing edge (0° incidence at the root and 5.0° incidence at the tip) and 7.0° of dihedral angle. Wing airfoil sections tapered from NACA 0009-64 at the root to NACA 0012-64 at the tip. The wing, which basically was positioned so that the trailing edge was flush with the base of the body, could be placed either forward or aft of this position by 0.970 cm (0.382 in.). (See fig. 1(b).) The full-span elevons could be deflected in 10° increments from -30° to 10°. The vertical tail had a 10° wedge section with a blunt trailing edge and 45° of leading-edge sweepback. Provision was made to deflect the rudder -20° (trailing edge right), and in addition, a rudder that could be flared with half-angle increments of 15° and 30° was provided on the trailing edge of the vertical tail. (See fig. 1(c).) Two all-movable ventral fins could be mounted at the base of the body. (See fig. 1(d).)

A modified fuselage which had a smaller chine flare forward of the wing was also provided. (See fig. 1(e).) The basic model is designated B_0W_0V. All control surfaces are at zero deflection unless otherwise noted.

Tunnel

The investigation was performed in the high Mach number test section of the Langley Unitary Plan wind tunnel, which is a variable-pressure, continuous-flow facility. The test section is about 1.49 m^2 (16 ft^2) in area and 2.13 m (7 ft) long, and the asymmetric-sliding-block nozzle leading to the test section permits a continuous variation in Mach number from about 2.3 to 4.7.

Test Conditions

Tests were conducted at the following conditions:

Mach number	Stagnation pressure		Stagnation temperature	
	kN/m^2	psia	K	^oF
2.50	101	14.7	338.7	150
3.90	225	32.6	352.6	175
4.60	312	45.2	352.6	175

Reynolds number was held constant at 8.2×10^6 per meter (2.5×10^6 per ft). The model was tested at angles of attack from about -4^o to 42^o and at sideslip angles from about -4^o to 8^o. Test-section dewpoint temperature was maintained sufficiently low to assure negligible condensation effects.

Transition strips composed of single-spaced No. 45 sand placed 3 diameters apart were affixed to the wing and tail surfaces 1.0 cm (0.4 in.) aft of the leading edges in a streamwise direction and 3.05 cm (1.2 in.) aft of the nose apex.

Measurements and Corrections

Aerodynamic forces and moments on the model were measured by means of an internally mounted, six-component electrical strain-gage balance, which, in turn, was rigidly fastened to the sting-support system. Pressures in the model chamber and at the model base were measured by means of single static-pressure orifices.

Angles of attack have been corrected for tunnel airflow misalinement, and angles of attack and sideslip have been corrected for sting-balance deflection due to aerodynamic loads on the model. The axial-force- and drag-coefficient data have been adjusted to correspond to free-stream static conditions acting over the total model base. Typical values of base and chamber drag coefficients may be seen in figure 3.

PRESENTATION OF RESULTS

The results of the tests are presented in the following figures:

DISCUSSION

Longitudinal Aerodynamic Characteristics

The pitching-moment variation with lift coefficient and the lift-coefficient variation with angle of attack for the basic configuration are relatively linear throughout the angle-of-attack range at all test Mach numbers. (See fig. 4.) Moving the wing forward about 6 percent $\bar{c}$ causes a noticeable decrease in the stability level, whereas moving the wing aft causes a noticeable increase in the stability level. (See fig. 5.) Although there is little or no effect of wing position on lift-curve slope at $M = 2.50$, there is a slight increase in C_{L_α} for both the forward- and aft-located wing configurations at the higher test Mach numbers.

The elevons are effective in providing pitching moments at all test Mach numbers and angles of attack. (See fig. 6.) The data indicate that for the test center of gravity and elevon deflection of -30°, the trim angle of attack of the orbiter is about 15° at $M = 2.50$ and about 36° at $M = 3.90$ and 4.60. The generally expected loss in lift with the negative elevon deflection for trim is apparent.

Other than an increase in drag coefficient, there is little effect of rudder or ventral-fin deflection on the longitudinal aerodynamic characteristics of the model. (See figs. 7 and 8.)

The rudder flare is an effective means of producing drag (figs. 9 and 10), and for the test vehicle, this effectiveness is considerably increased with increase in rudder flare deflection angle. The effectiveness does decrease with increase in angle of attack, and the flared rudder becomes ineffective in producing drag at $\alpha \approx 40^{\circ}$ for $M = 2.50$ and at $\alpha \approx 24^{\circ}$ for $M = 4.60$. It appears that the flared rudder induces a high-pressure field on the aft top of the body that leads to a decrease in lift coefficient and a positive $C_{m,o}$. The chine flare change on the modified fuselage had essentially no effect on the body or wing-body longitudinal aerodynamic characteristics. (See fig. 11.)

A summary of longitudinal aerodynamic characteristics is shown in figure 12, and the generally typical decrease in C_{L_α}, $(L/D)_{max}$, and $C_{D,o}$ with increase in Mach number is indicated. Essentially the same amount of forward movement in aerodynamic-center location with increase in Mach number may be noted for all wing positions investigated.

Lateral Aerodynamic Characteristics

The rudder is effective in producing yawing moment; however, the effectiveness reduces with increase in Mach number and particularly with increase in angle of attack. For example, the rudder is ineffective in producing C_n at $\alpha \approx 40^{\circ}$ for $M = 2.50$ and at $\alpha \approx 30^{\circ}$ for $M = 4.60$. (See fig. 13.) The ventral fins, although not as effective as the rudder at low α, maintain a small amount of control effectiveness throughout the test angle-of-attack and Mach number range. (See fig. 14.) The data of figure 15 indicate that there is little or no effect of the rudder flare deflection on the lateral aerodynamic characteristics with the rudder at 0°. The data of figure 16 however, indicate that when the rudder is deflected -20°, the flared rudder induces more positive yawing moments with increased flare angle in the low to moderate angle-of-attack range.

Variations of the lateral aerodynamic characteristics of the model in sideslip are relatively linear throughout the angle-of-attack and test Mach number range. (See fig. 17.)

The basic model is directionally stable only to an angle of attack of about 10° at $M = 2.50$ and is directionally unstable at Mach numbers of 3.90 and 4.60 throughout the

entire test angle-of-attack range. (See fig. 18.) Addition of the ventral fins has little or no effect upon the directional stability of the vehicle. The data of figure 19 indicate that the small changes in the longitudinal position of the wing do not significantly affect the lateral stability of the model. The rudder flared to 30° produces an increase in C_{n_β} such that the vehicle is directionally stable at all test Mach numbers to an angle of attack of about 13°. (See fig. 20.) The data of figure 21 indicate that the modified chine flare has little effect on the lateral stability characteristics of the body alone or the wing-body configuration.

CONCLUSIONS

Tests have been performed in the Langley Unitary Plan wind tunnel to determine the static aerodynamic characteristics of a model of a 60° swept delta-wing space shuttle orbiter at Mach numbers of 2.50, 3.90, and 4.60.

The results of the tests indicate the following conclusions:

(1) For the test center of gravity, the elevons are effective in producing pitching moment and provided a stable trim angle of attack of about 36° at a Mach number of 3.90 and 4.60 and about 15° at a Mach number of 2.50.

(2) The rudder flare is effective in producing drag at large flare angles and low angles of attack but becomes ineffective at high angles of attack. Increase in rudder flare also produces an accompanying increase in pitching-moment coefficient at zero lift.

(3) The rudder is effective in producing yawing moments at low angles of attack, but the effectiveness is reduced considerably at high angles of attack. The ventral fins, although not as effective as the rudder at low angles of attack, maintain effectiveness throughout the test angle-of-attack range.

(4) The basic model was directionally stable only for a Mach number of 2.50 and angles of attack less than 10°. Full rudder flare deflection provided directional stability at all test Mach numbers but only at angles of attack up to about 13°.

(5) The modified fuselage chine had essentially no effect on the aerodynamic characteristics at the test Mach numbers.

Langley Research Center,
National Aeronautics and Space Administration,
Hampton, Va., April 21, 1972.

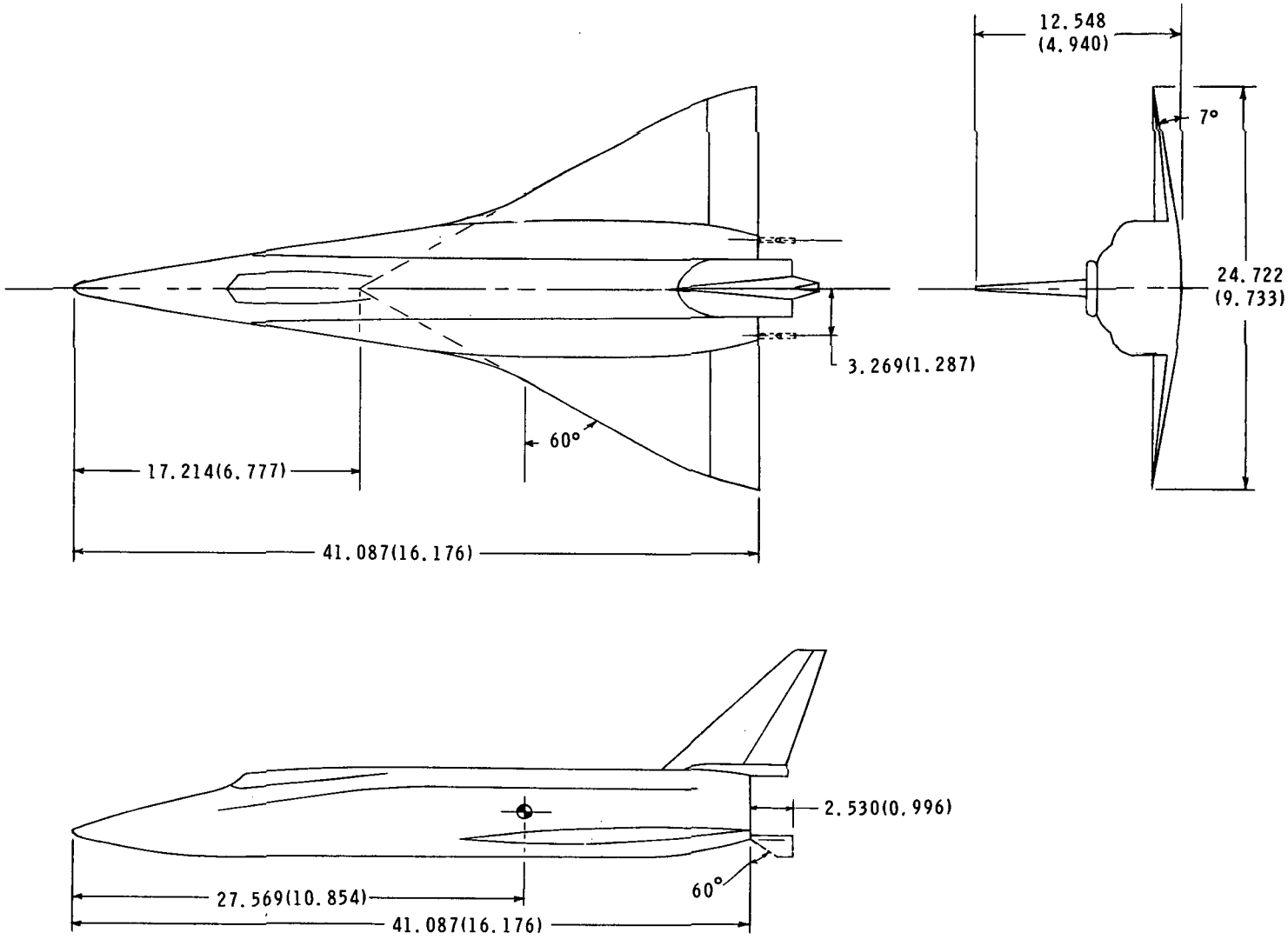

(a) Basic configuration.

Figure 1.- Drawing of model. All dimensions in centimeters (inches) unless otherwise noted.

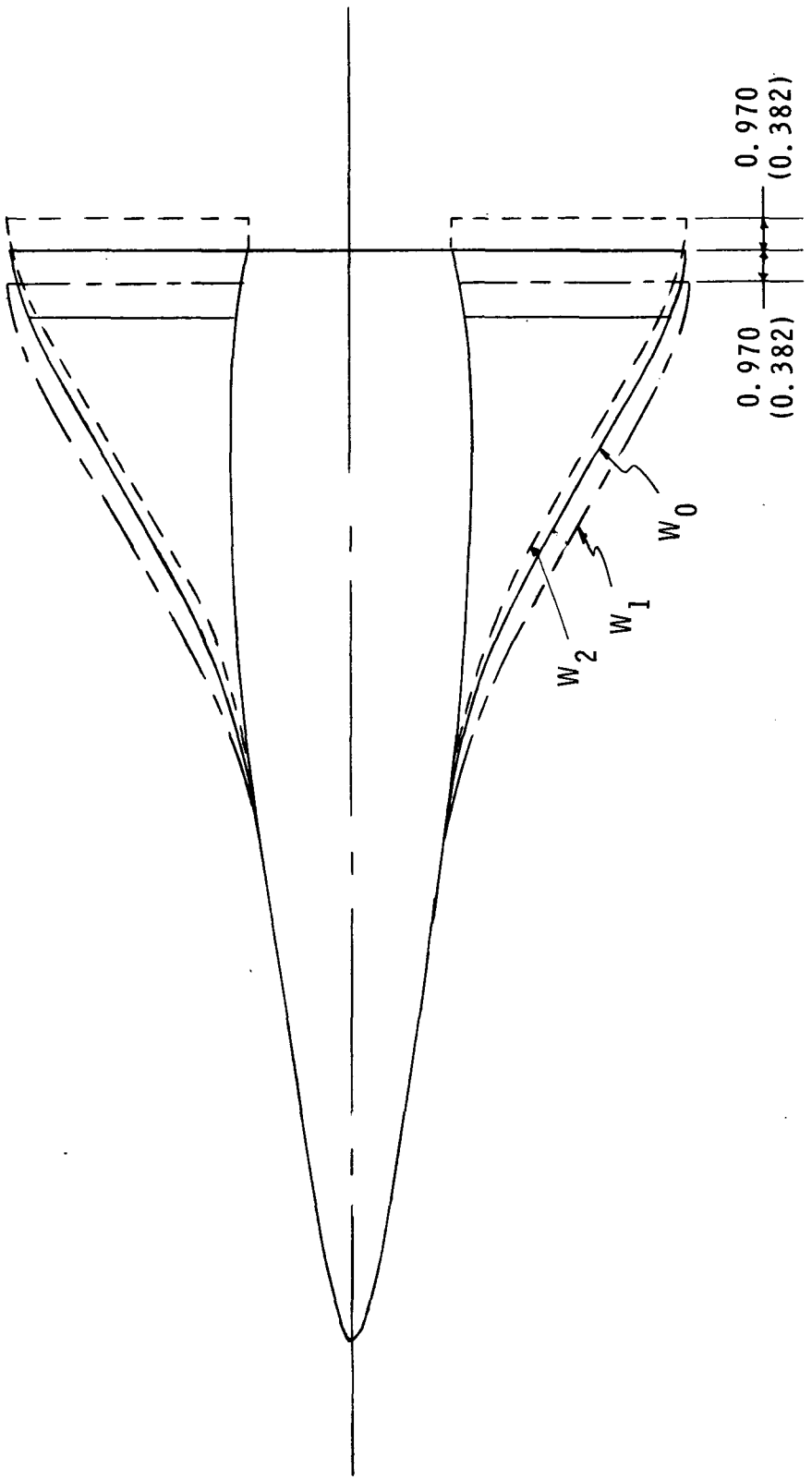

(b) Wing positions.

Figure 1.- Continued.

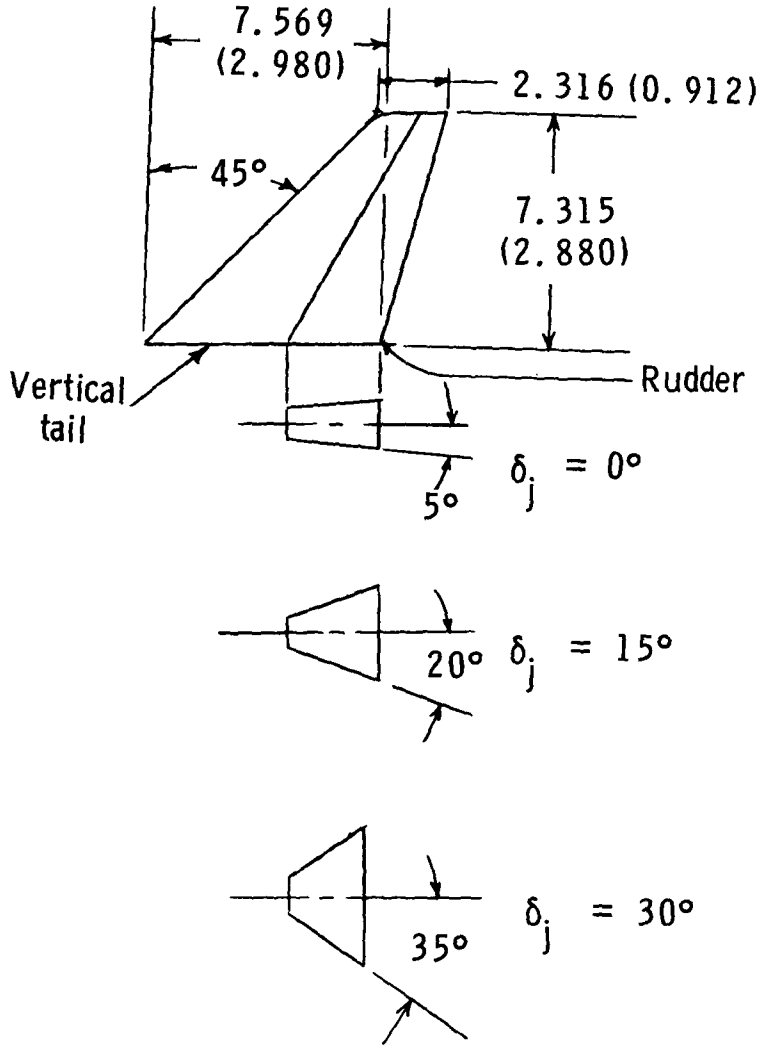

(c) Vertical tail and rudder.

Figure 1.- Continued.

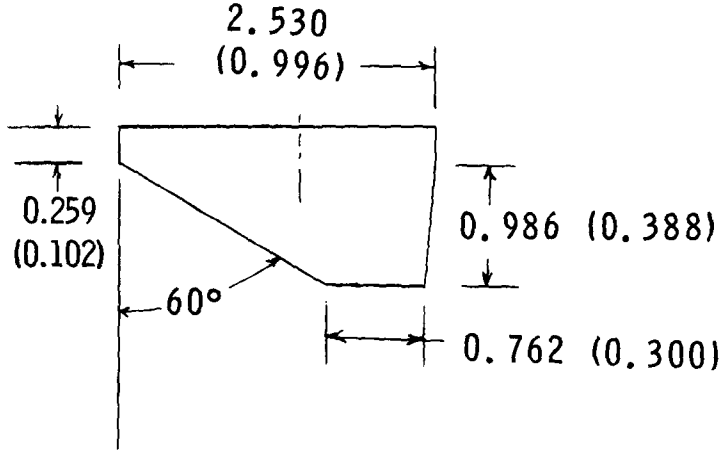

(d) Ventral fin.

Figure 1.- Continued.

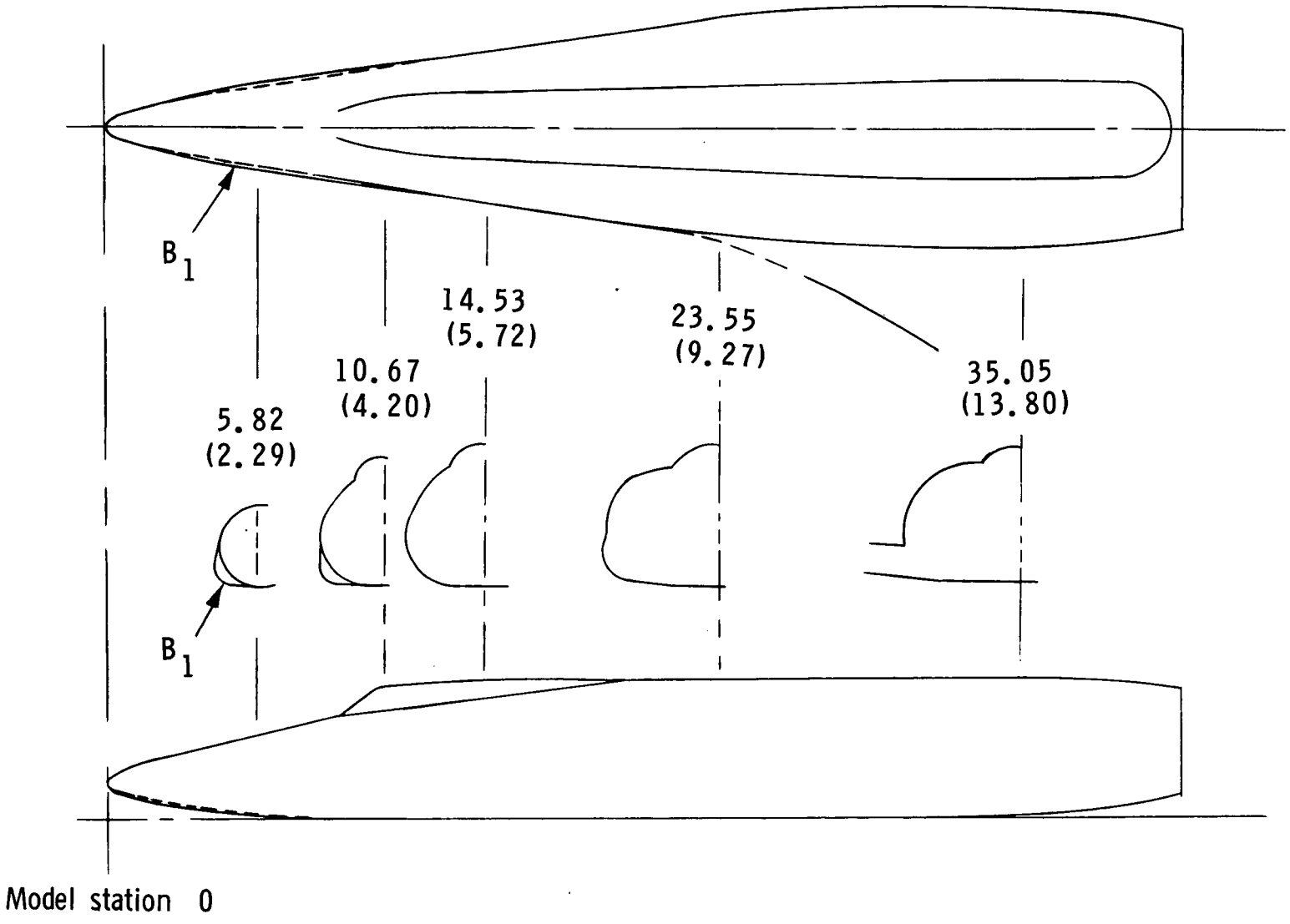

(e) Modified chine flare (B_1).

Figure 1.- Concluded.

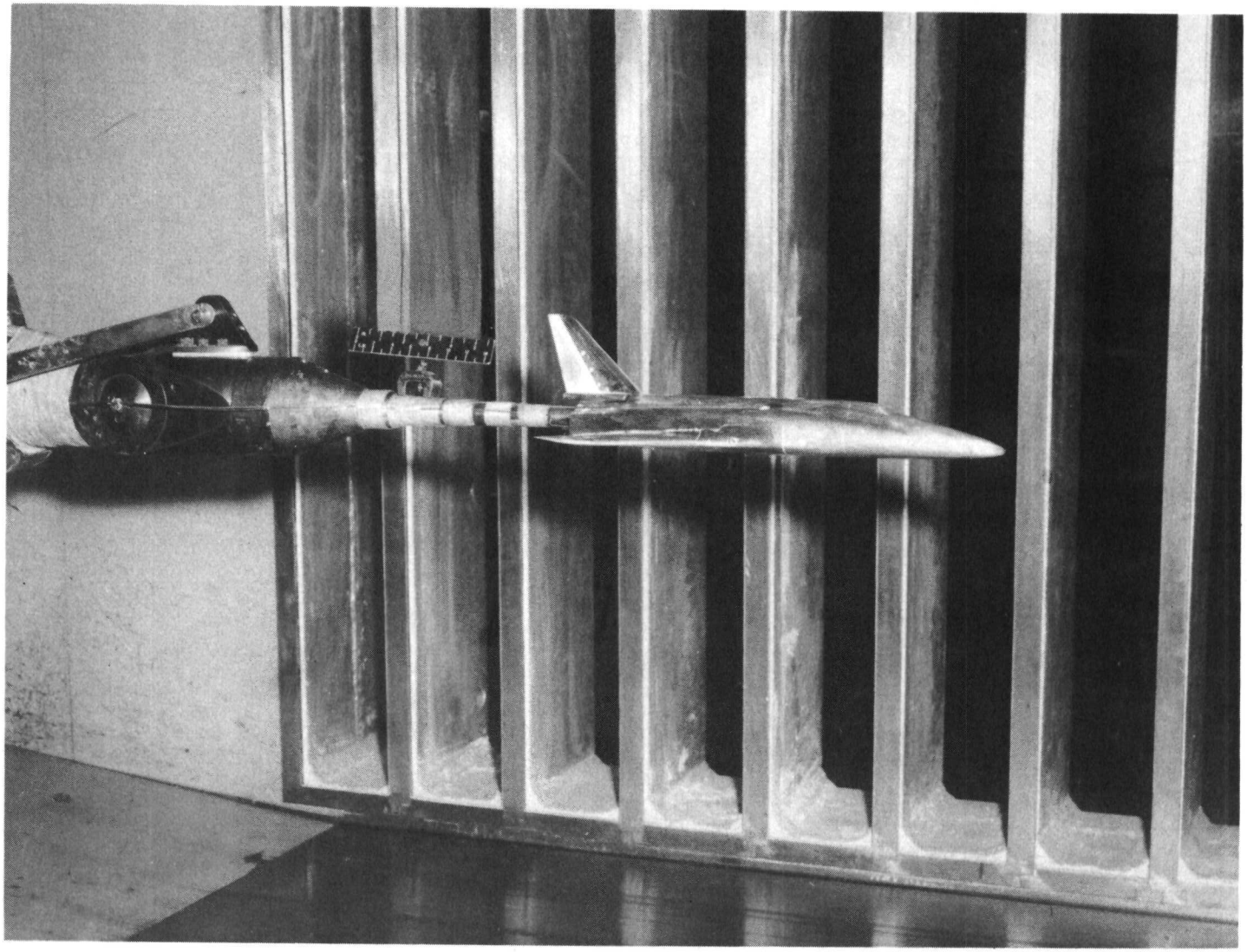

L-71-2478

Figure 2.- Photograph of model.

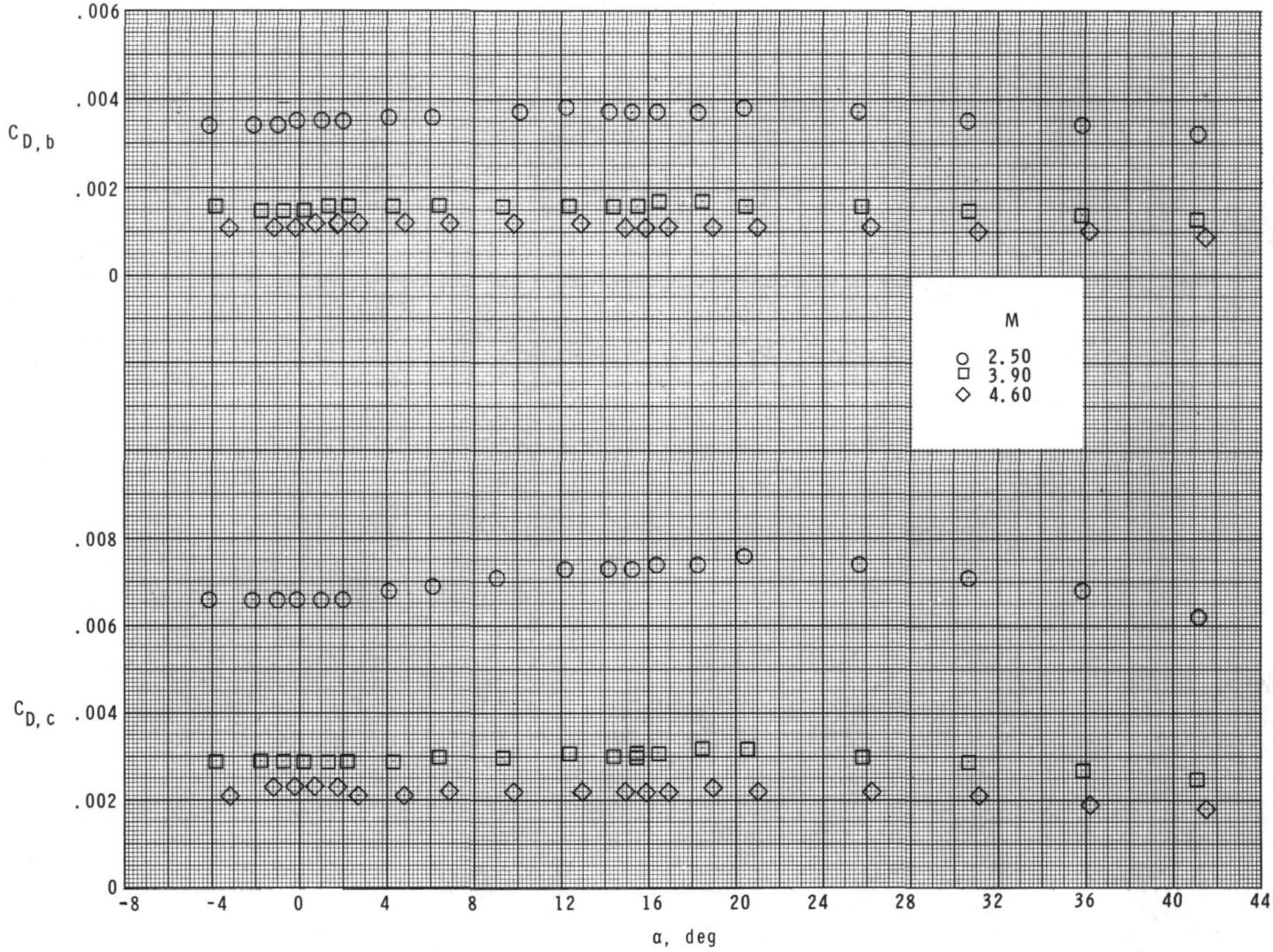

Figure 3.- Typical variation of base and chamber drag coefficients.

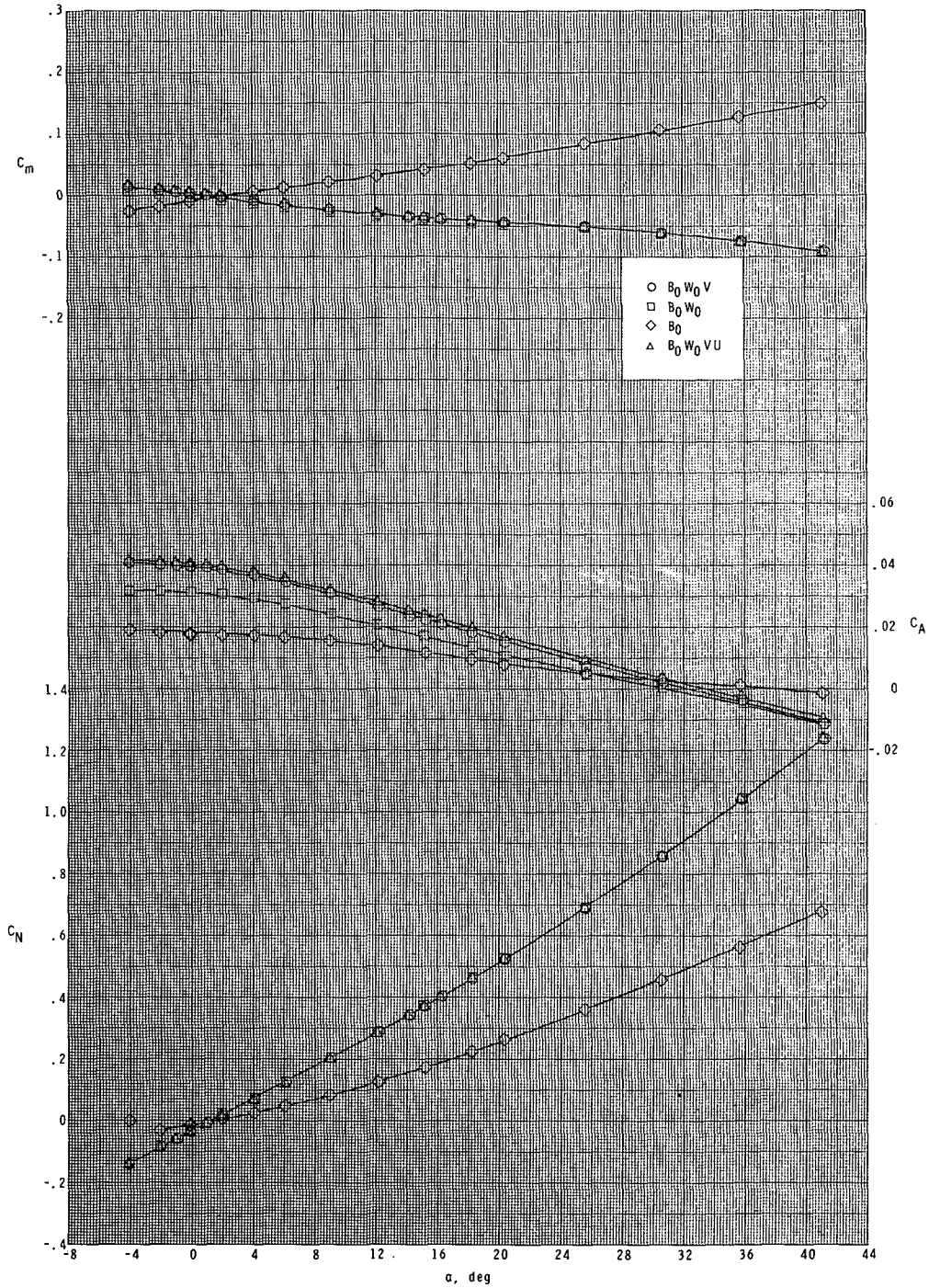

(a) M = 2.50.

Figure 4.- Effect of model components on longitudinal aerodynamic characteristics.

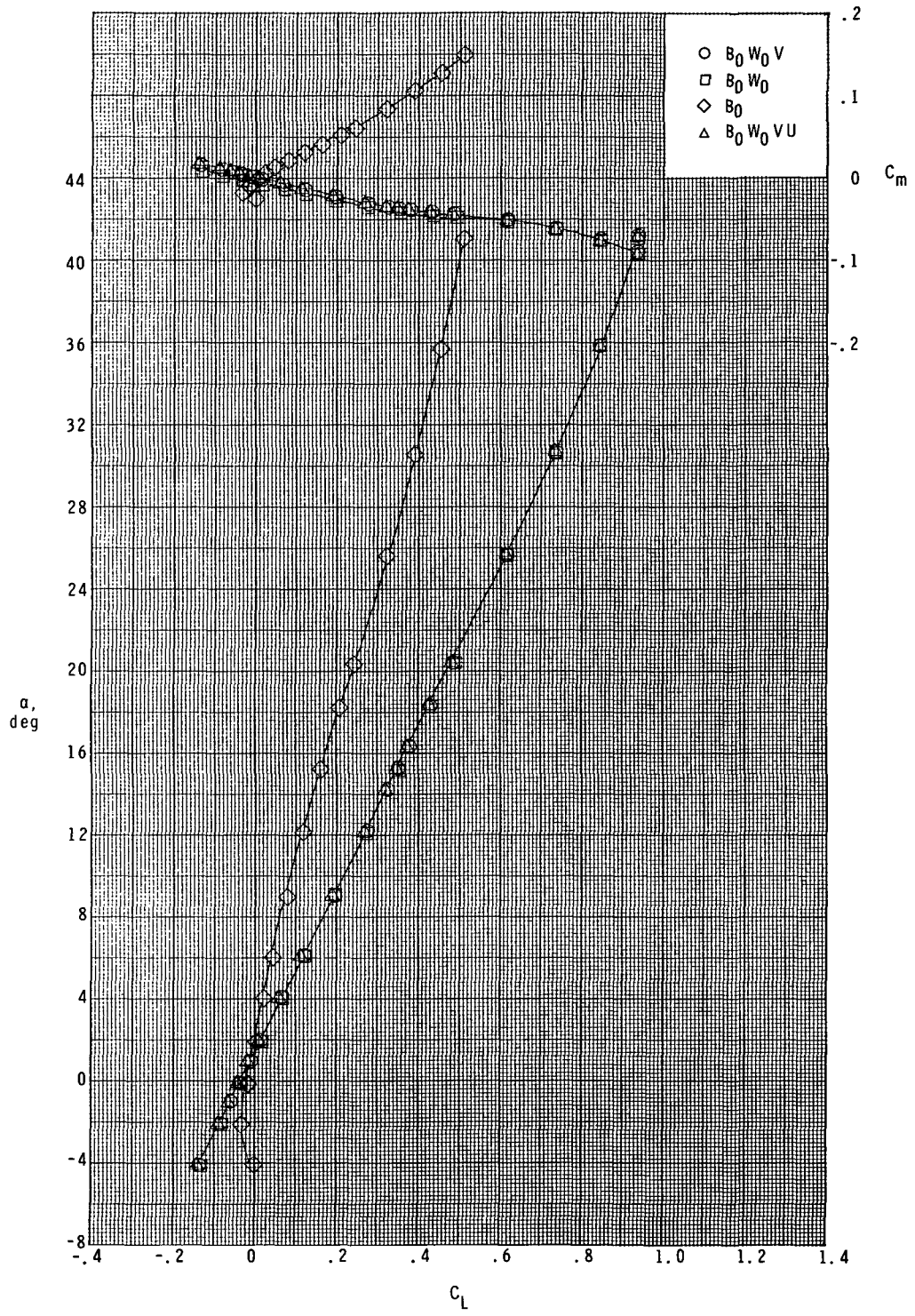

(a) Continued.

Figure 4.- Continued.

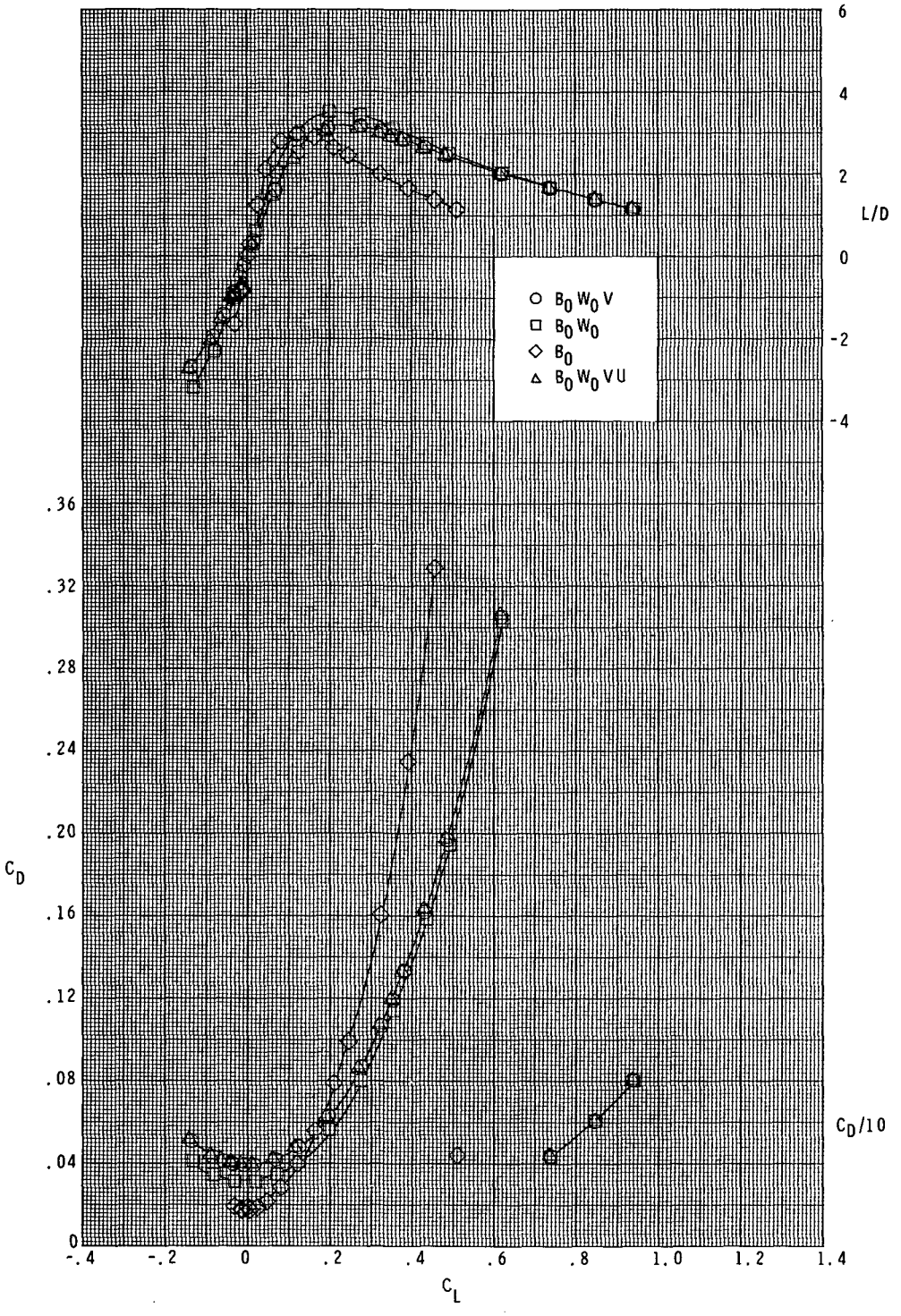

(a) Concluded.

Figure 4.- Continued.

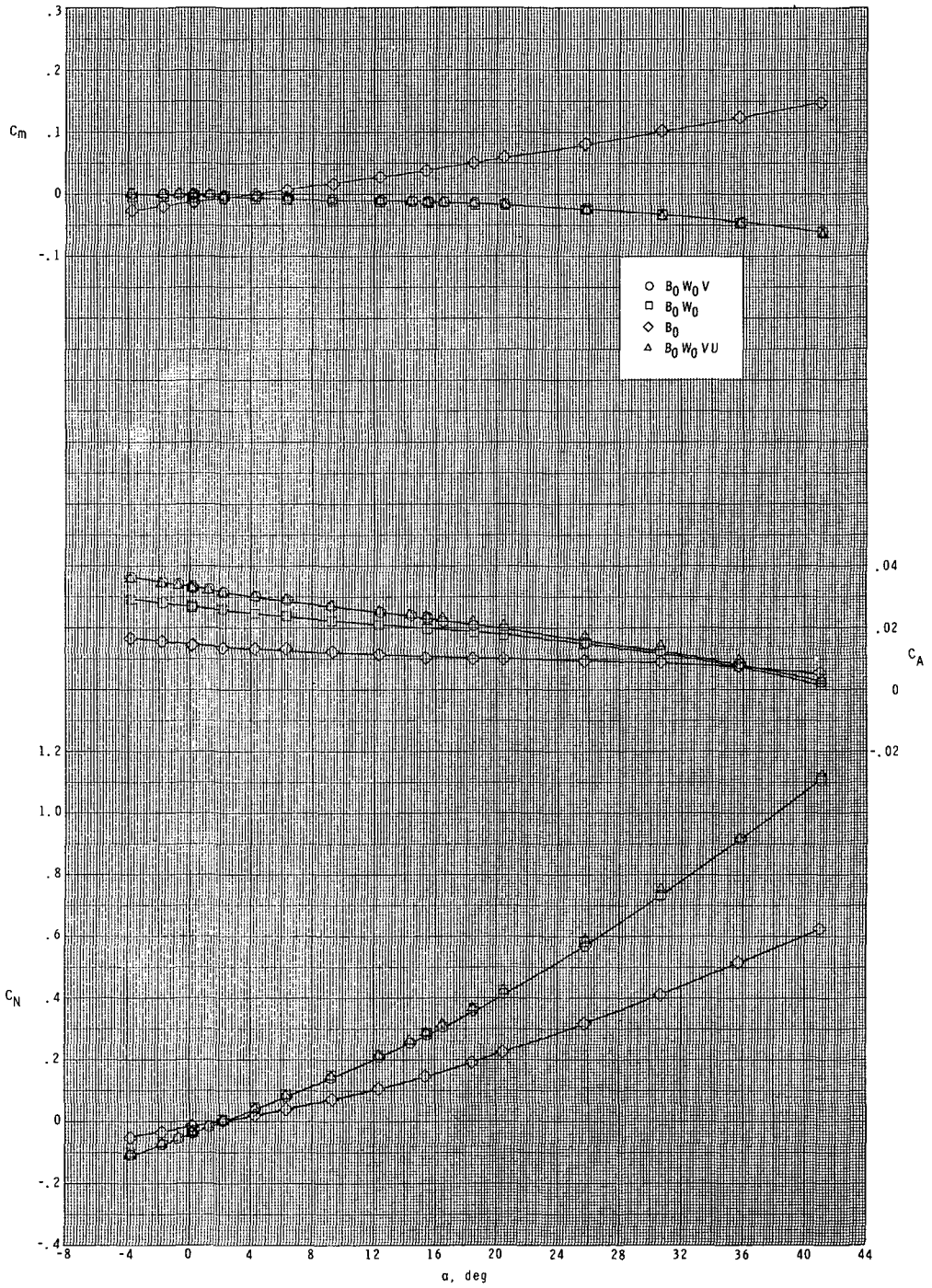

(b) M = 3.90.

Figure 4.- Continued.

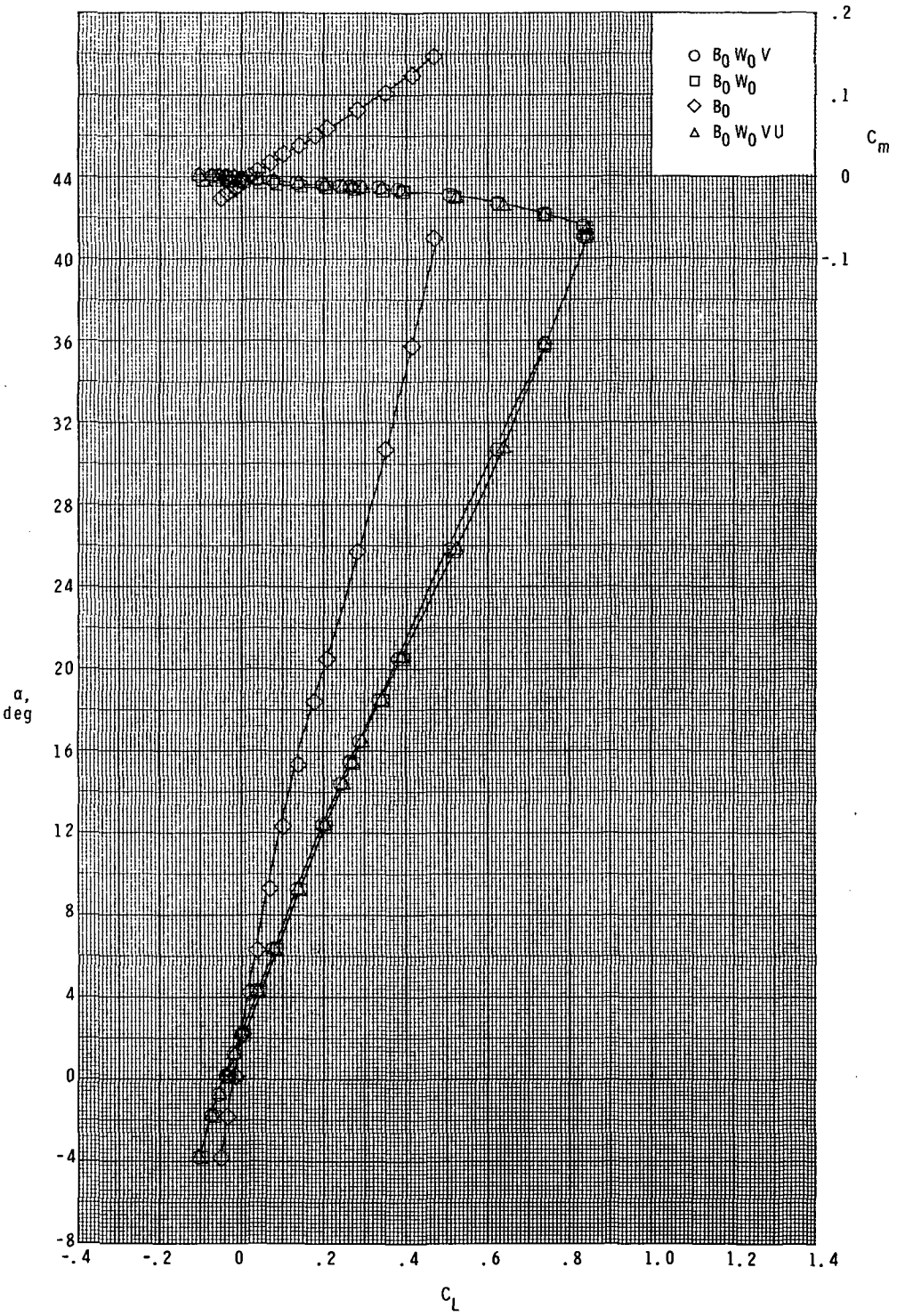

(b) Continued.

Figure 4.- Continued.

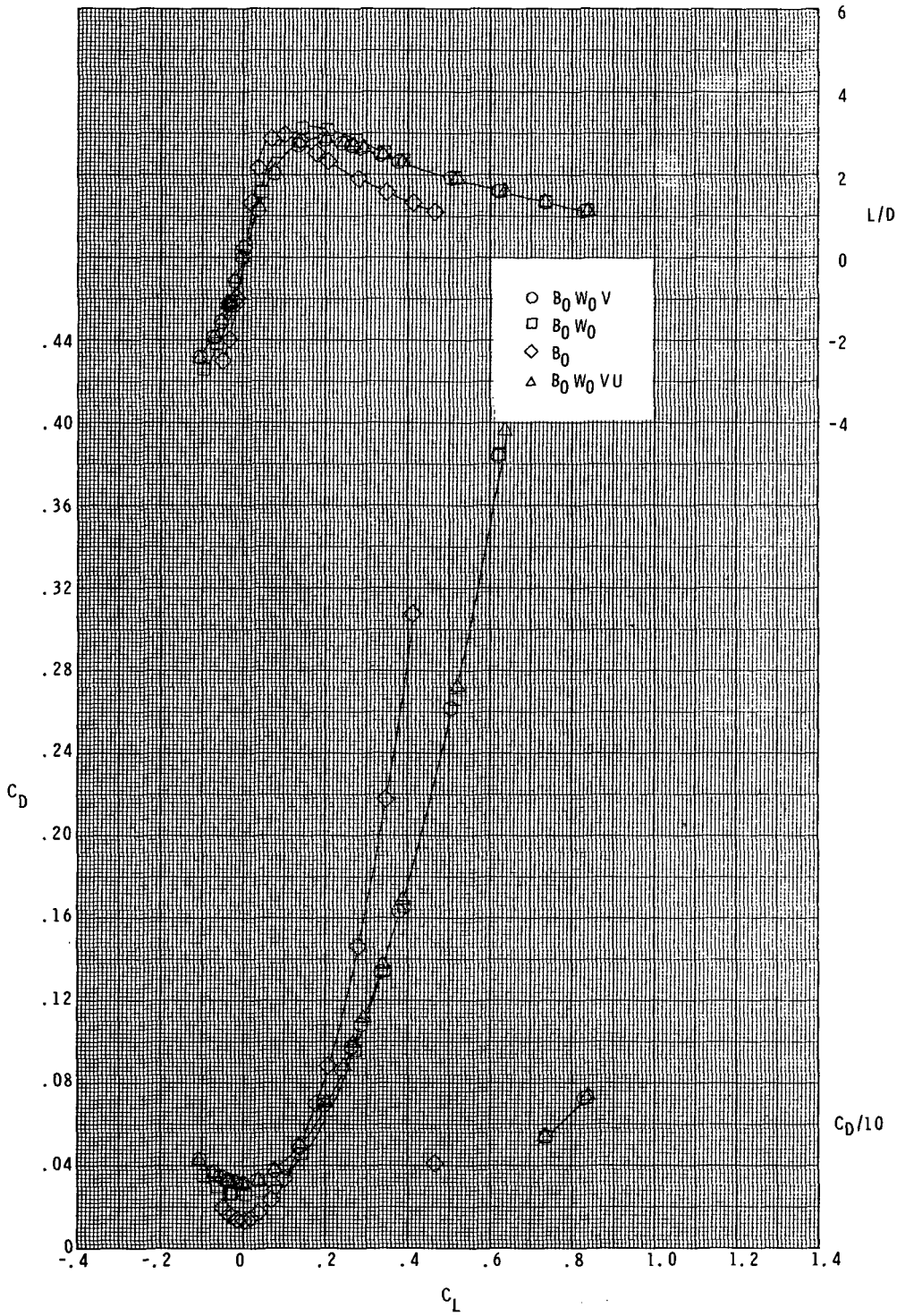

(b) Concluded.

Figure 4.- Continued.

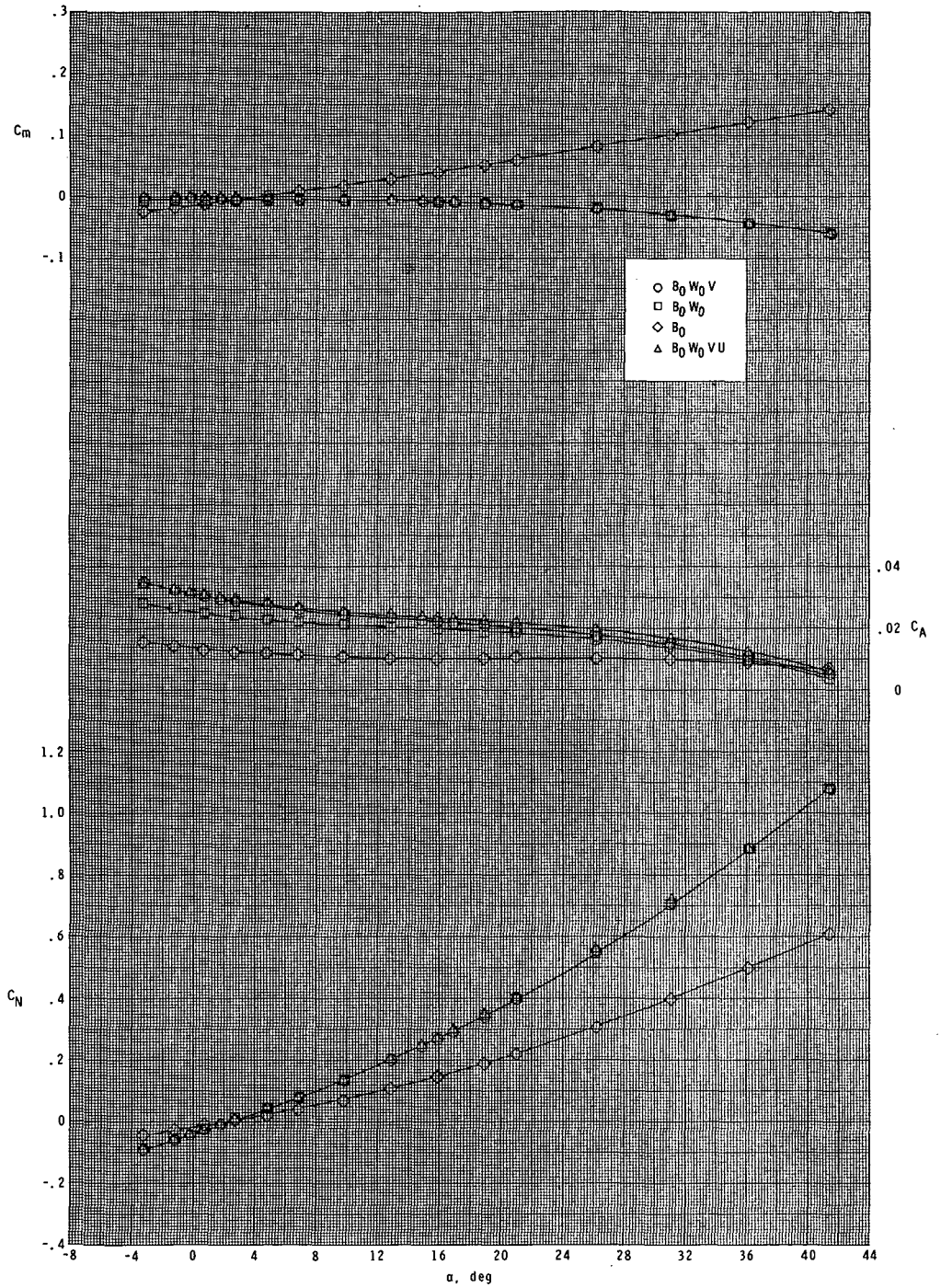

(c) M = 4.60.

Figure 4.- Continued.

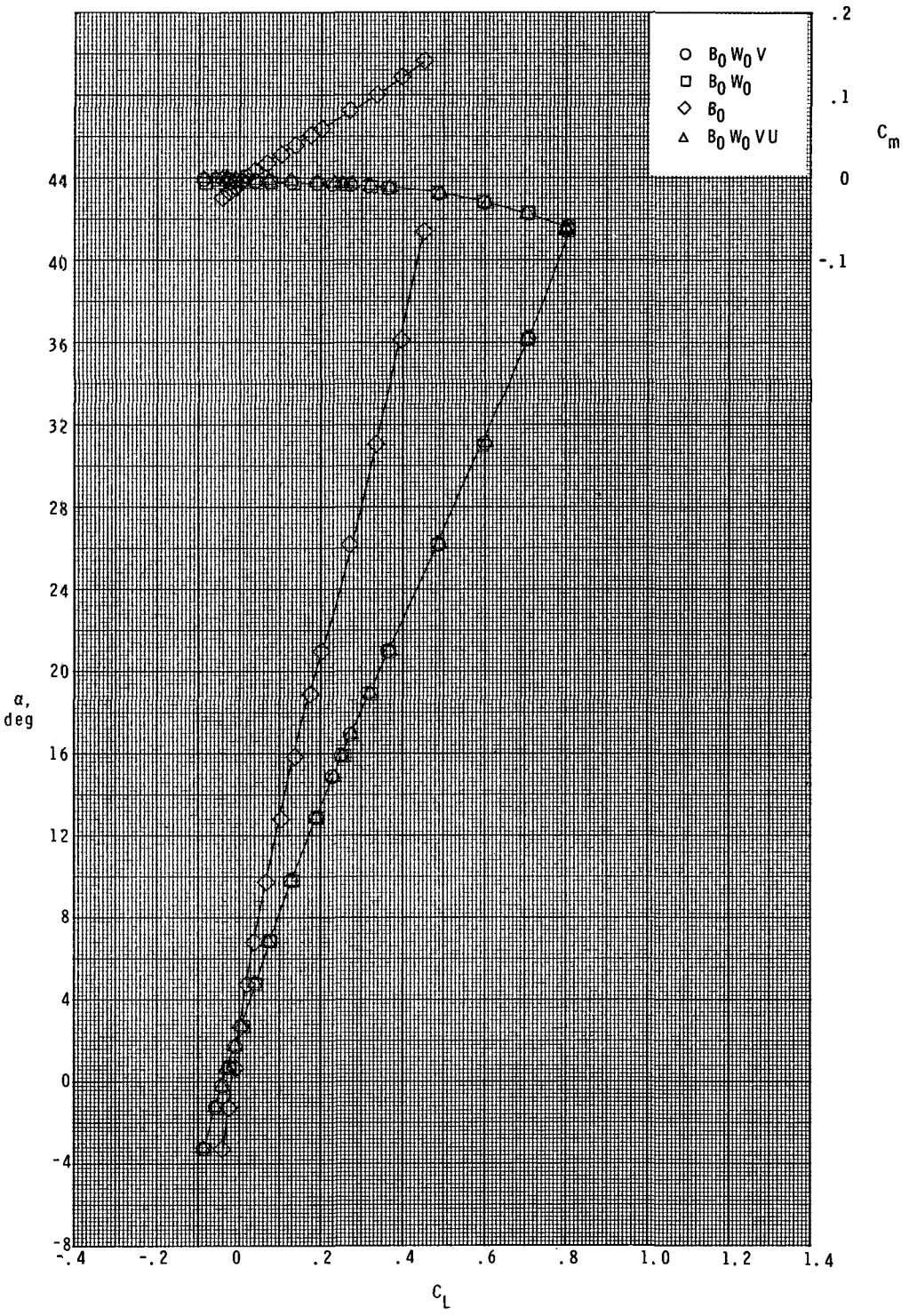

(c) Continued.

Figure 4.- Continued.

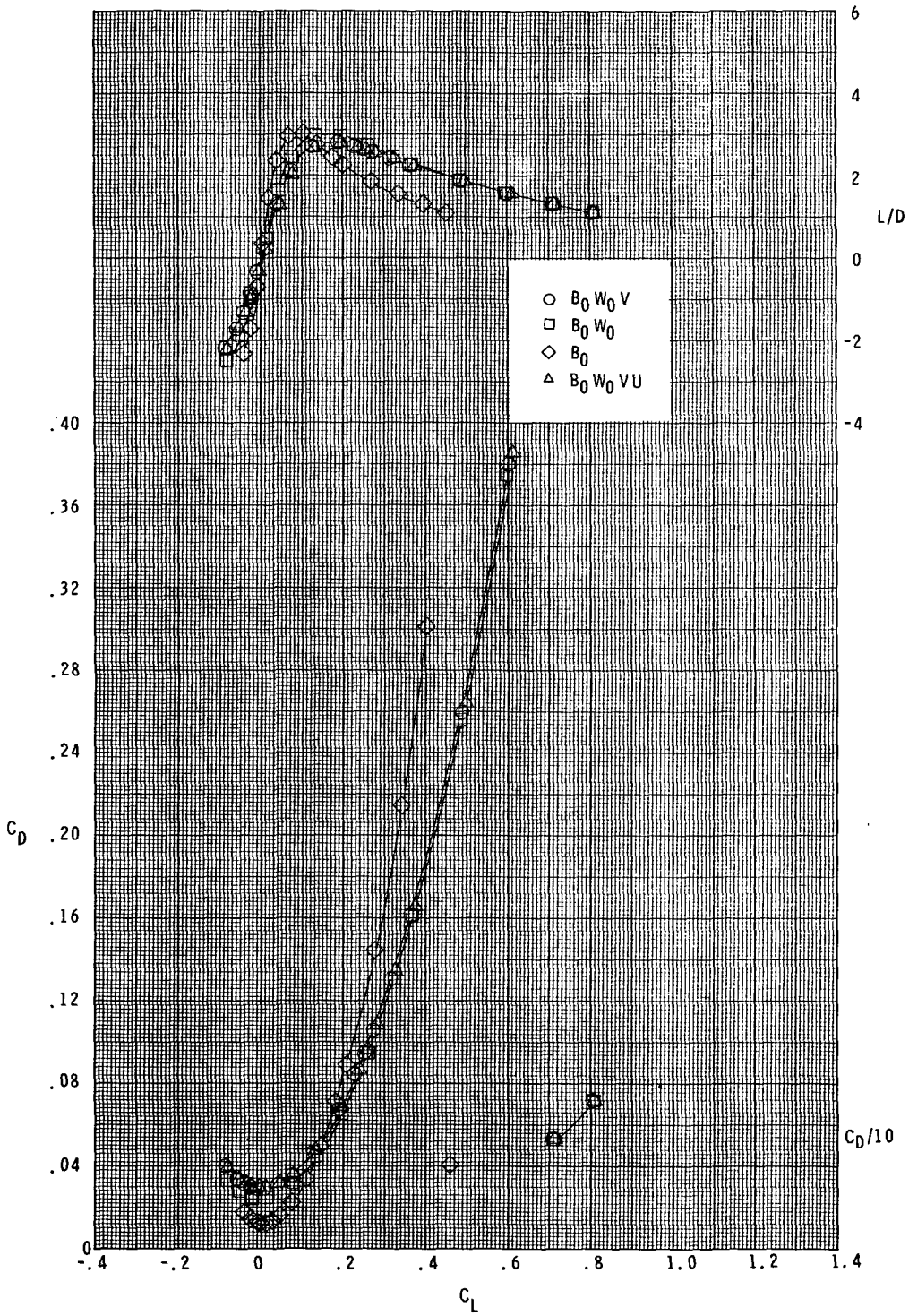

(c) Concluded.

Figure 4.- Concluded.

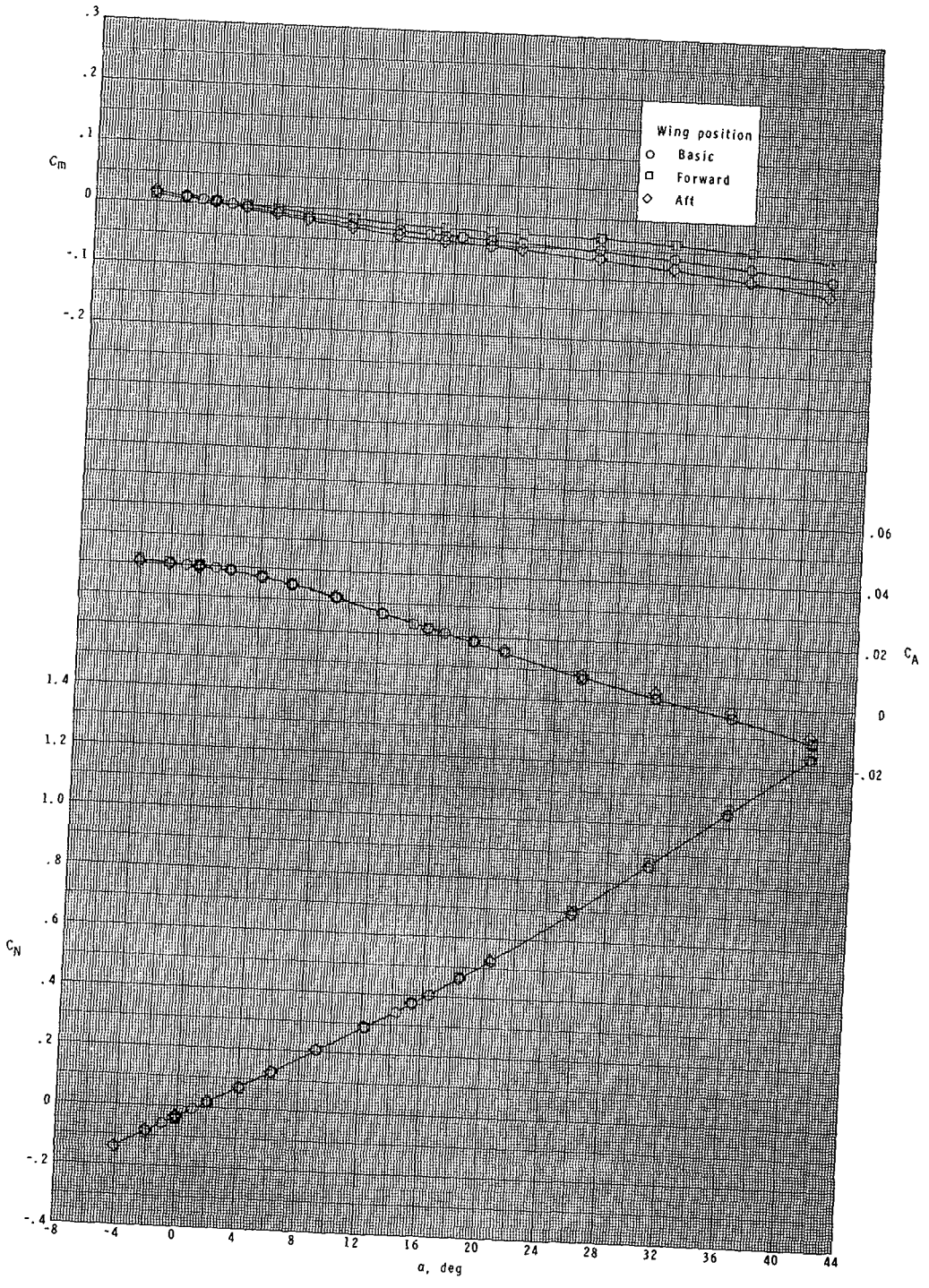

(a) M = 2.50.

Figure 5.- Effect of wing position on longitudinal aerodynamic characteristics.

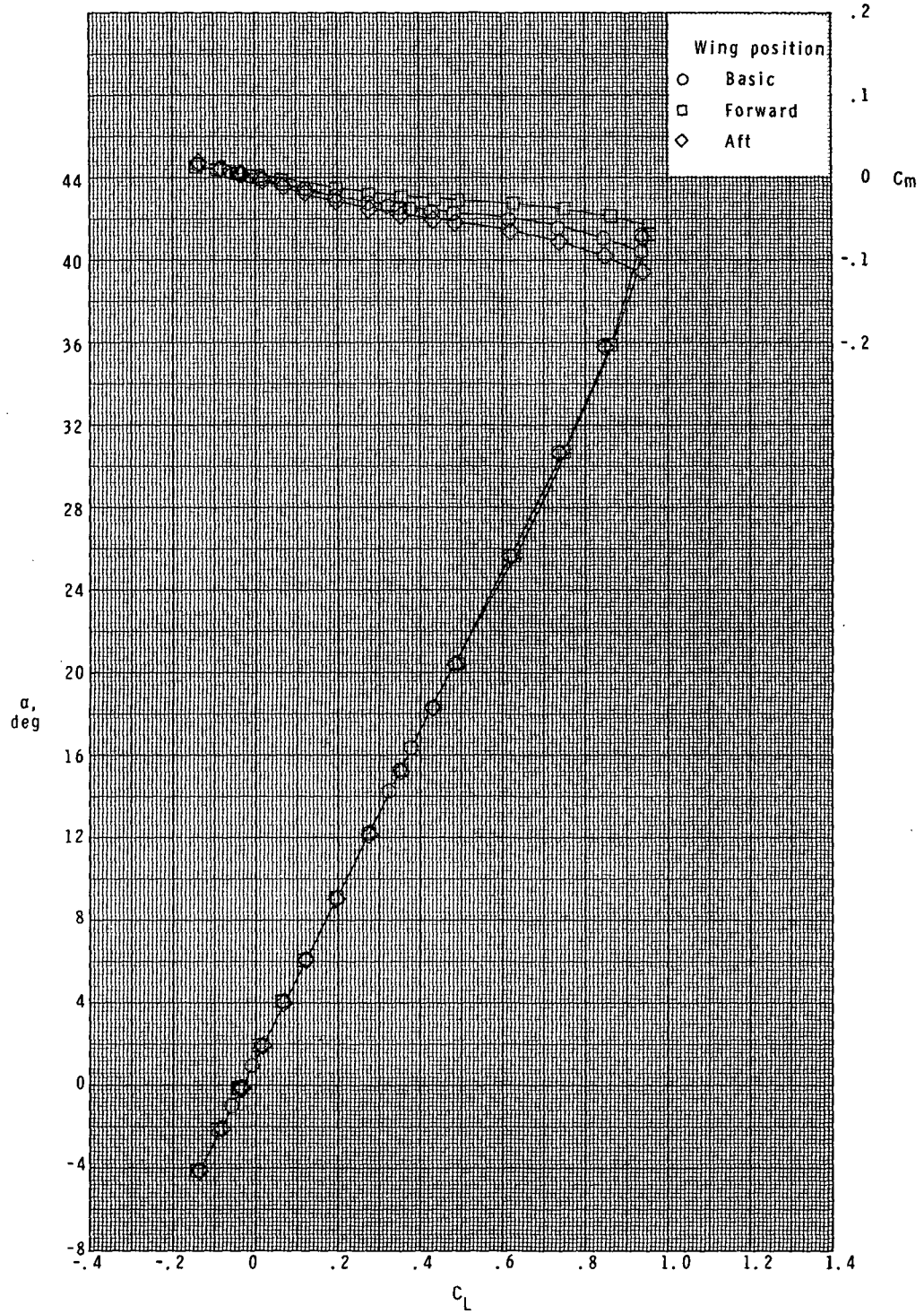

(a) Continued.

Figure 5.- Continued.

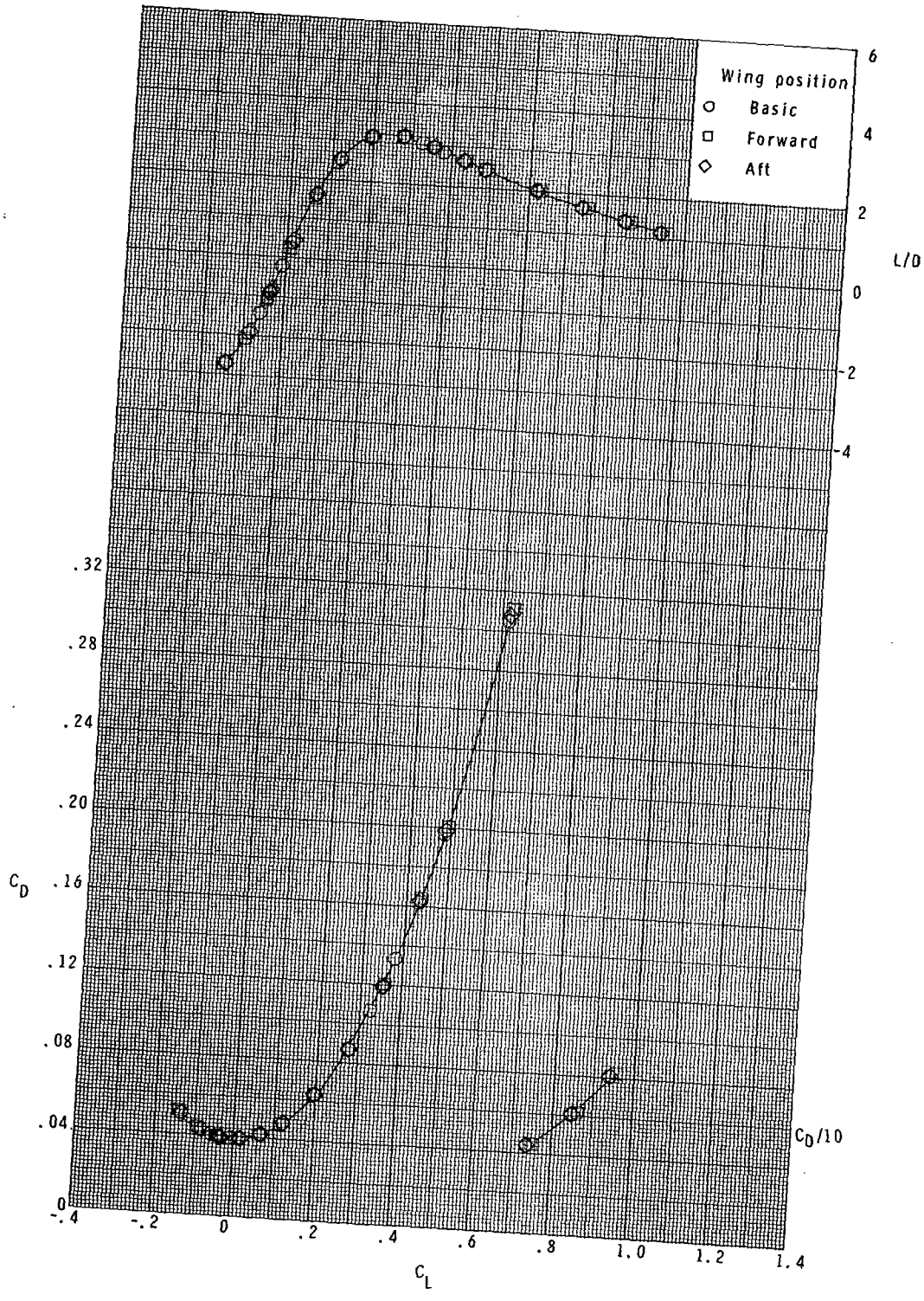

(a) Concluded.

Figure 5.- Continued.

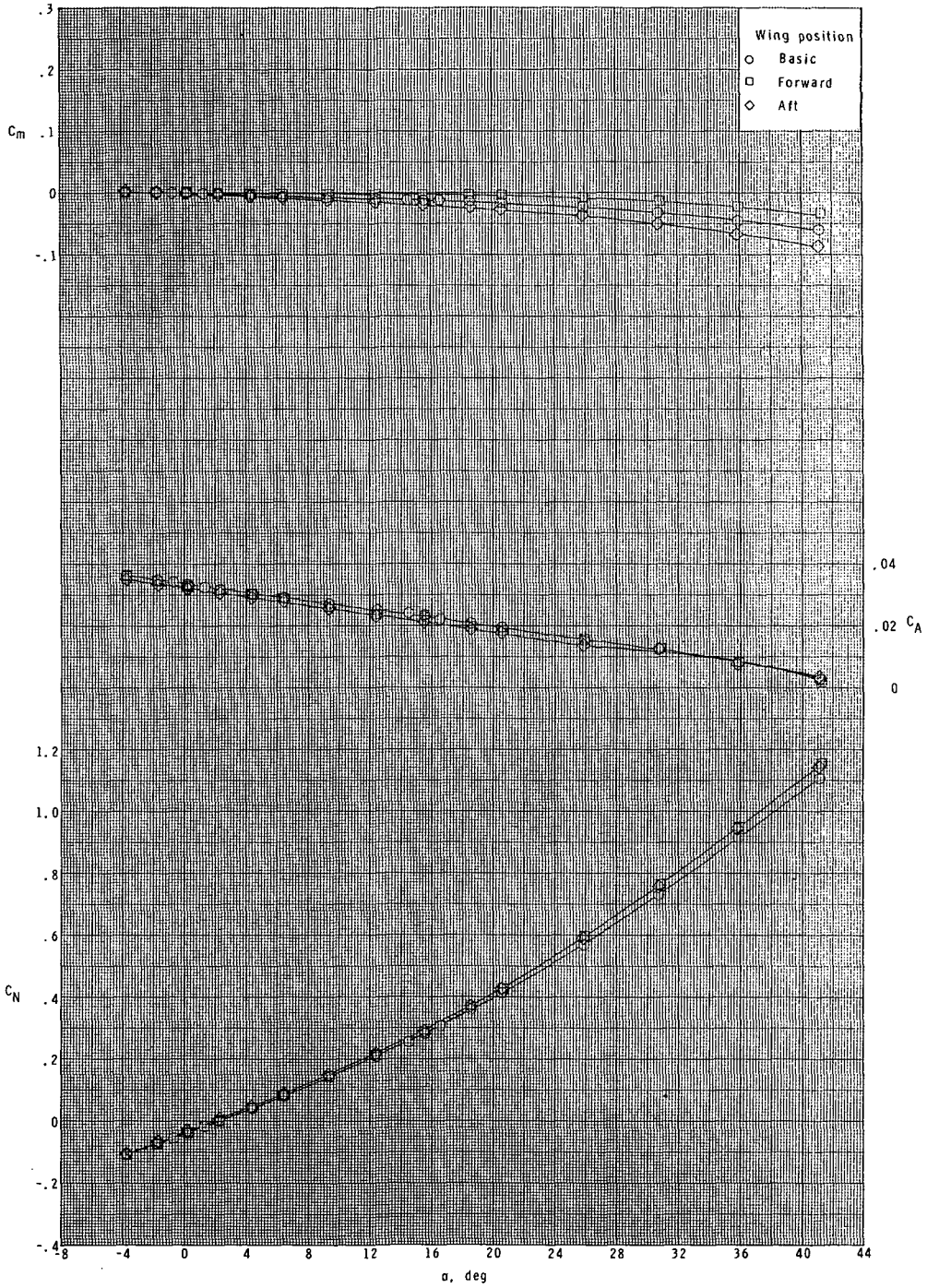

(b) M = 3.90.

Figure 5.- Continued.

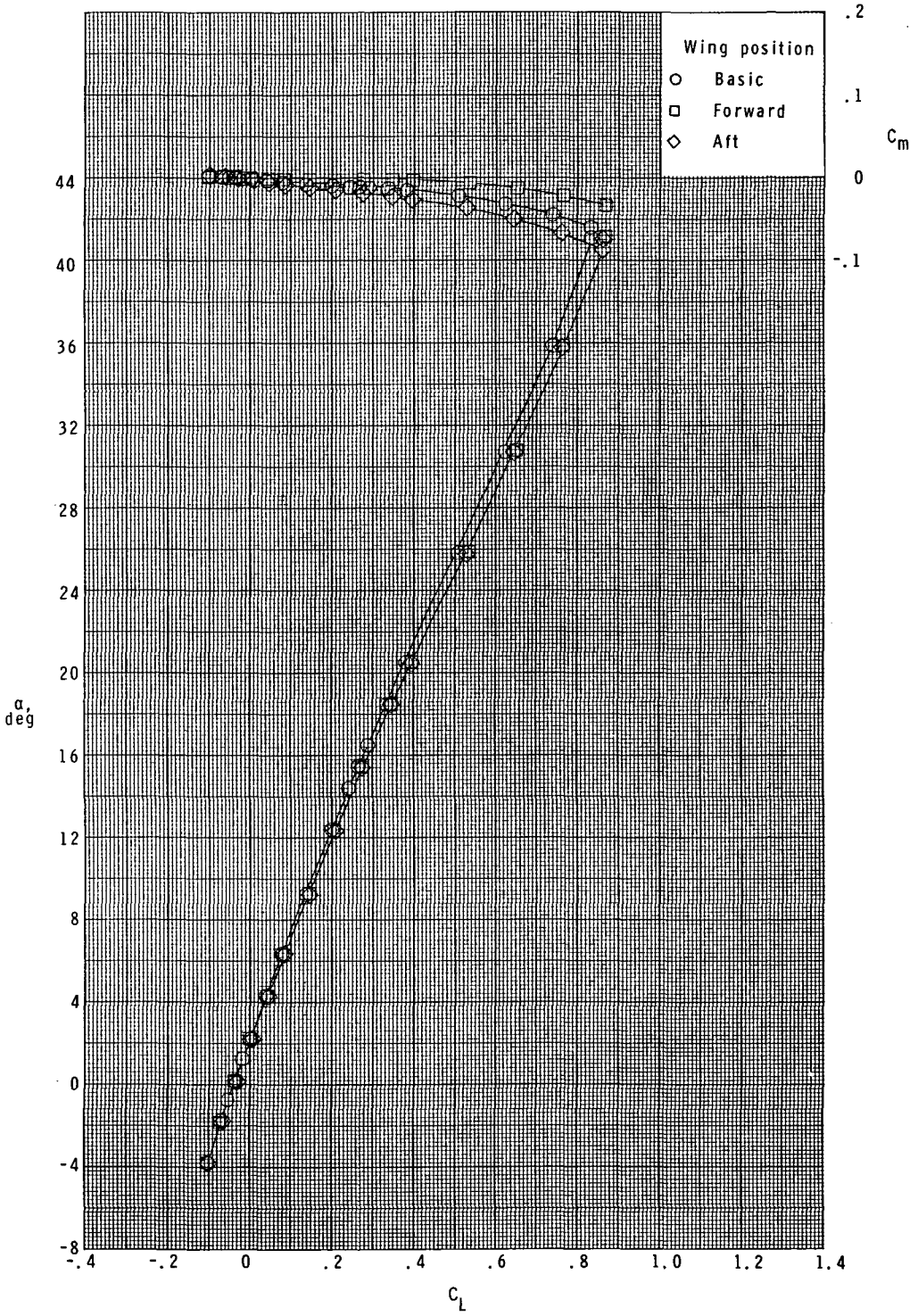

(b) Continued.

Figure 5.- Continued.

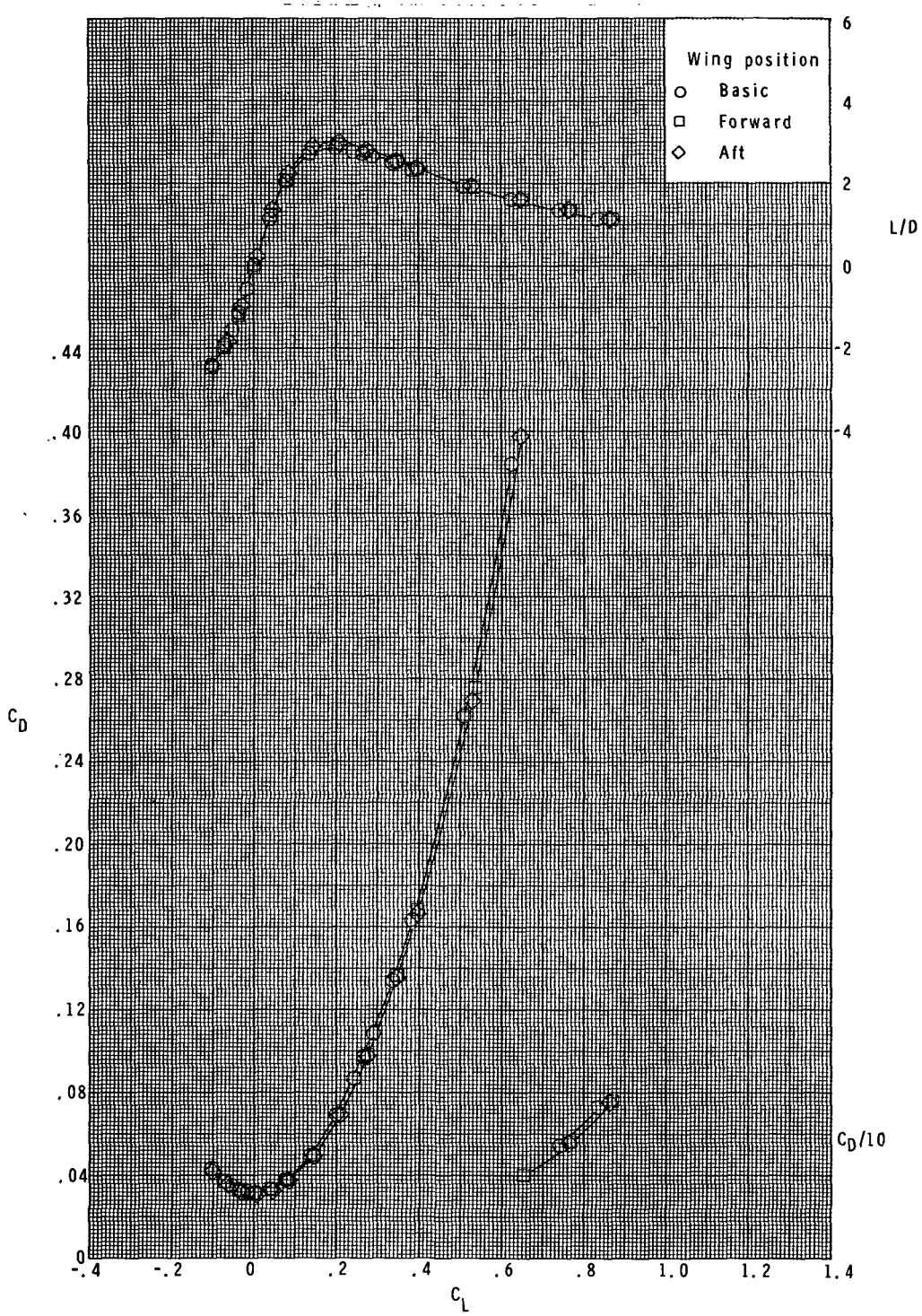

(b) Concluded.

Figure 5.- Continued.

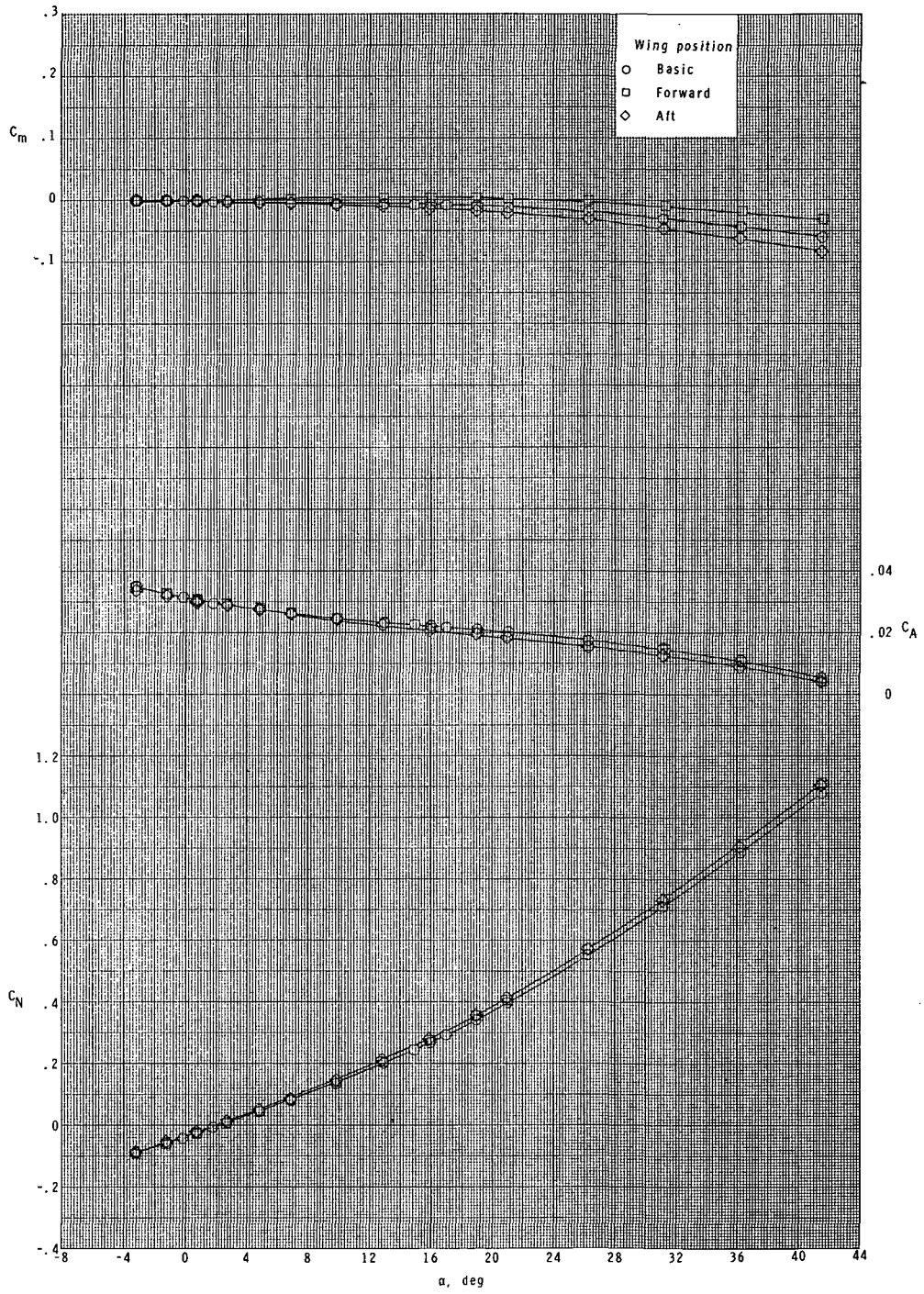

(c) M = 4.60.

Figure 5.- Continued.

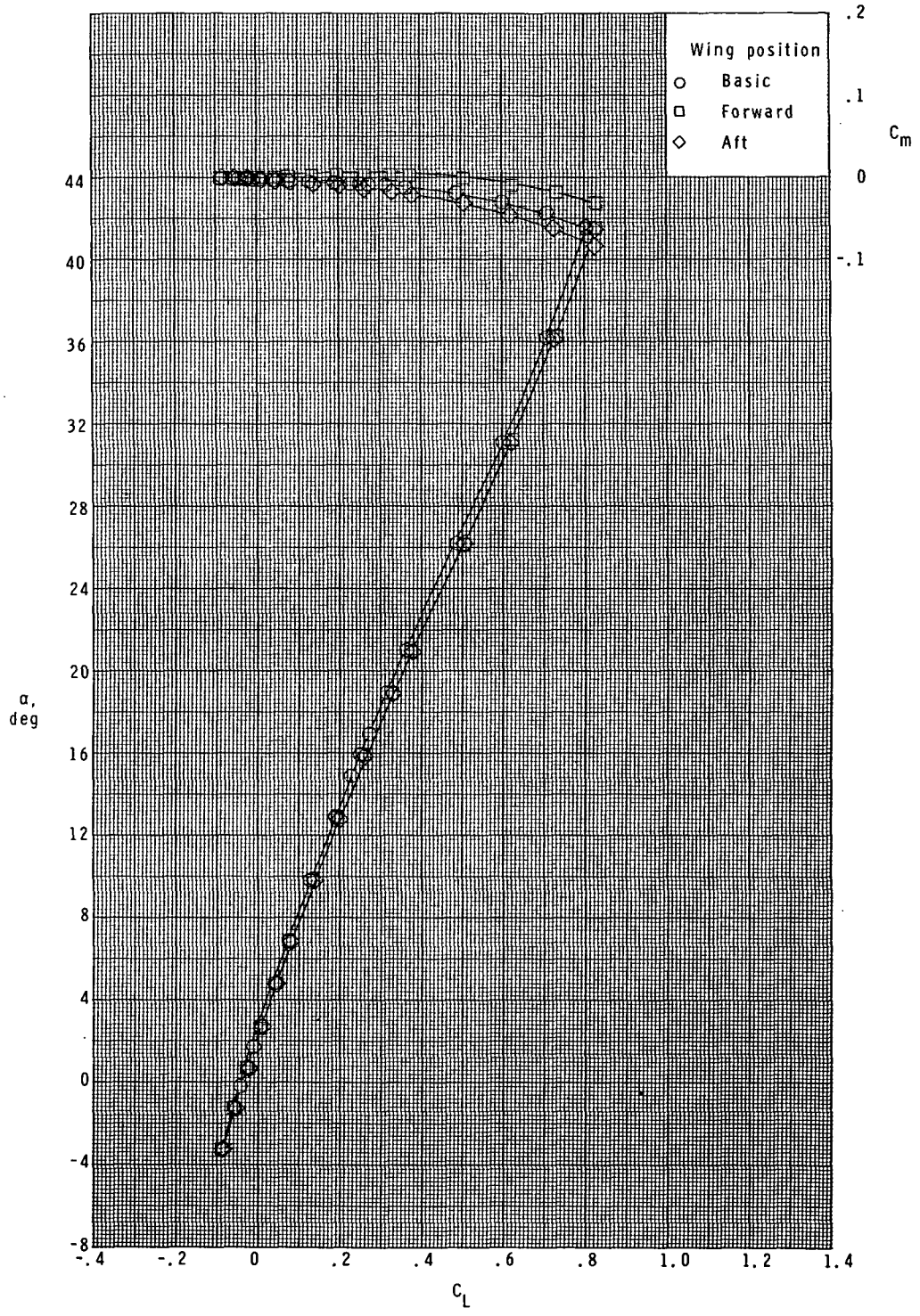

(c) Continued.

Figure 5.- Continued.

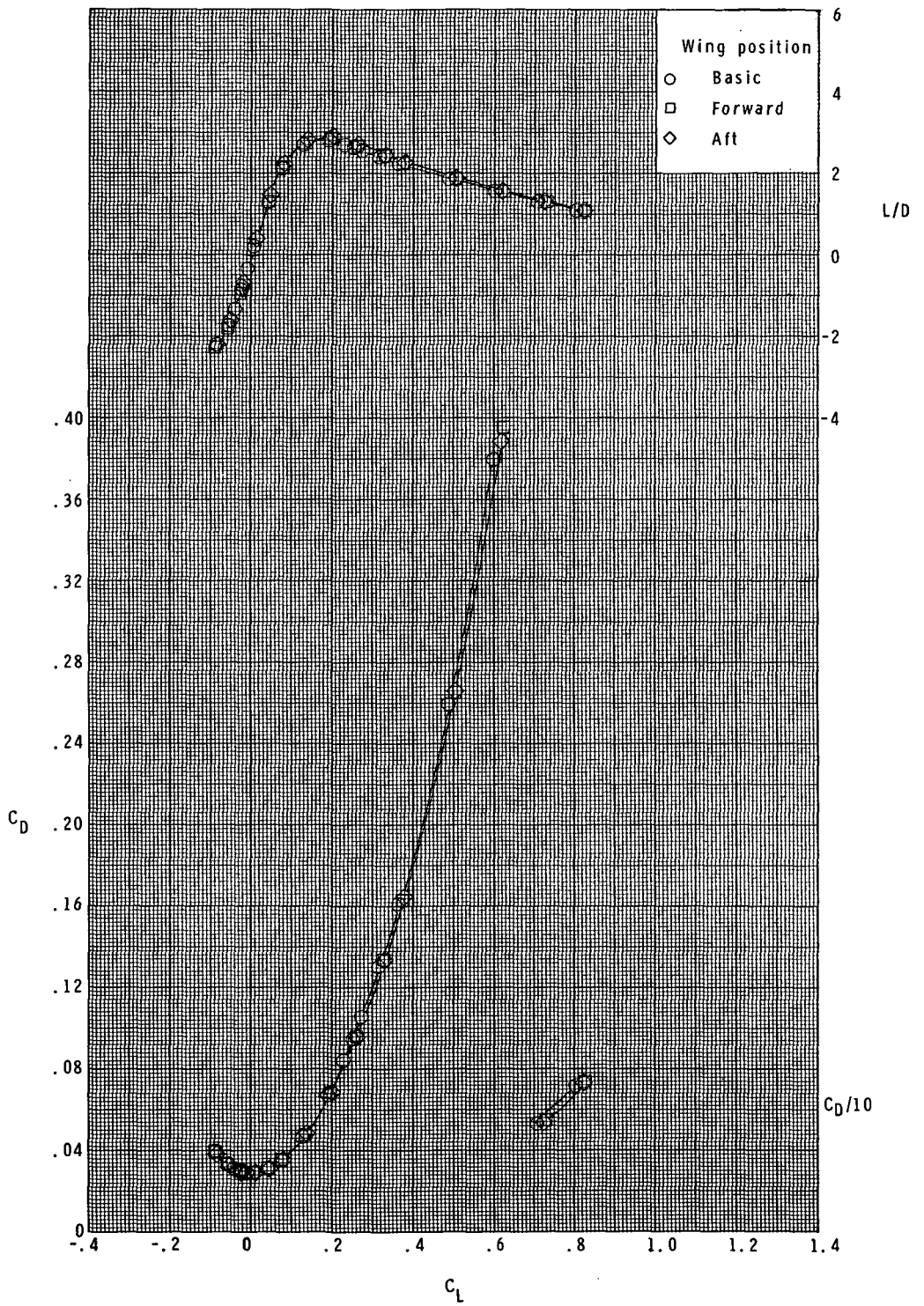

(c) Concluded.

Figure 5.- Concluded.

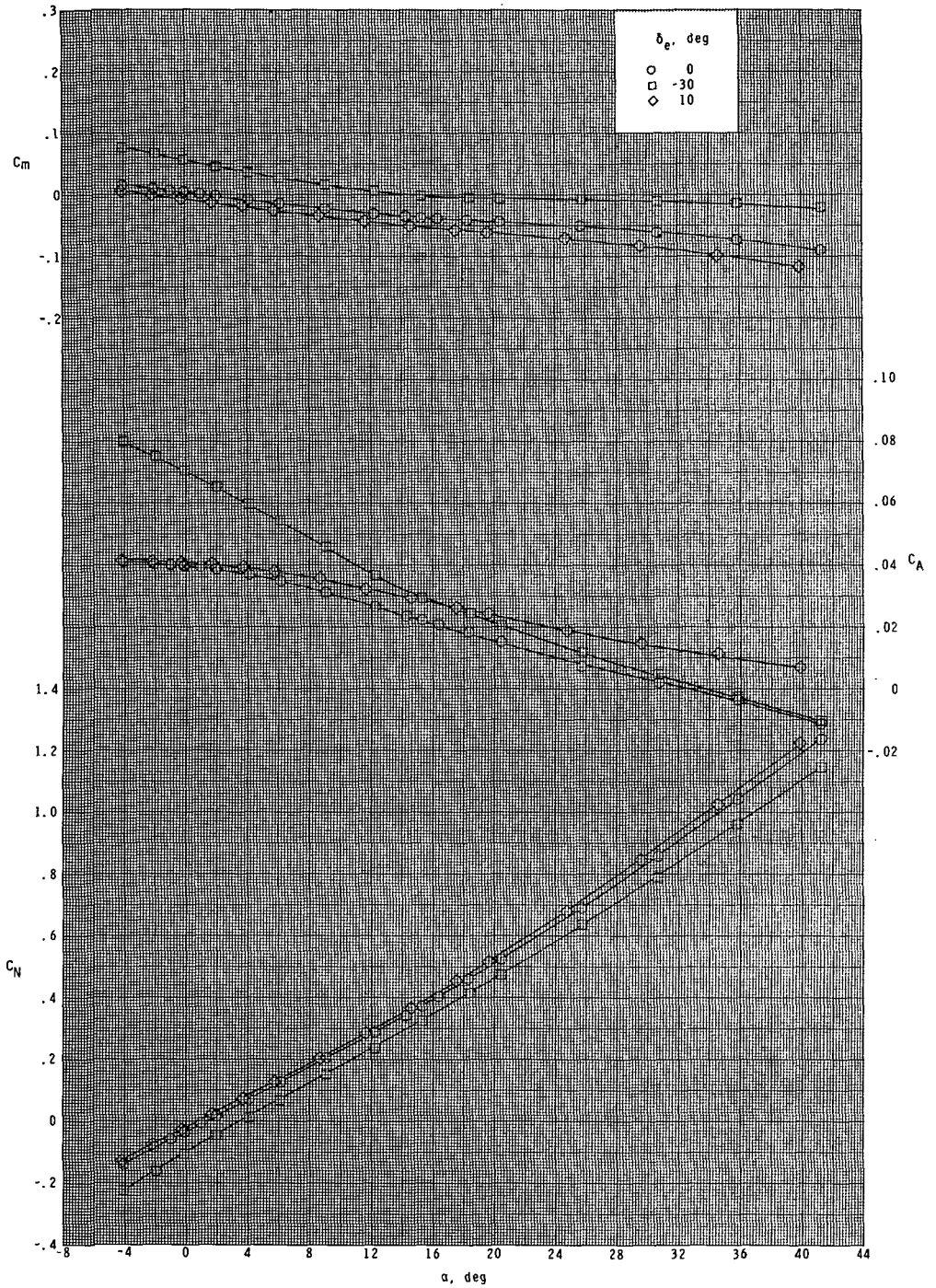

(a) M = 2.50.

Figure 6.- Elevon pitch-control effectiveness.

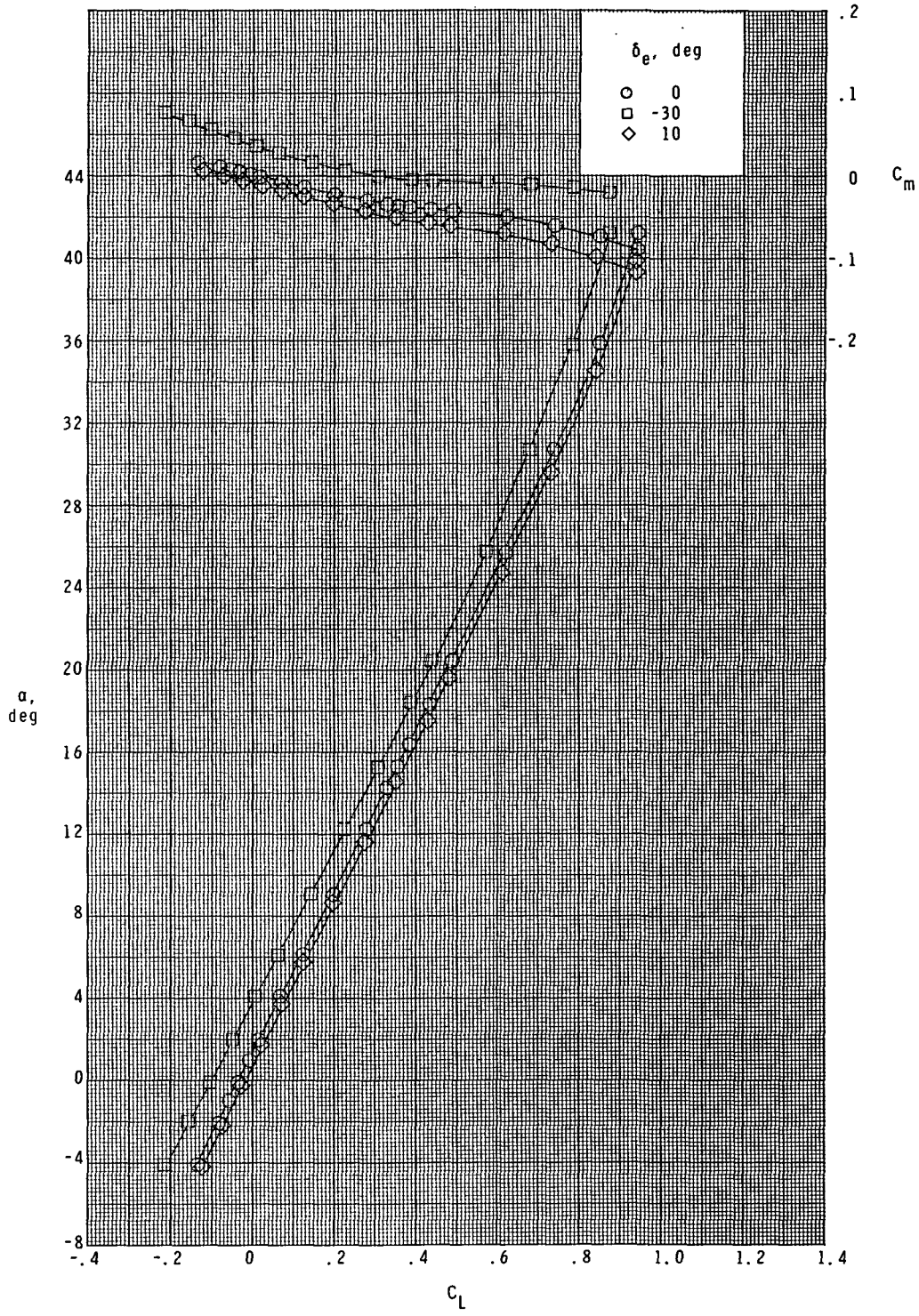

(a) Continued.

Figure 6.- Continued.

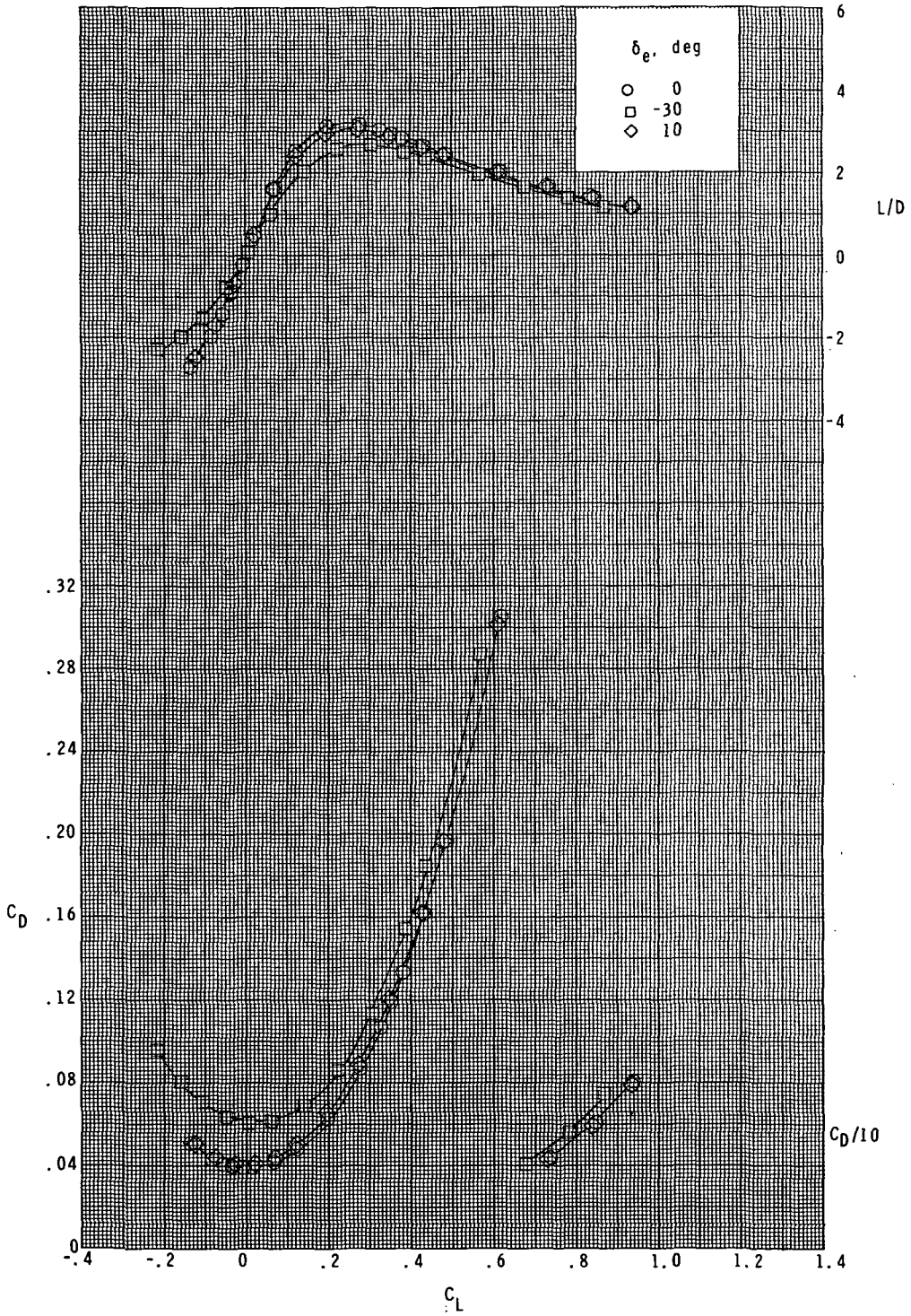

(a) Concluded.

Figure 6.- Continued.

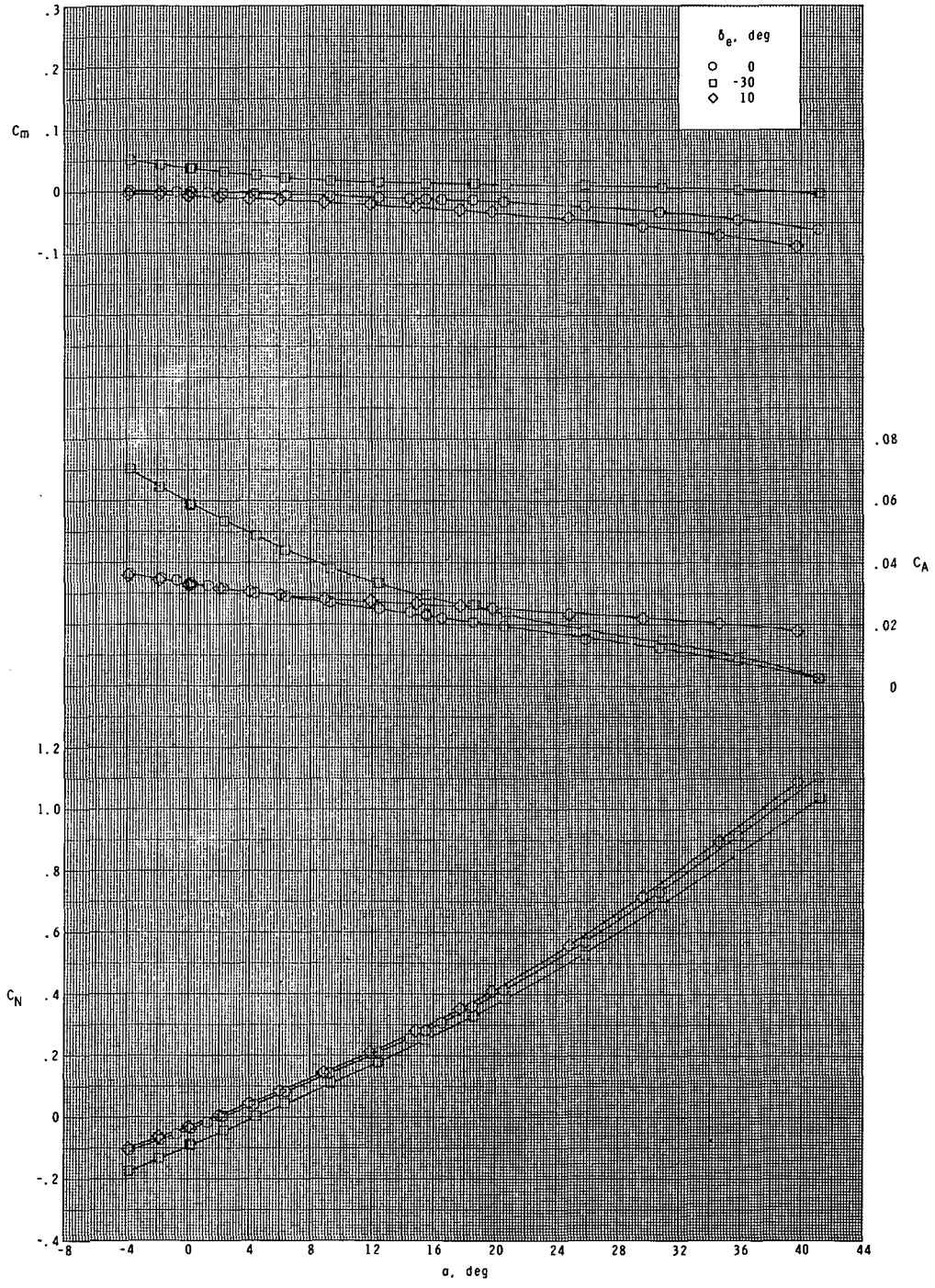

(b) M = 3.90.

Figure 6.- Continued.

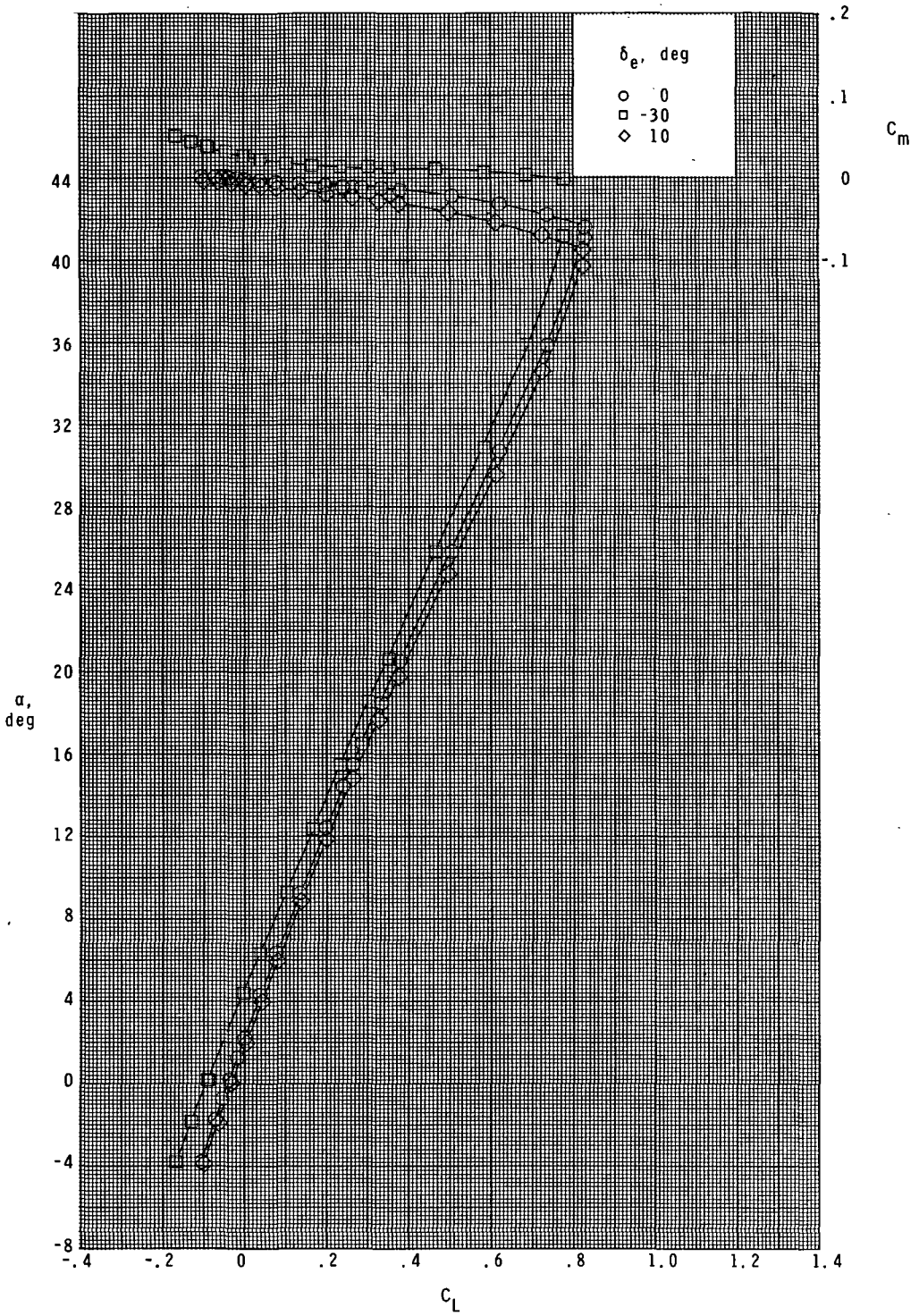

(b) Continued.

Figure 6.- Continued.

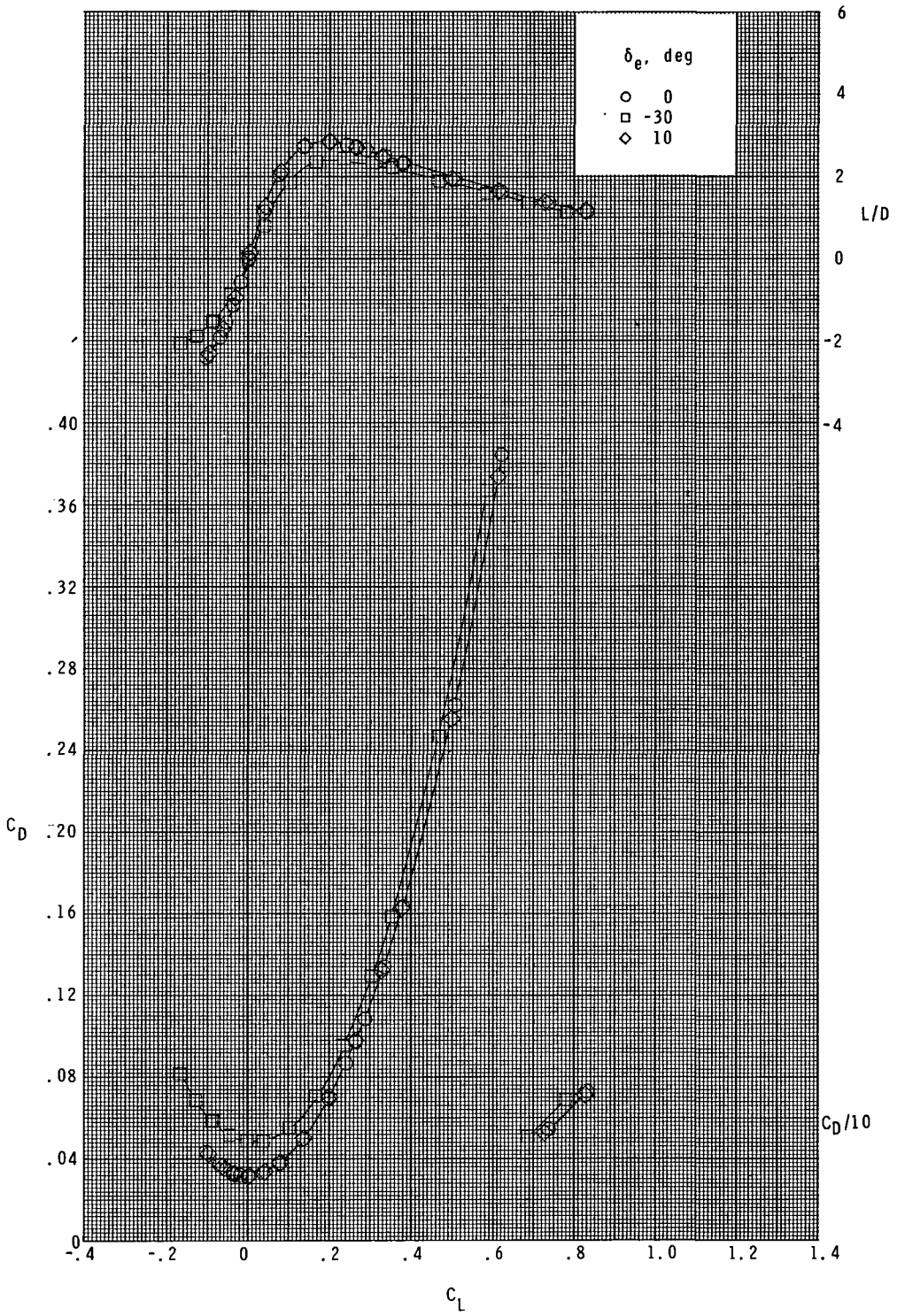

(b) Concluded.

Figure 6.- Continued.

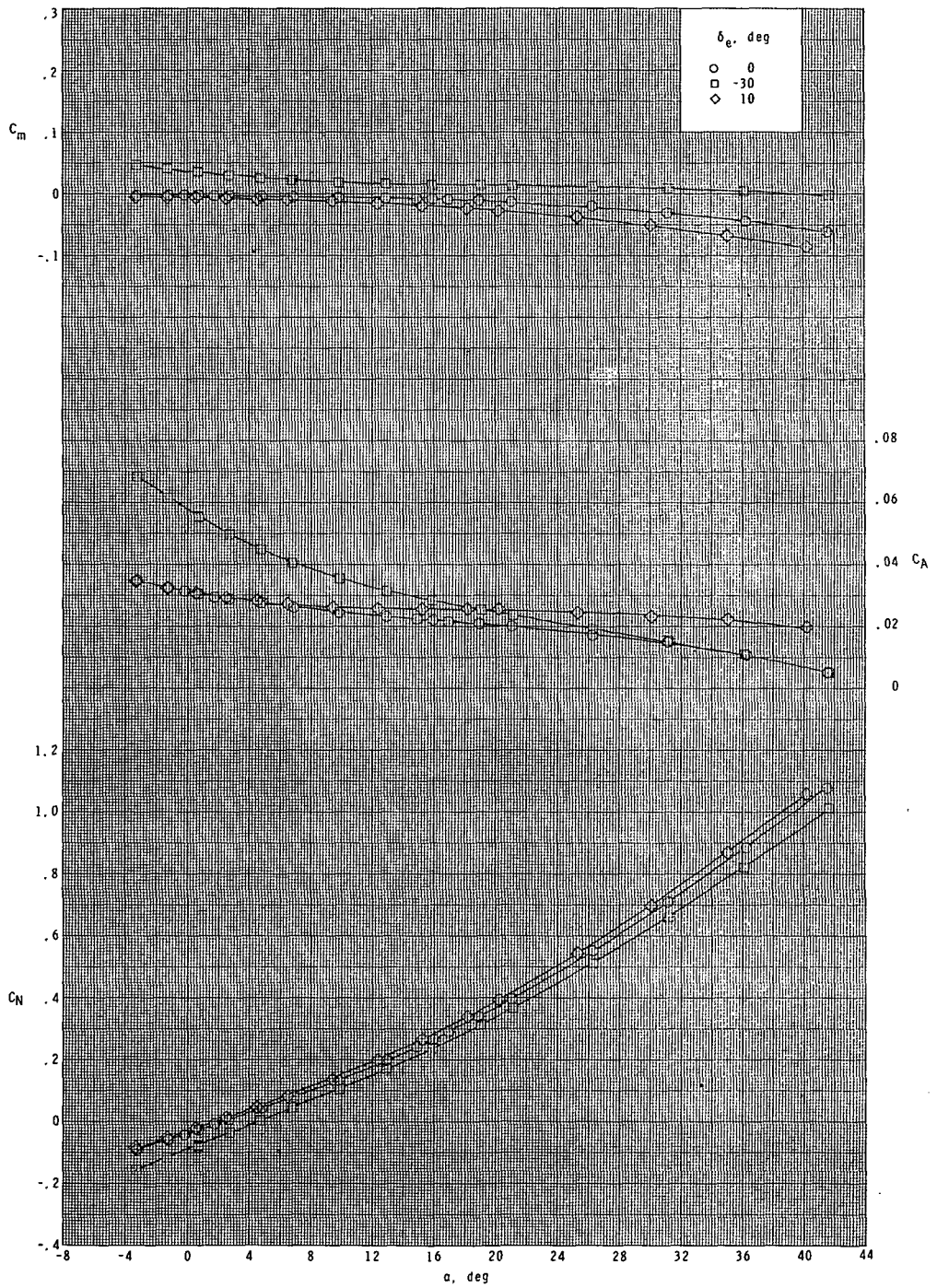

(c) M = 4.60.

Figure 6.- Continued.

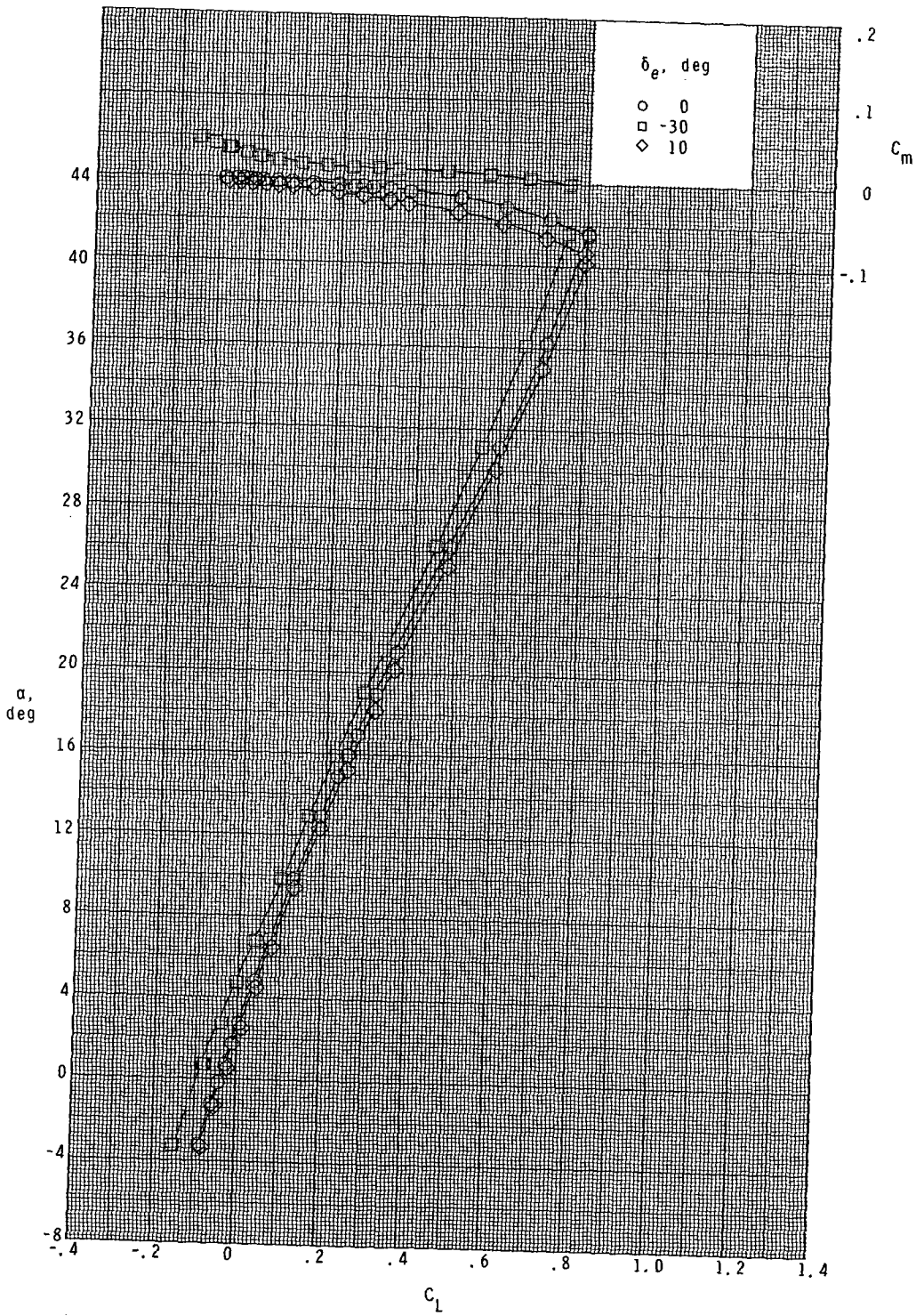

(c) Continued.

Figure 6.- Continued.

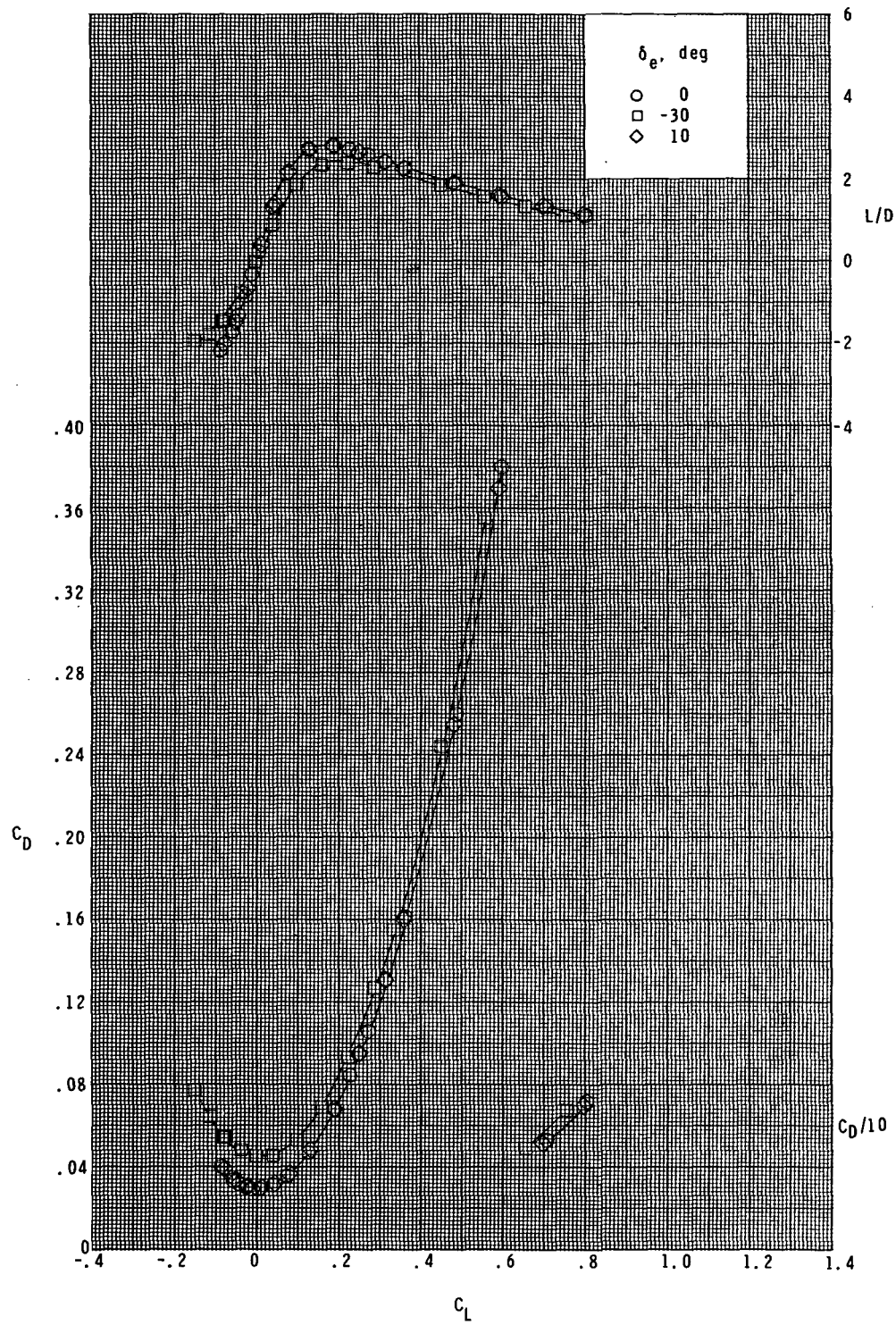

(c) Concluded.

Figure 6.- Concluded.

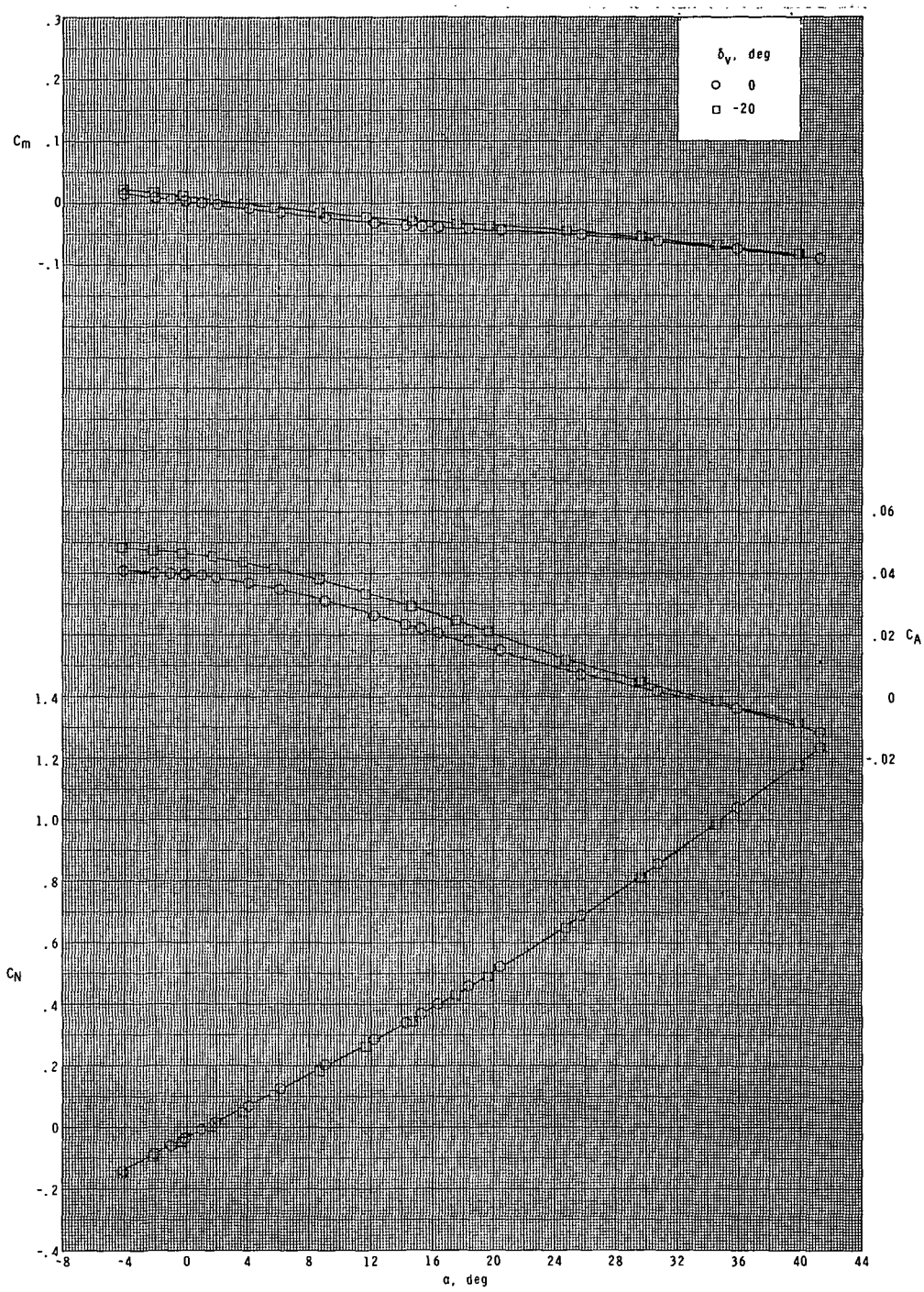

(a) M = 2.50.

Figure 7.- Effect of rudder deflection on longitudinal aerodynamic characteristics.

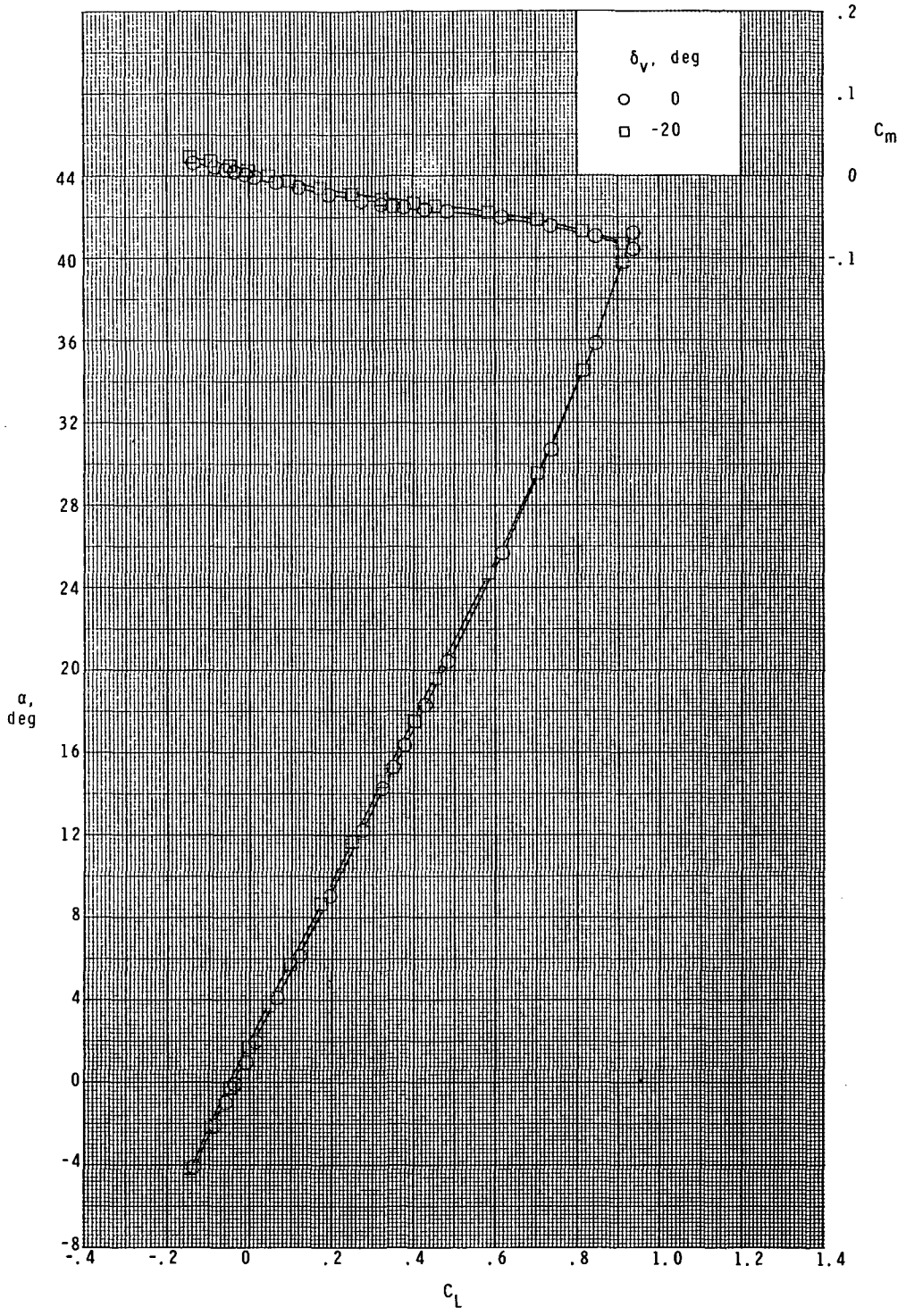

(a) Continued.

Figure 7.- Continued.

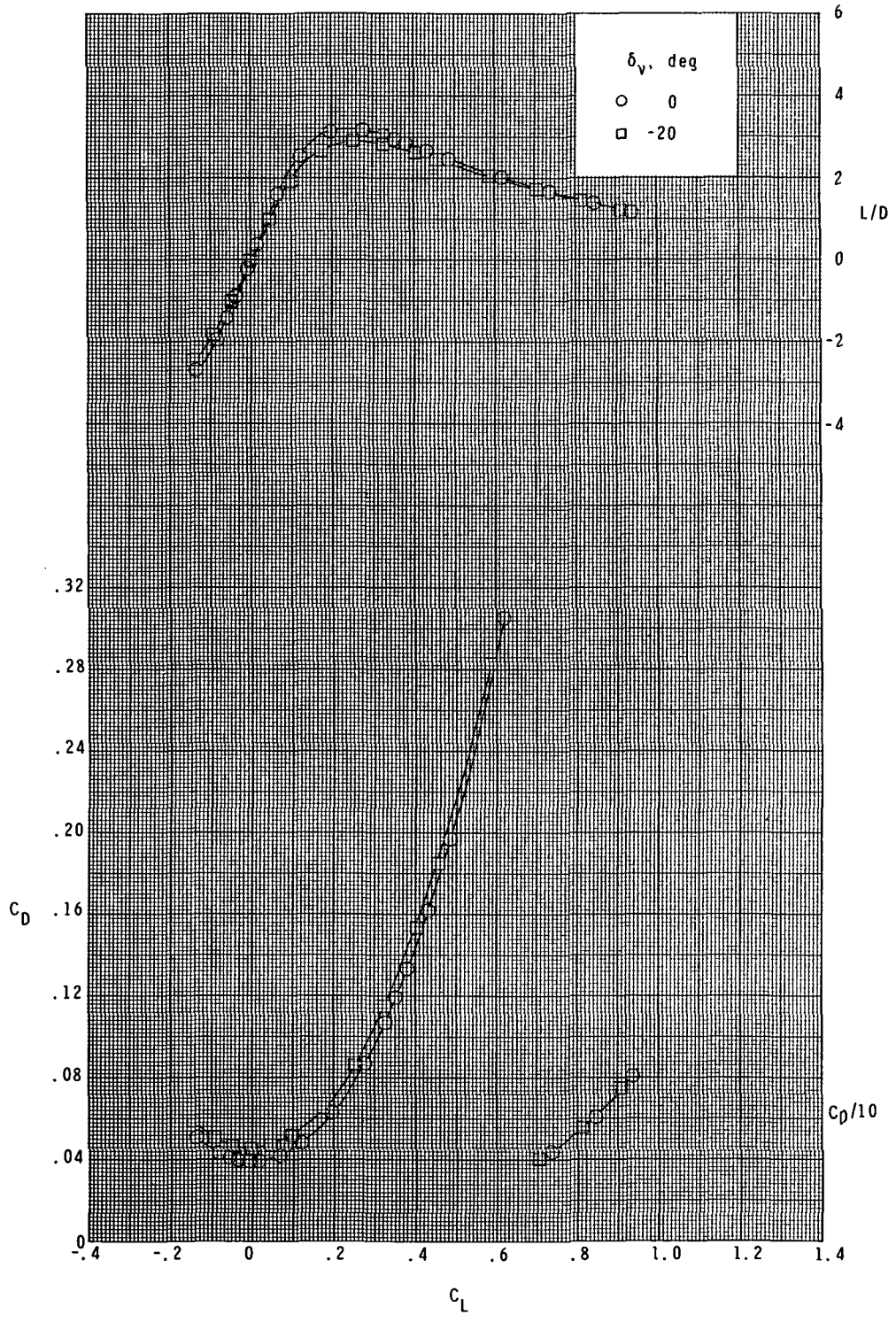

(a) Concluded.

Figure 7.- Continued.

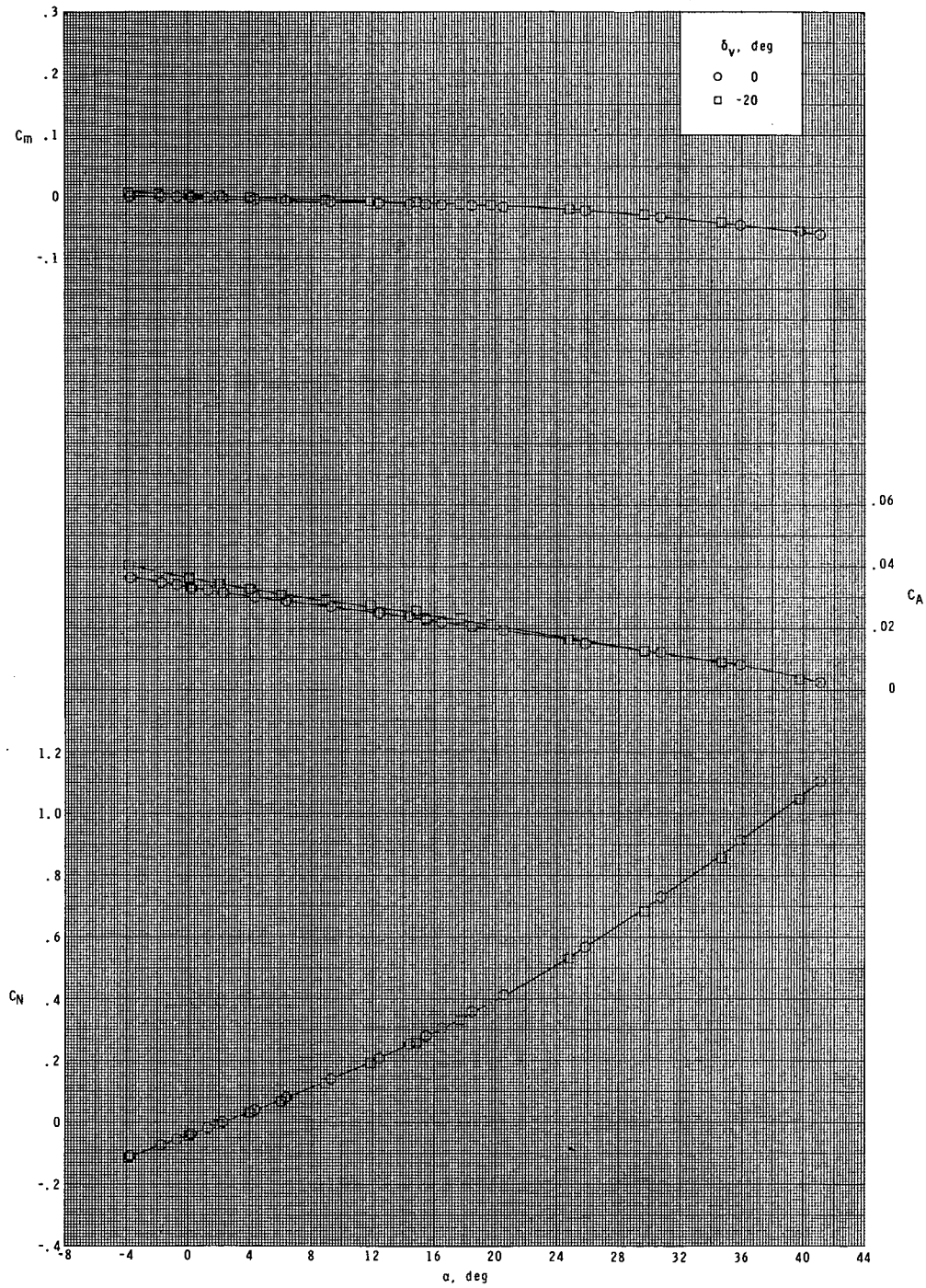

(b) M = 3.90.

Figure 7.- Continued.

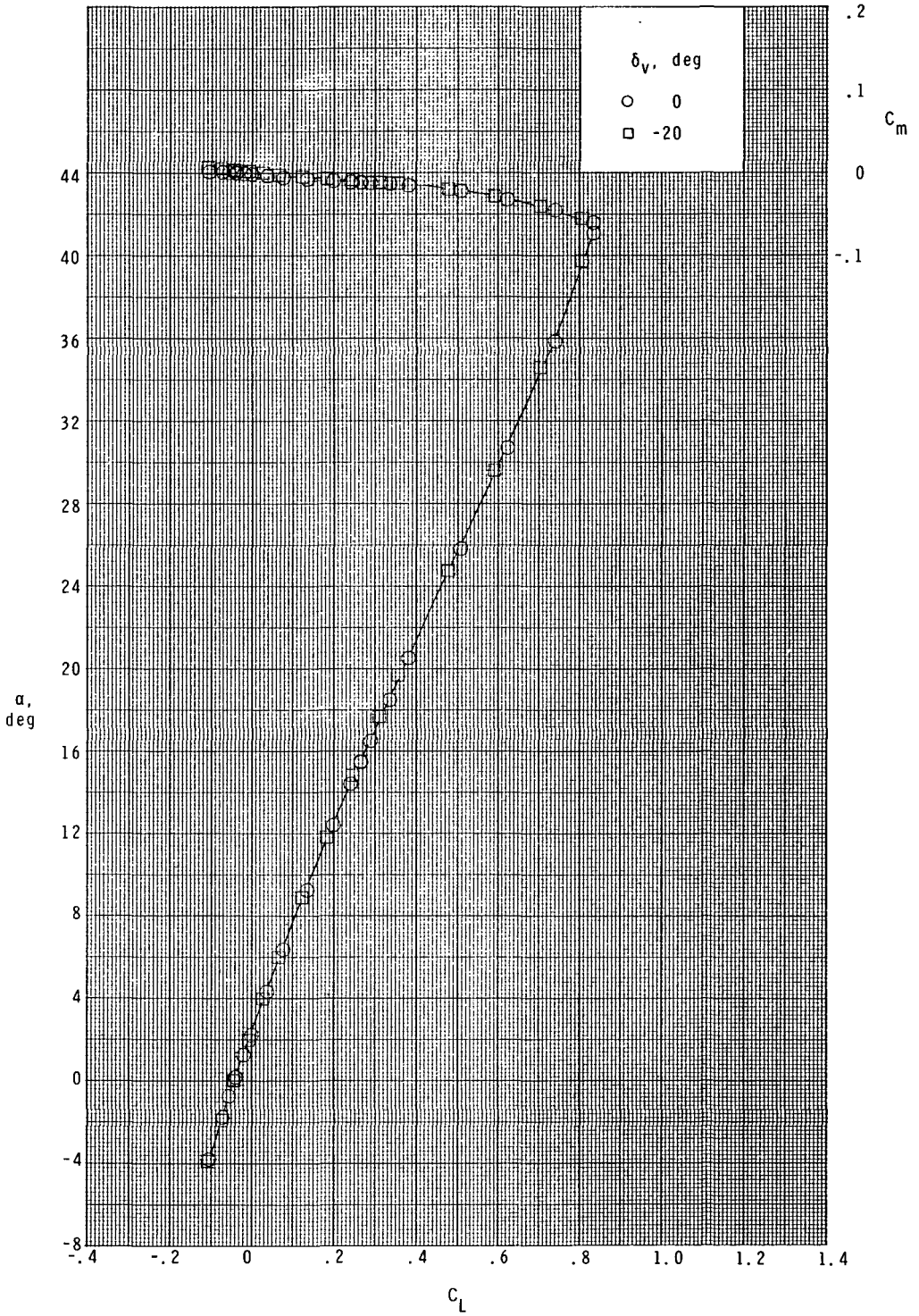

(b) Continued.

Figure 7.- Continued.

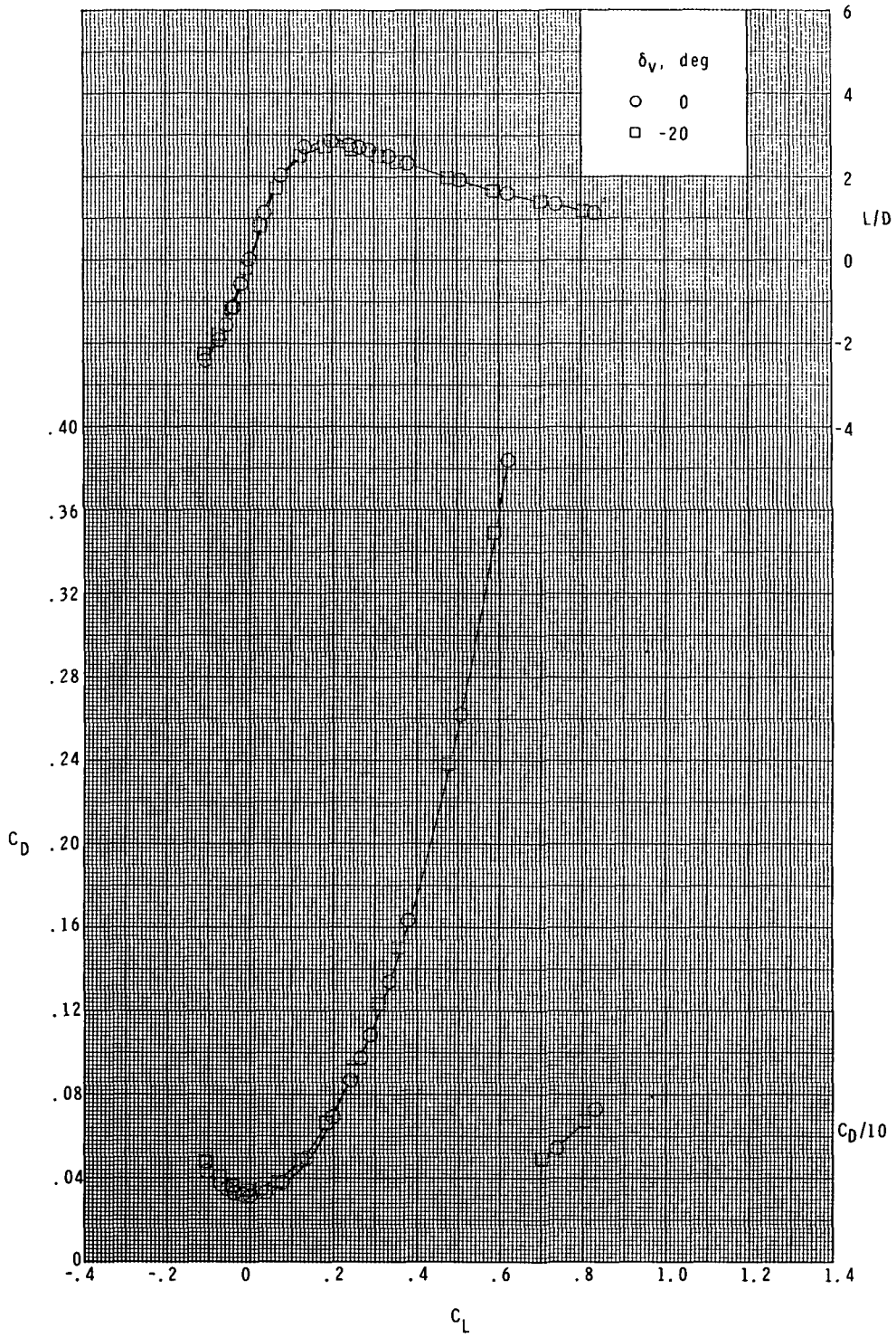

(b) Concluded.

Figure 7.- Continued.

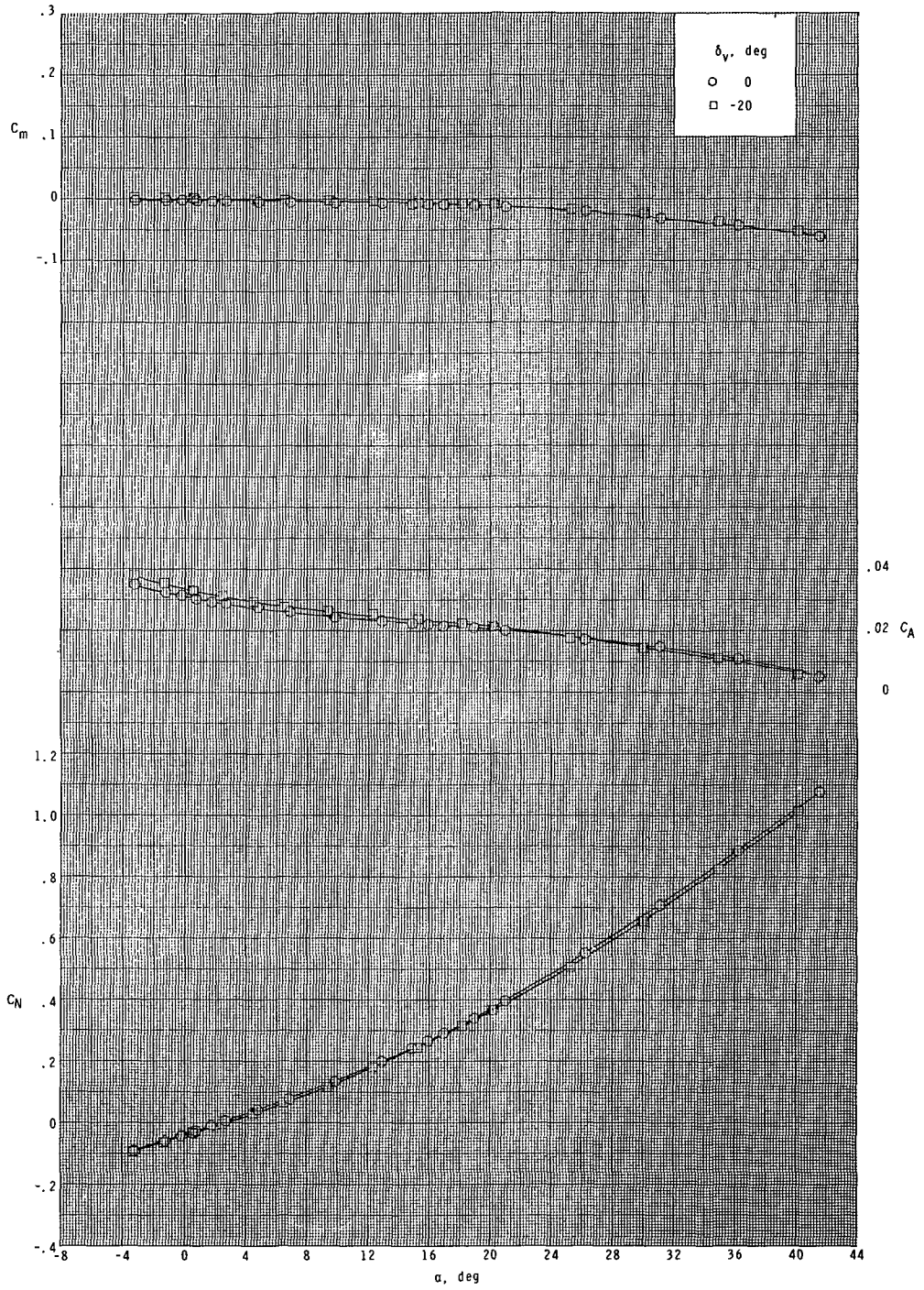

(c) M = 4.60.

Figure 7.- Continued.

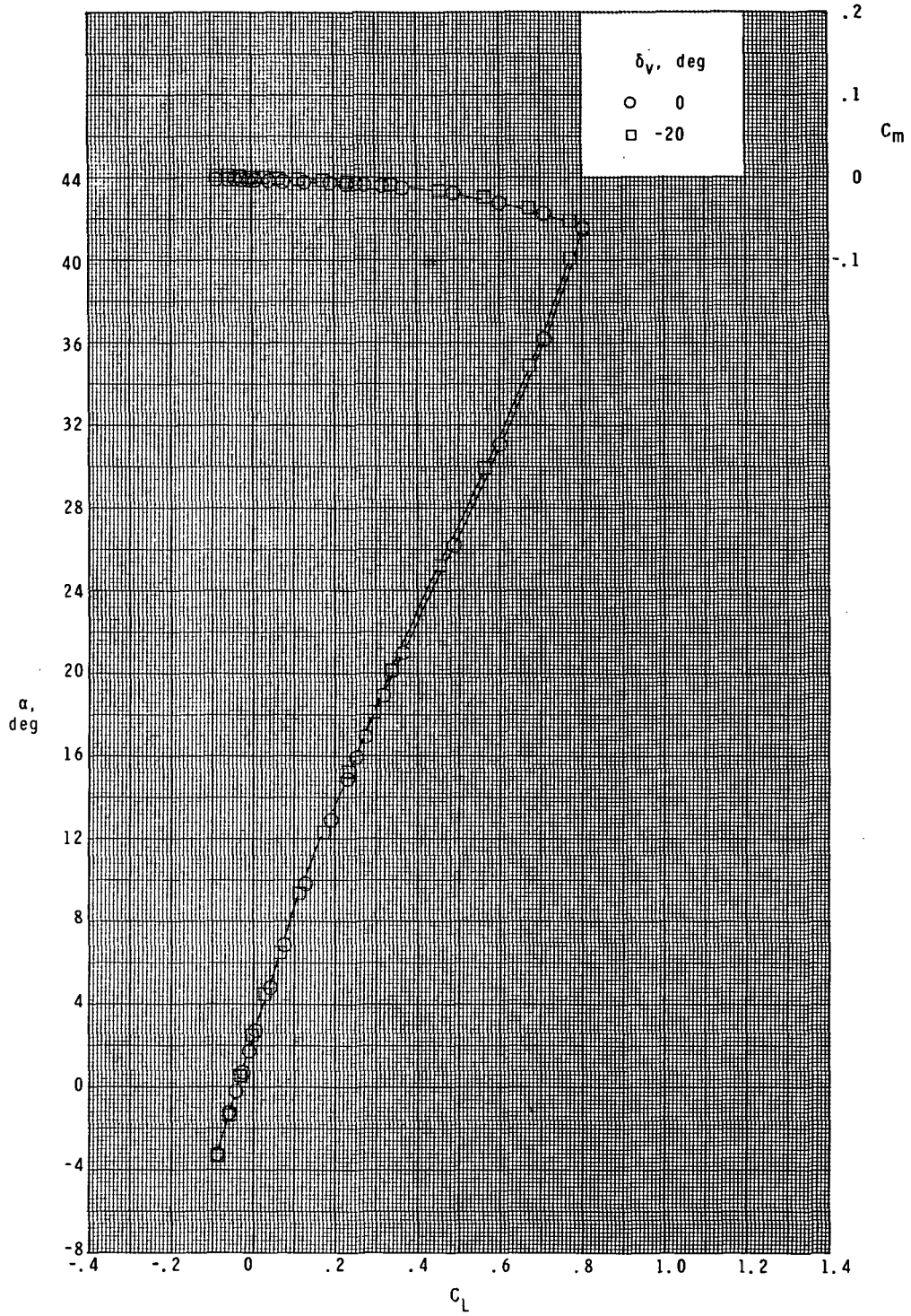

(c) Continued.

Figure 7.- Continued.

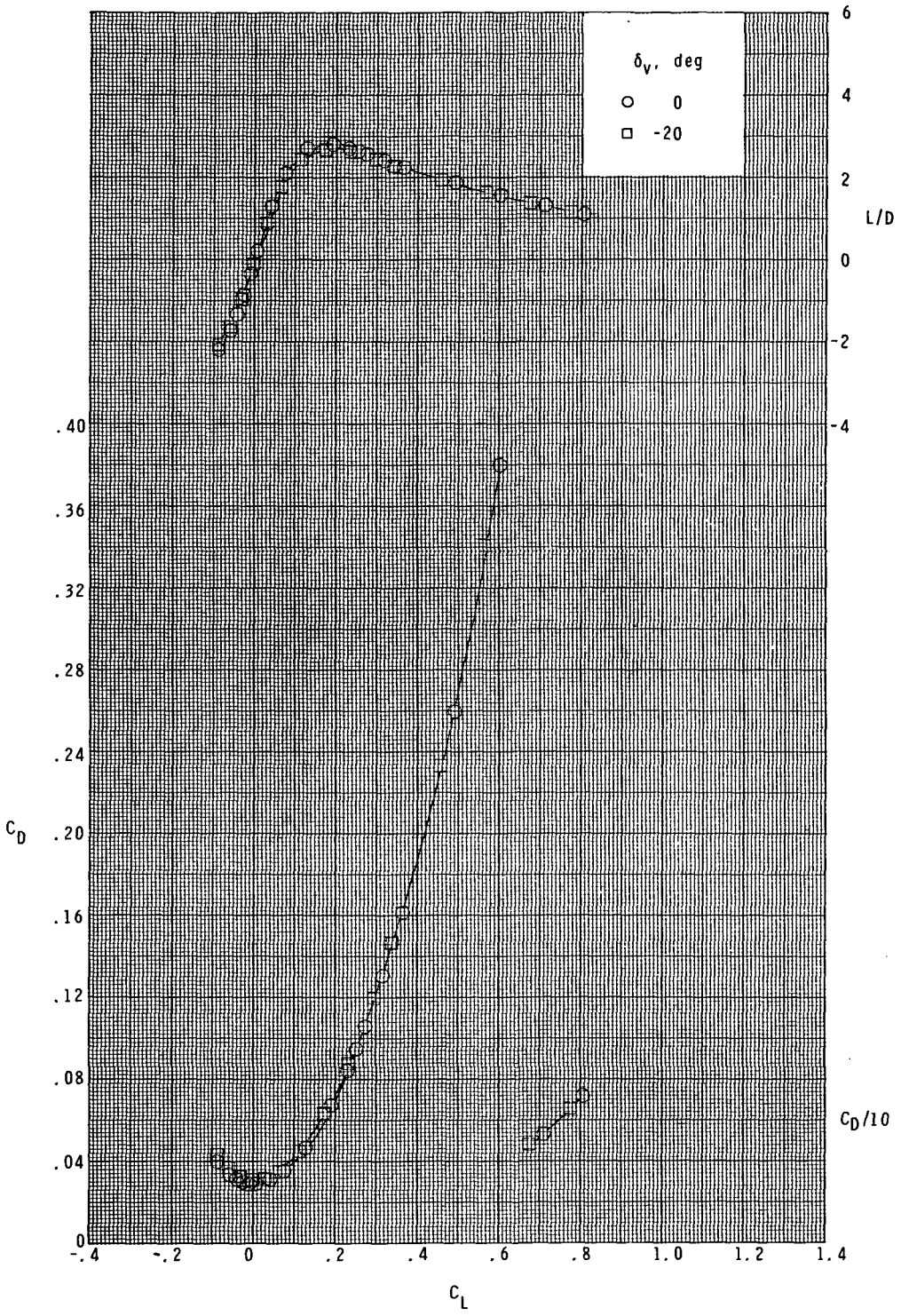

(c) Concluded.

Figure 7.- Concluded.

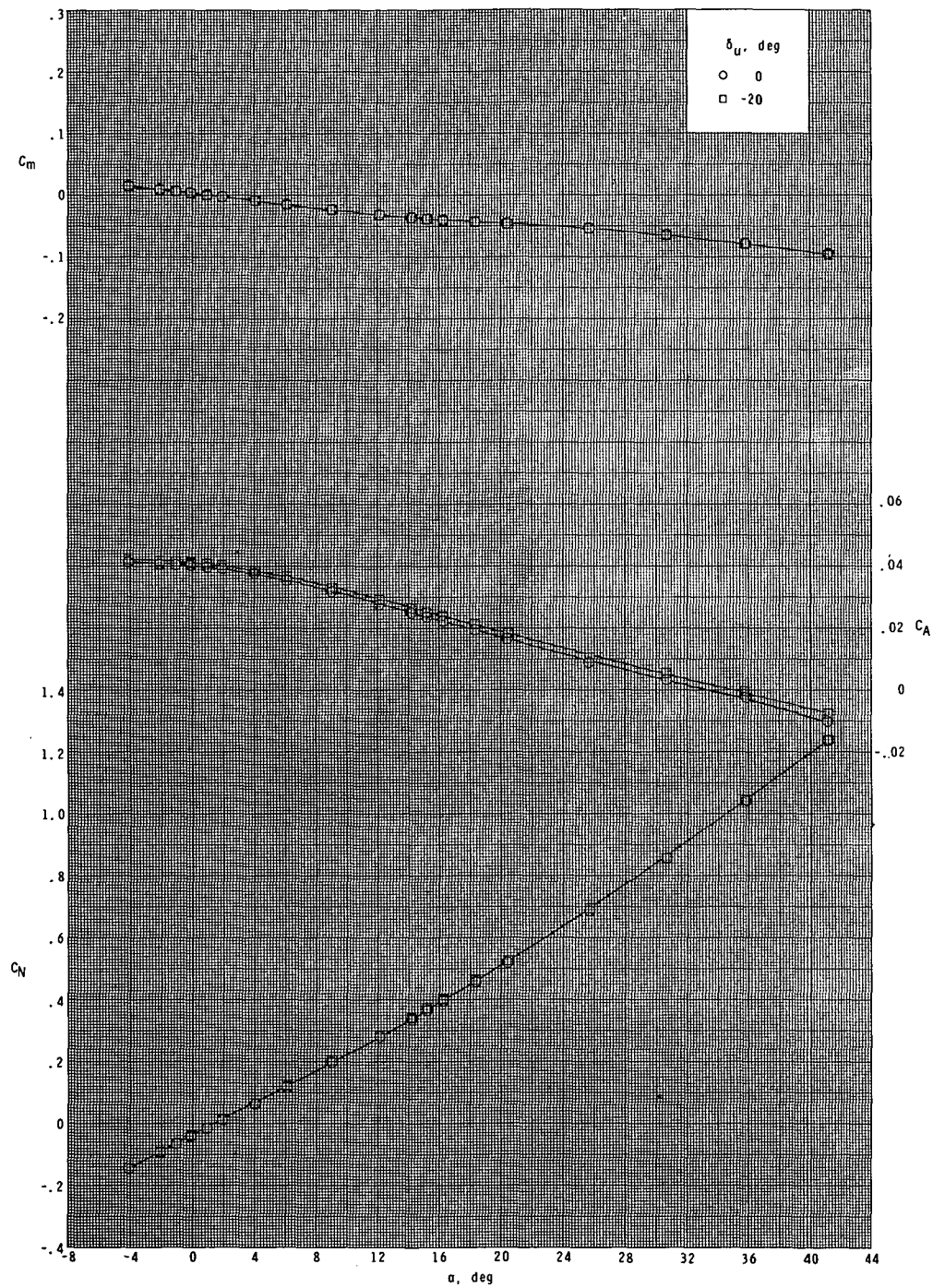

(a) M = 2.50.

Figure 8.- Effect of ventral-fin deflection on longitudinal aerodynamic characteristics.

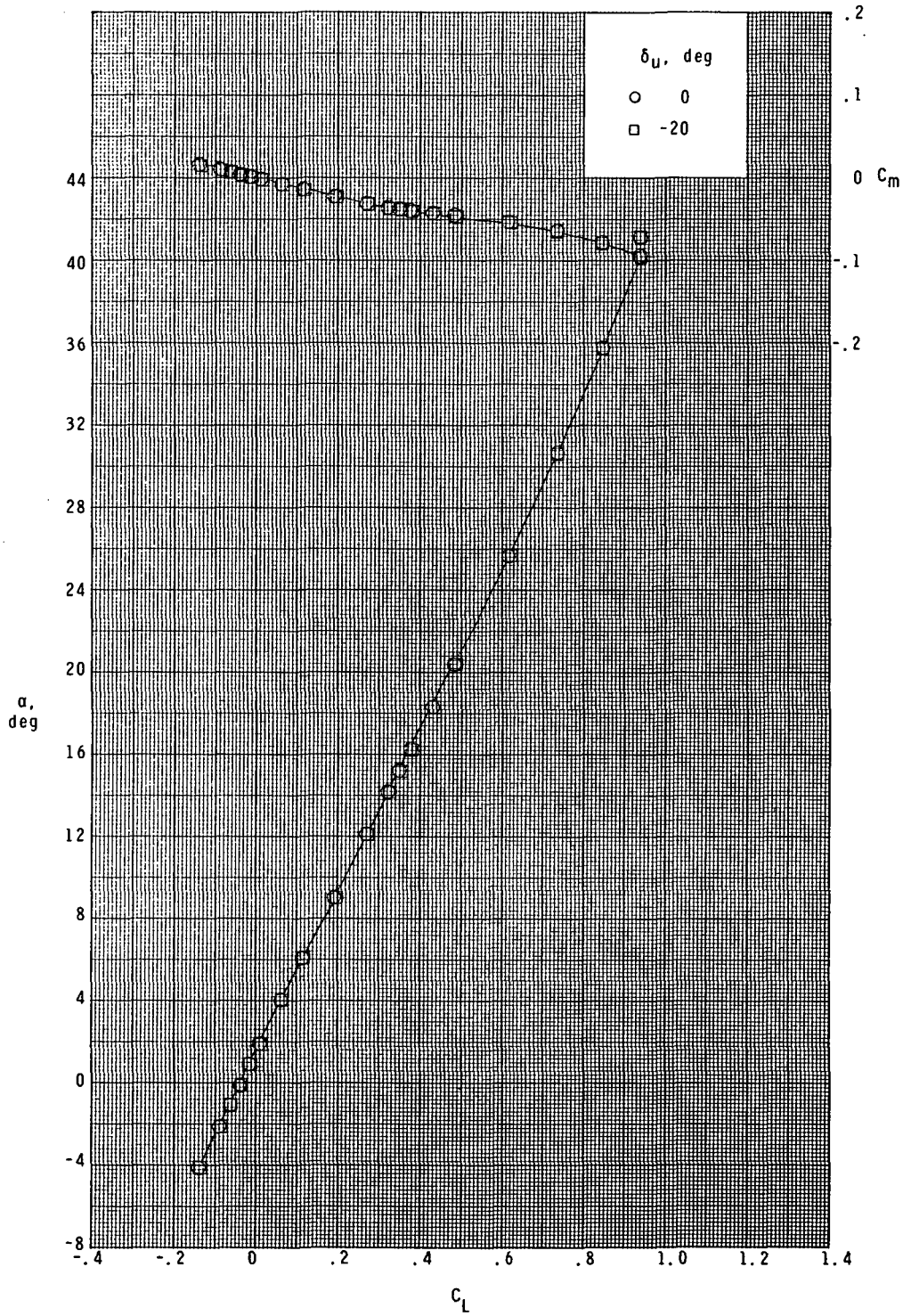

(a) Continued.

Figure 8.- Continued.

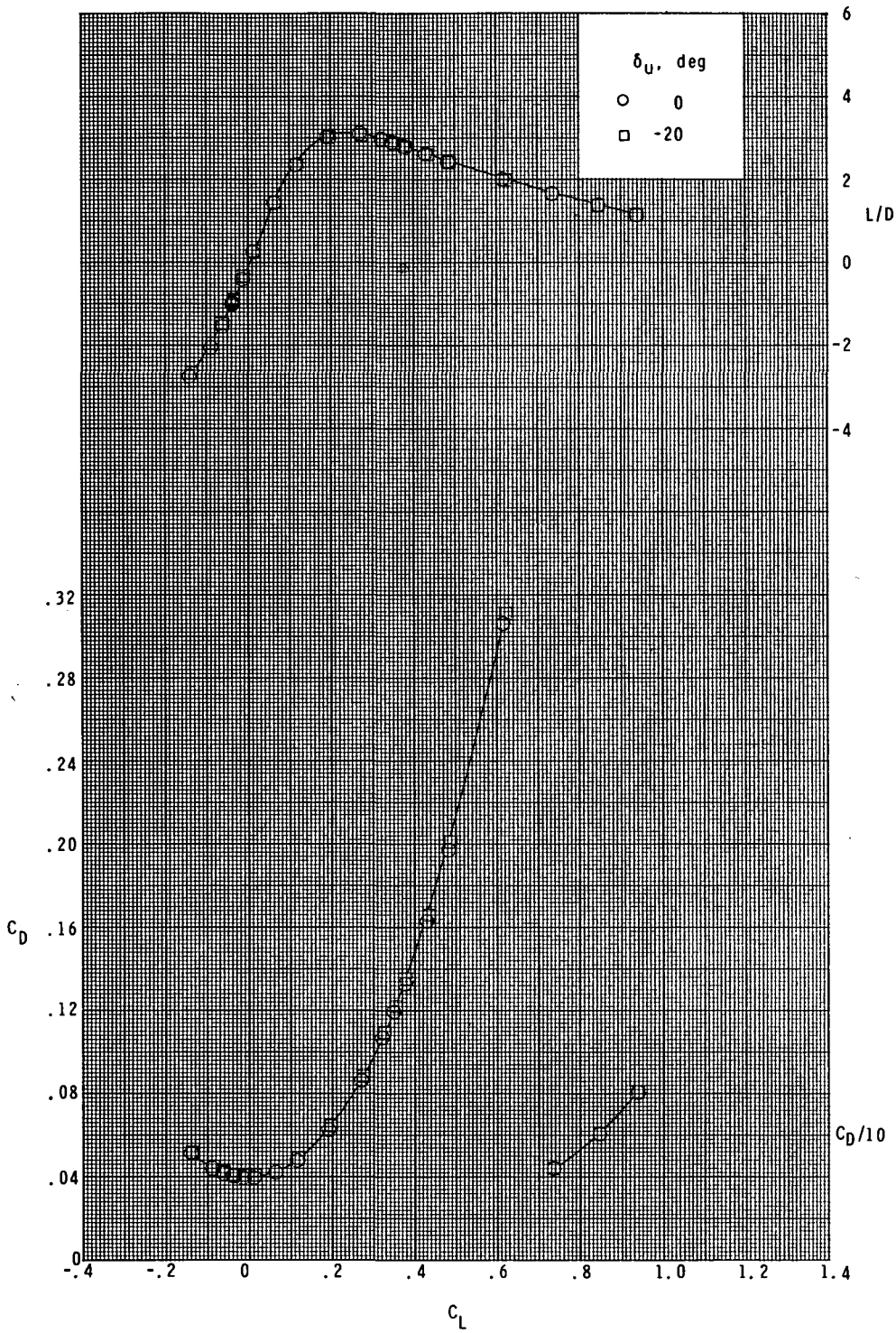

(a) Concluded.

Figure 8.- Continued.

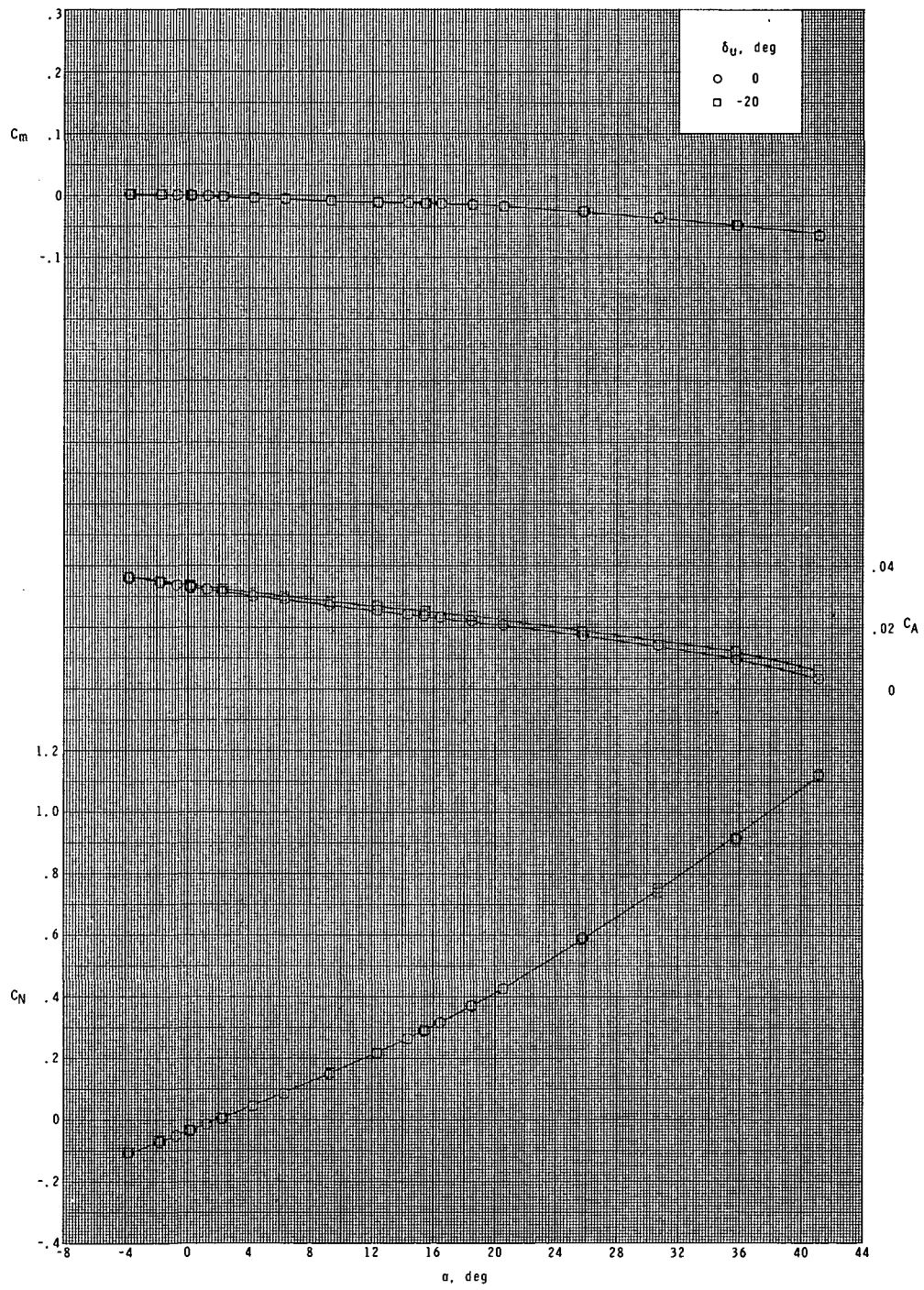

(b) M = 3.90.

Figure 8.- Continued.

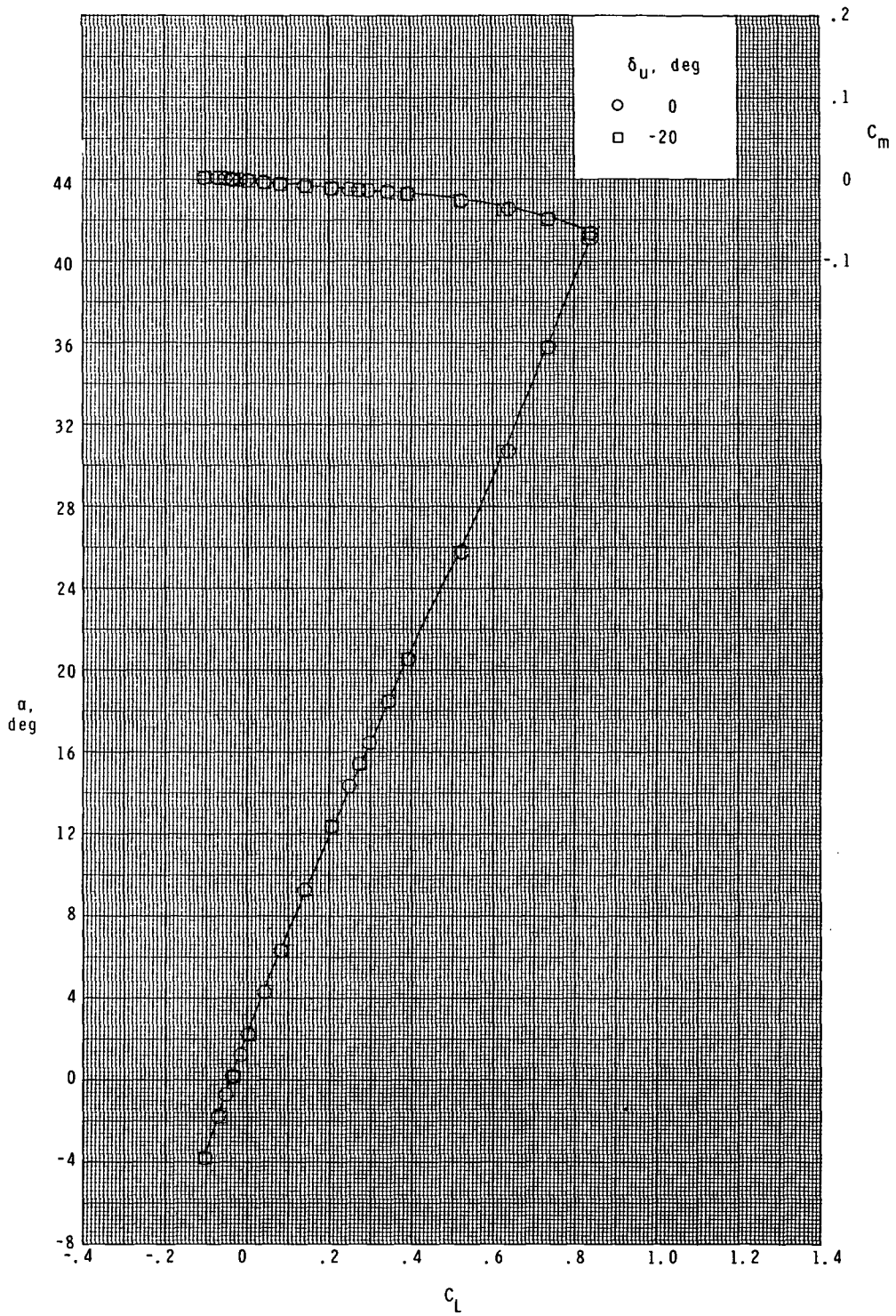

(b) Continued.

Figure 8.- Continued.

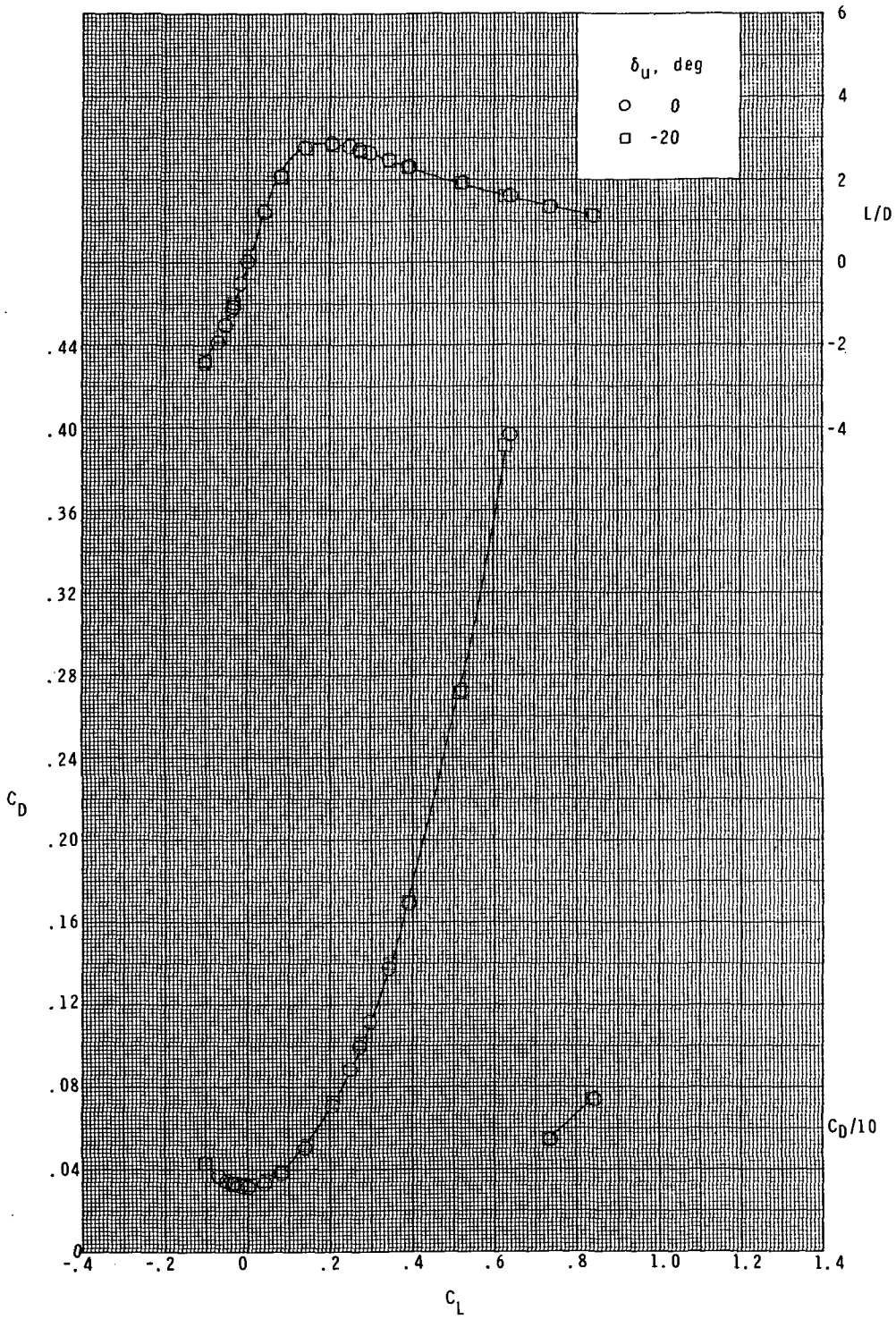

(b) Concluded.

Figure 8.- Continued.

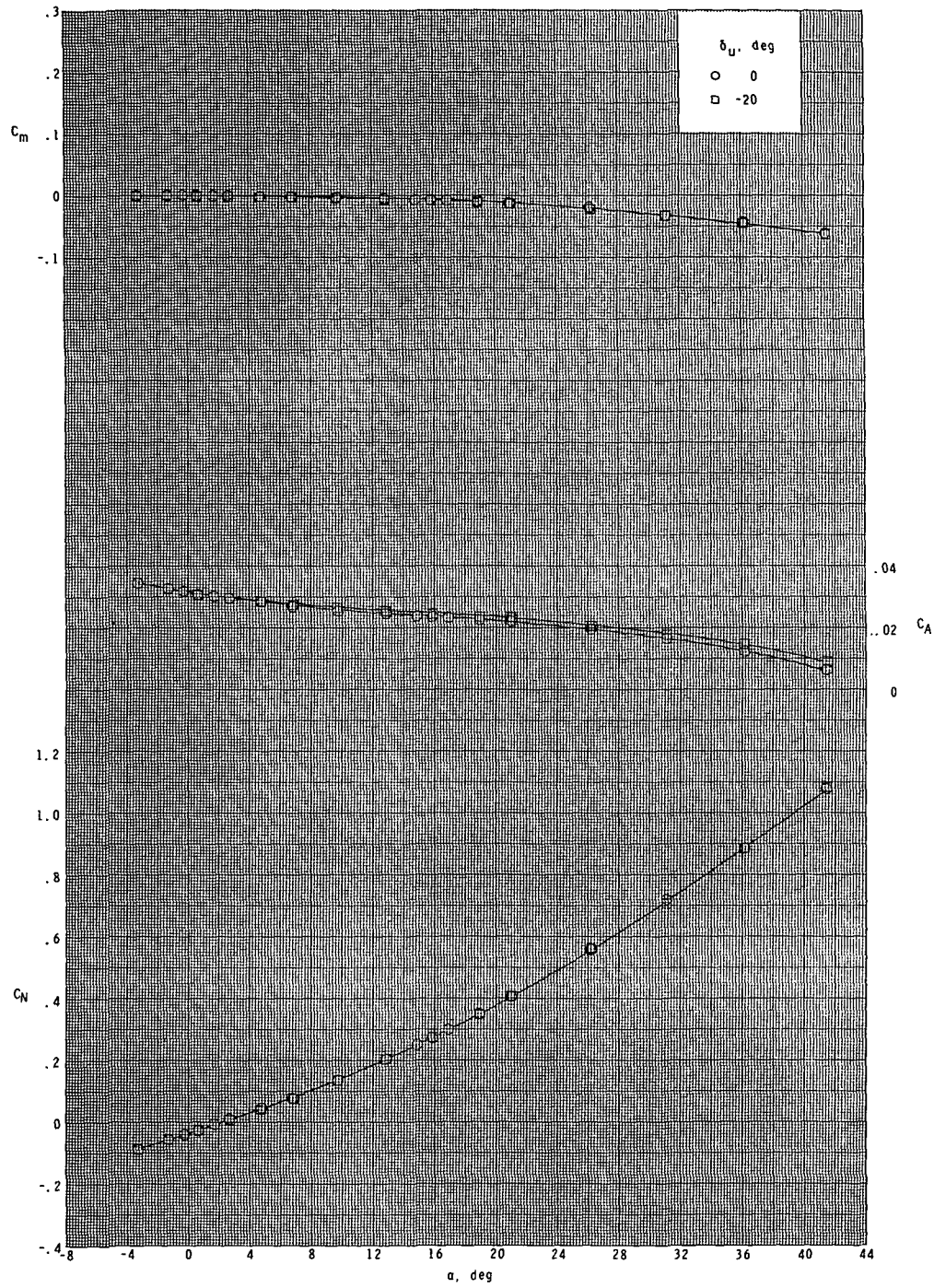

(c) M = 4.60.

Figure 8.- Continued.

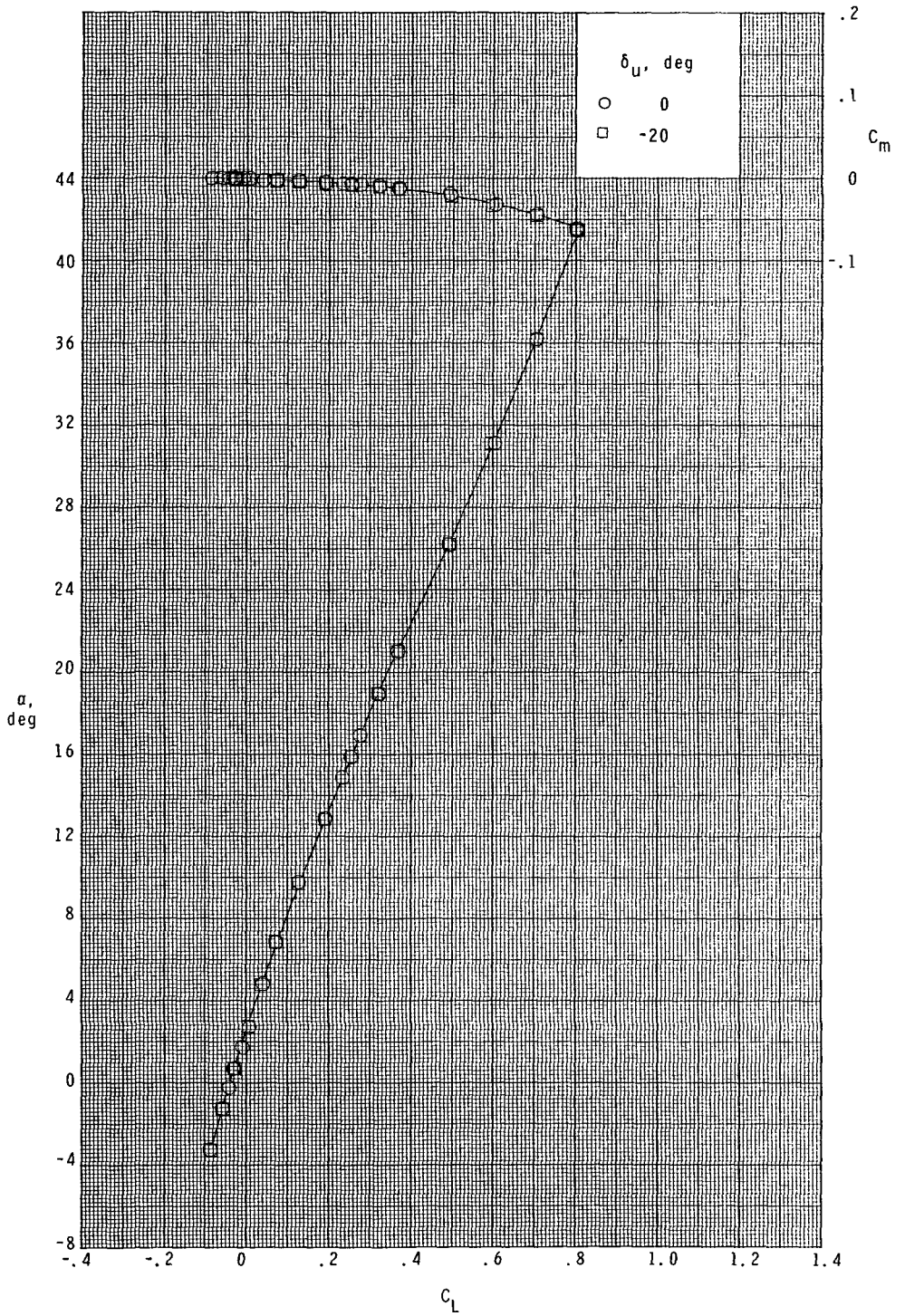

(c) Continued.

Figure 8.- Continued.

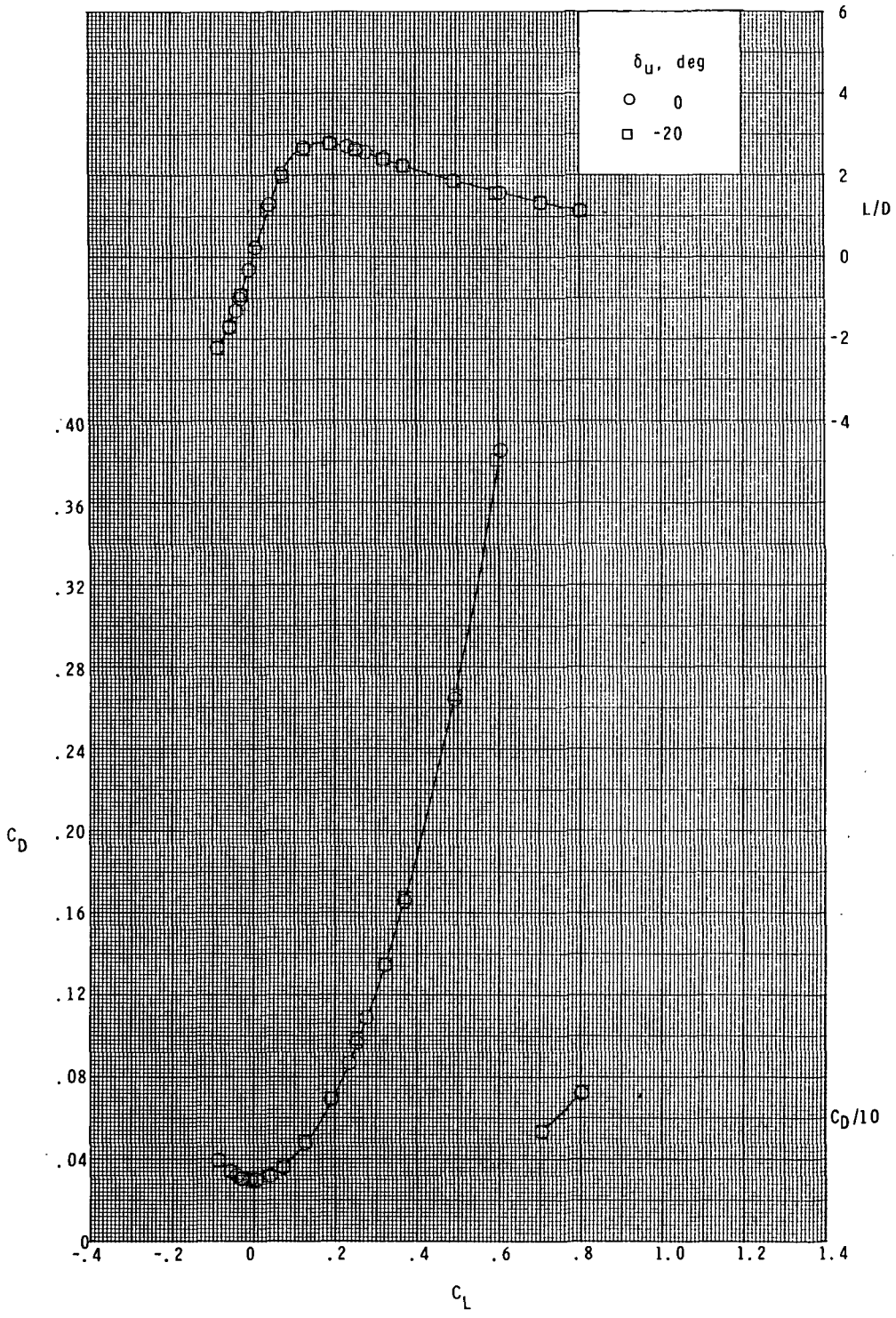

(c) Concluded.

Figure 8.- Concluded.

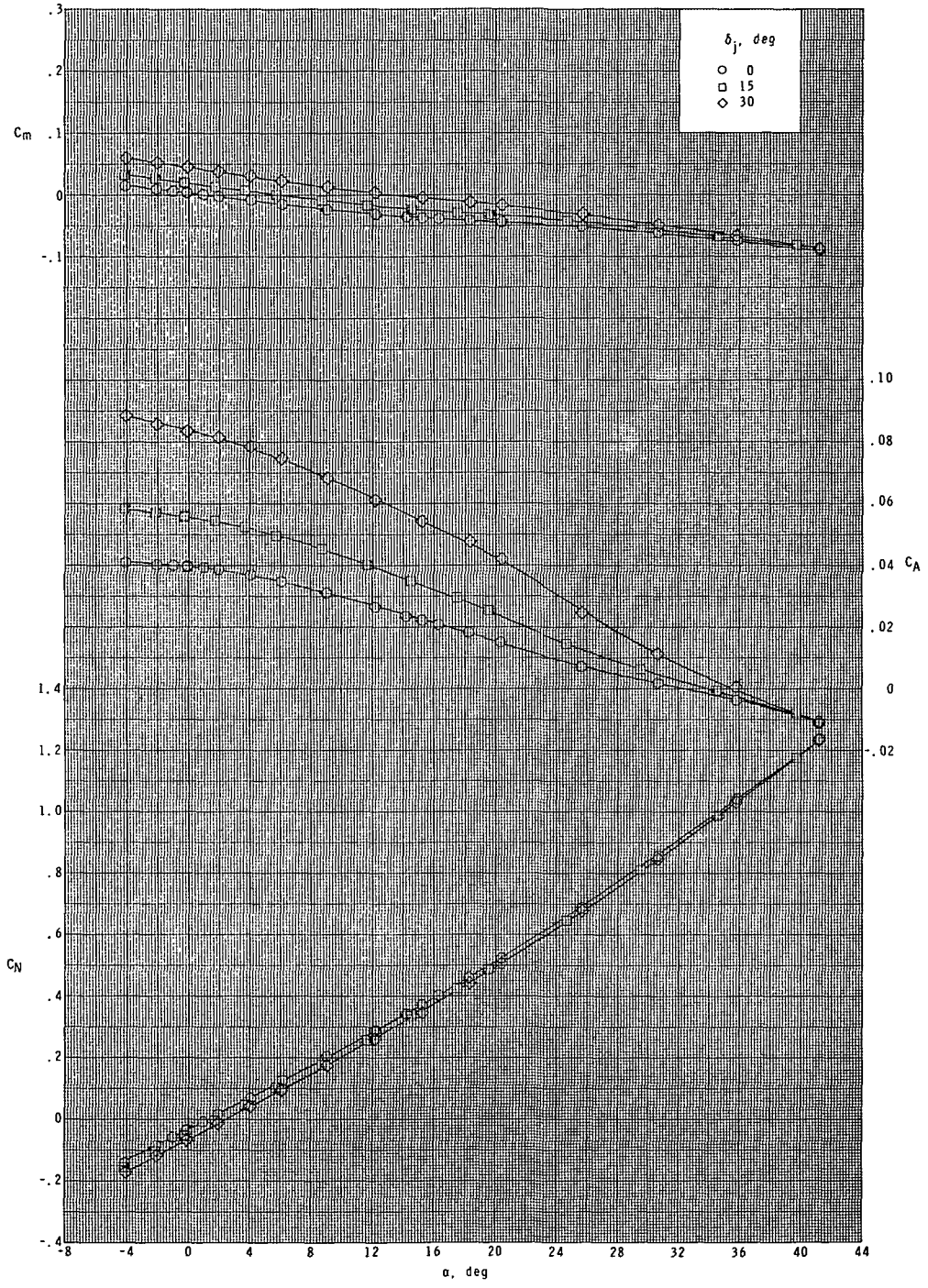

(a) M = 2.50.

Figure 9.- Effect of rudder flare deflection on longitudinal aerodynamic characteristics. $\delta_v = 0^o$.

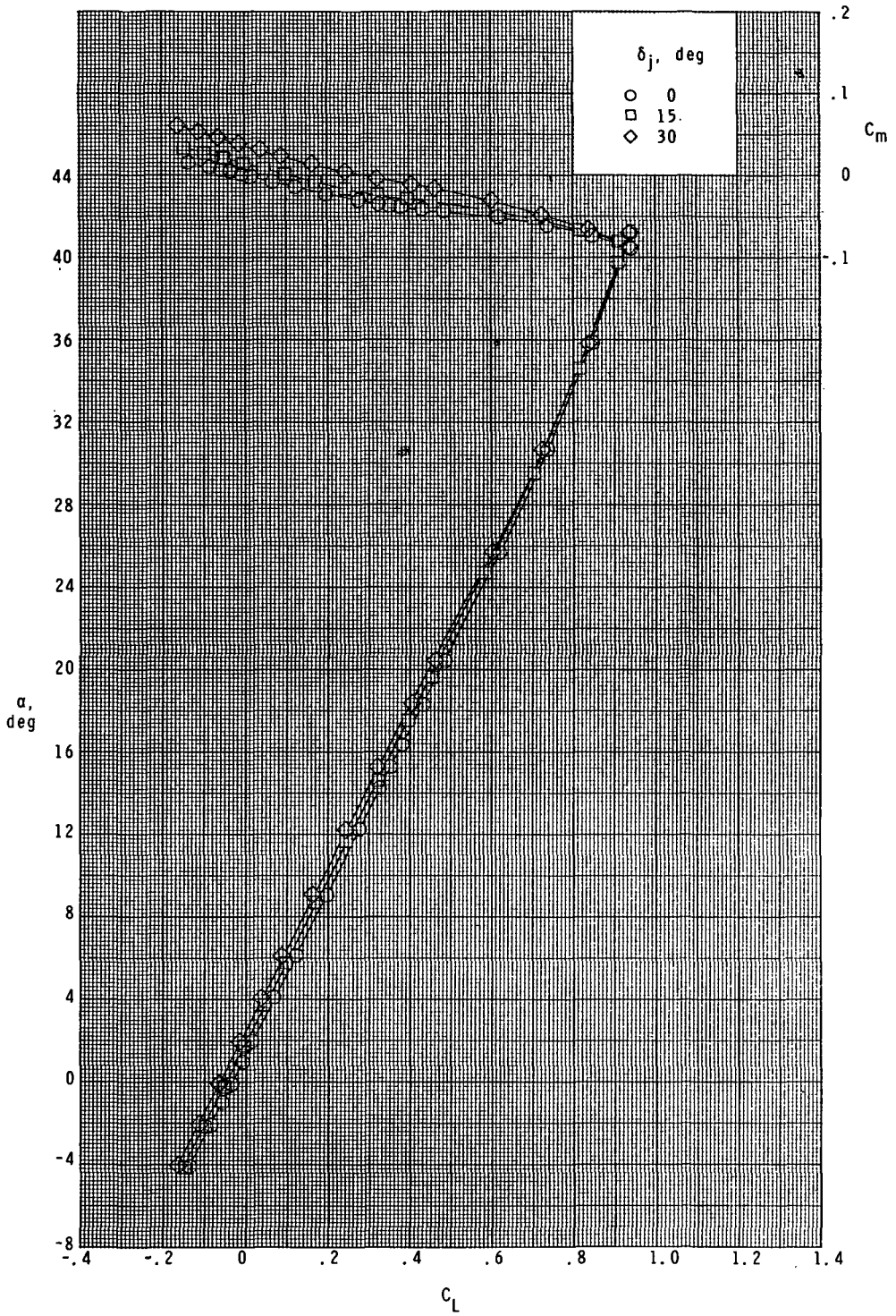

(a) Continued.

Figure 9.- Continued.

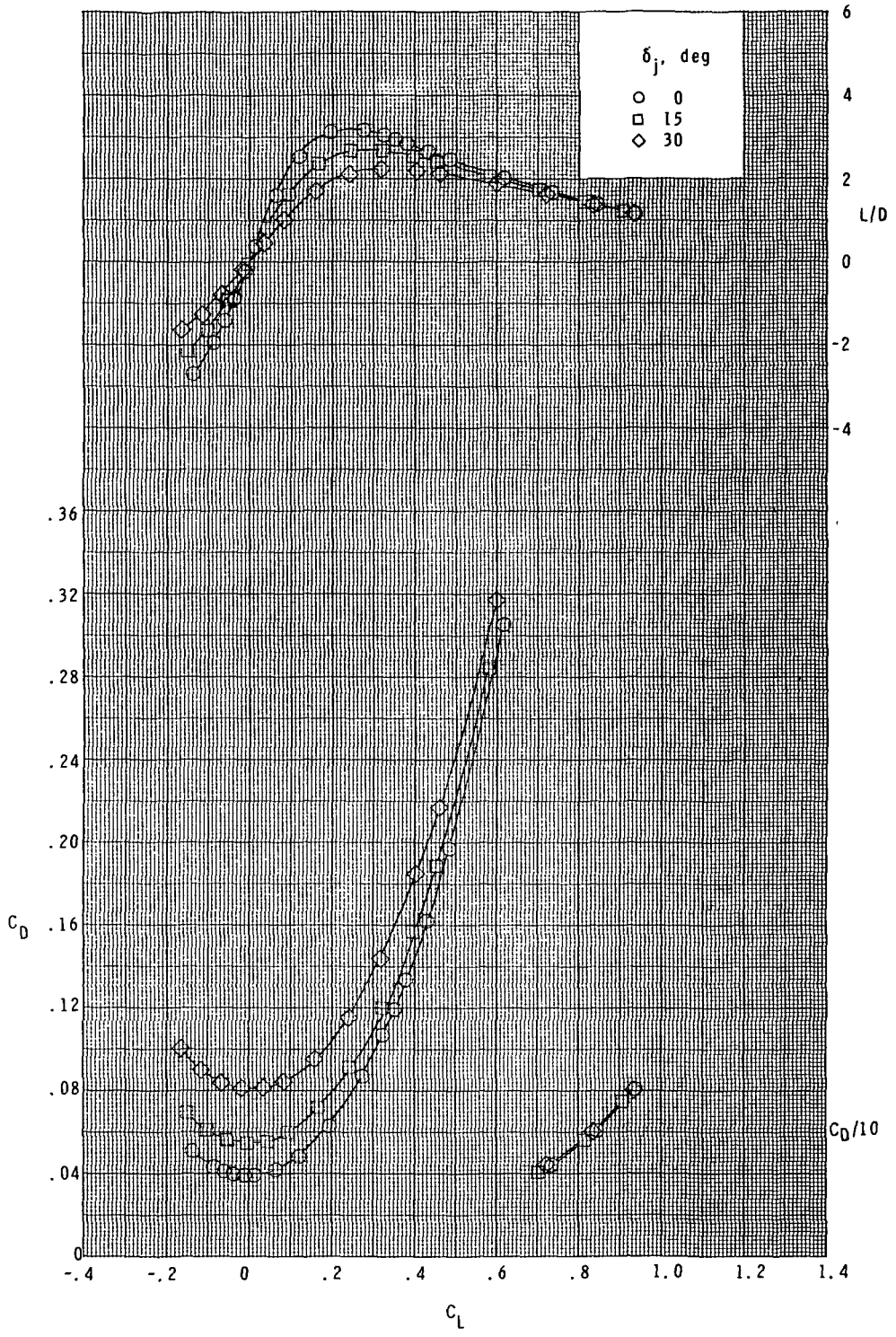

(a) Concluded.

Figure 9.- Continued.

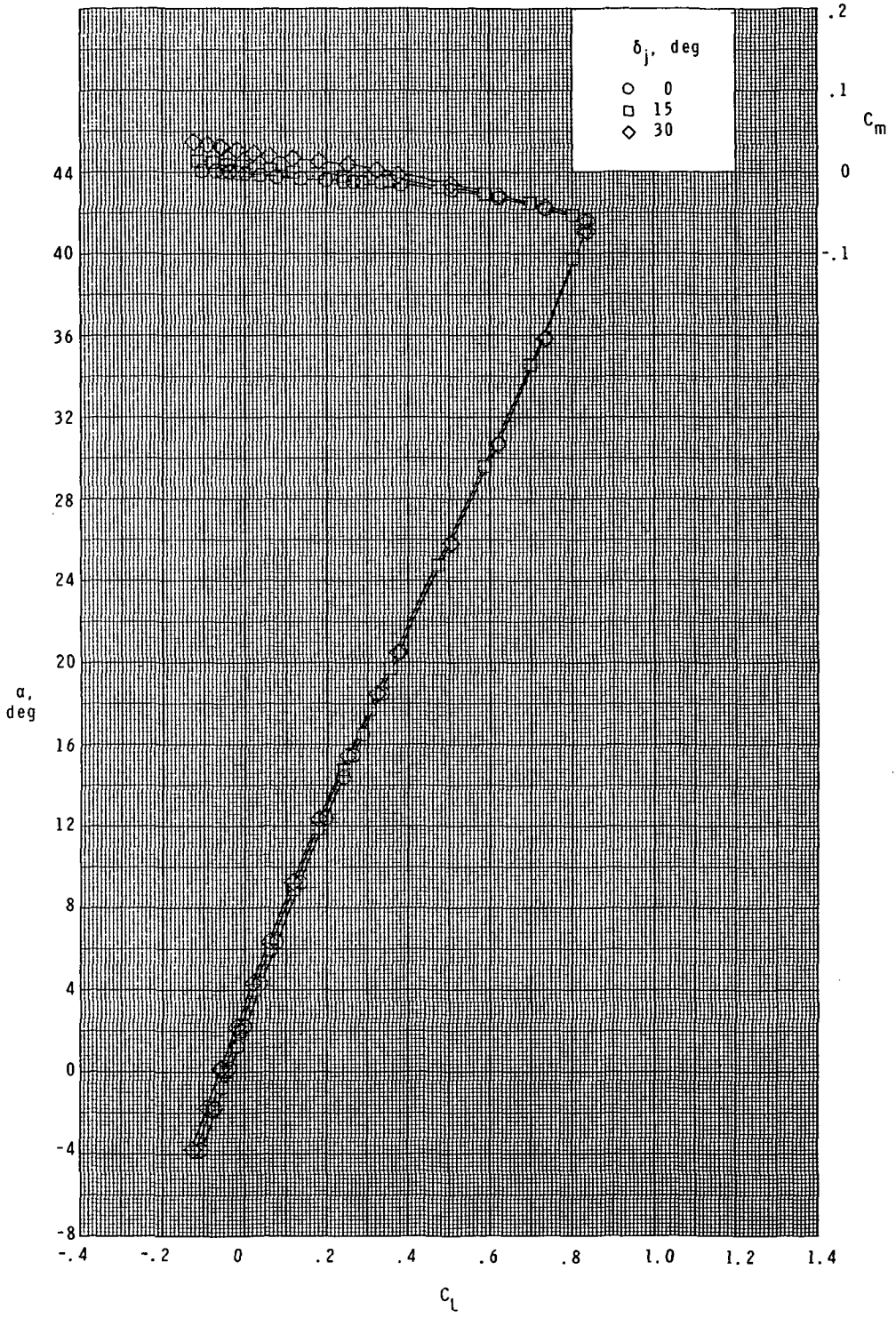

(b) Continued.

Figure 9.- Continued.

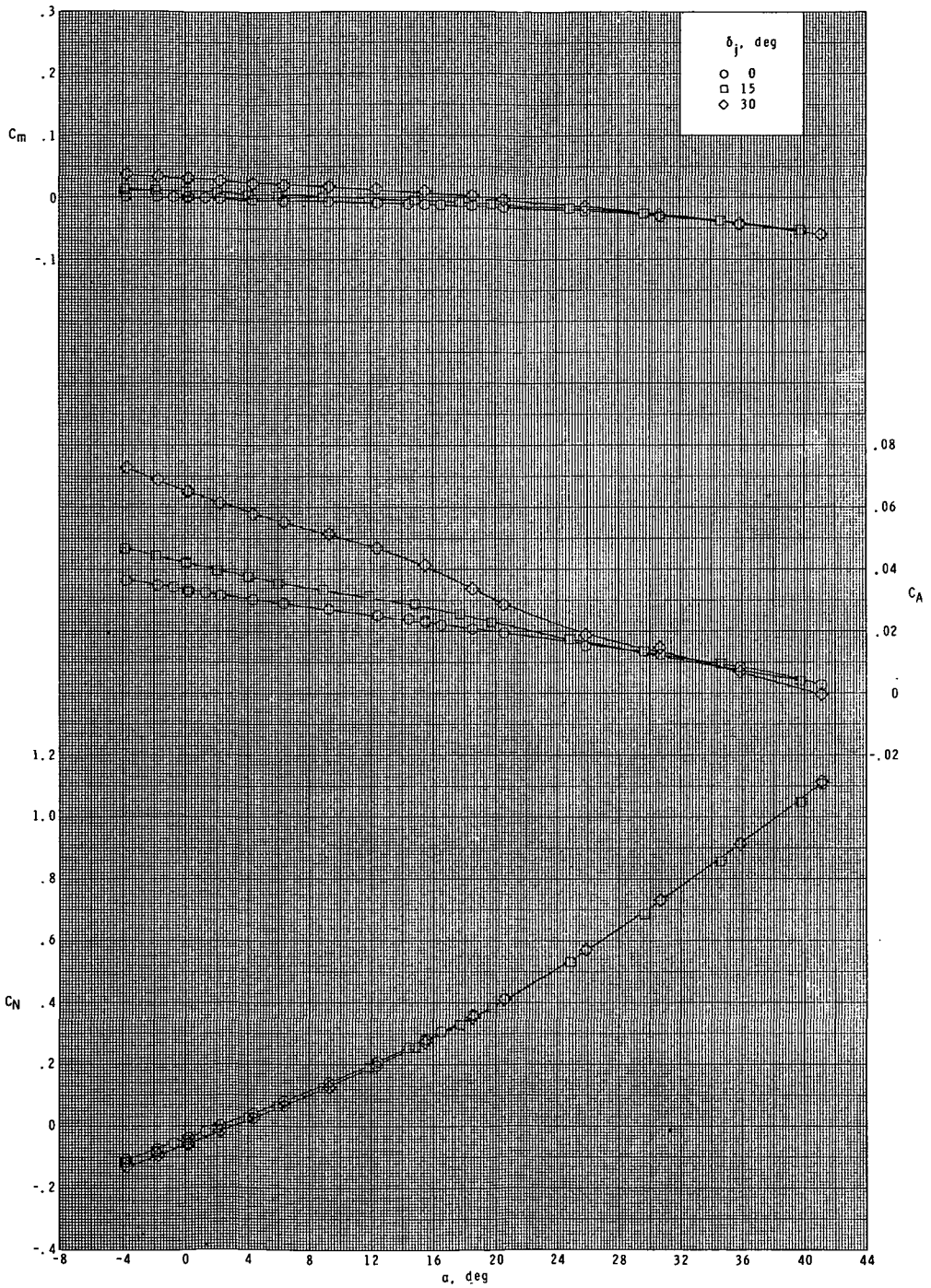

(b) M = 3.90.

Figure 9.- Continued.

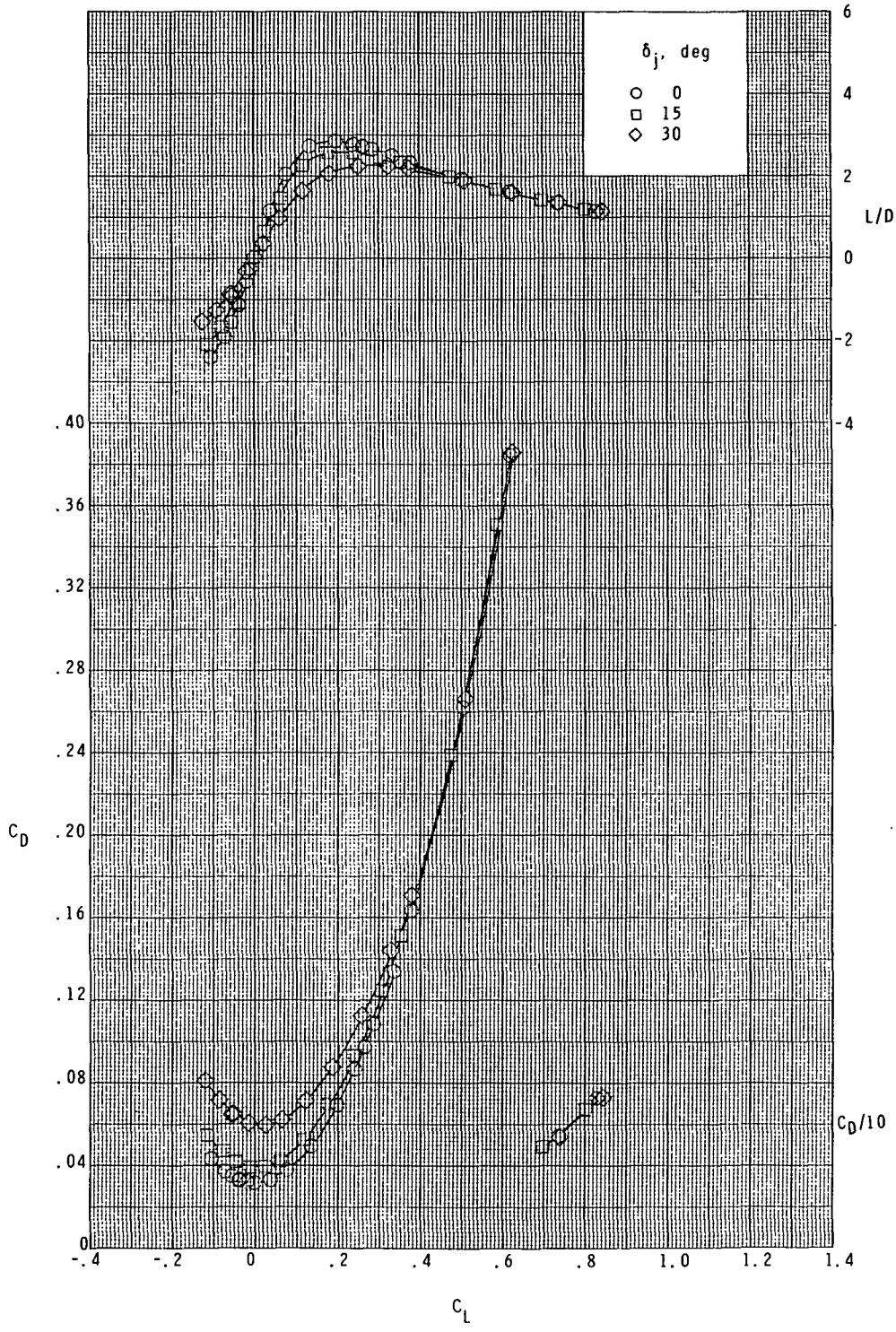

(b) Concluded.

Figure 9.- Continued.

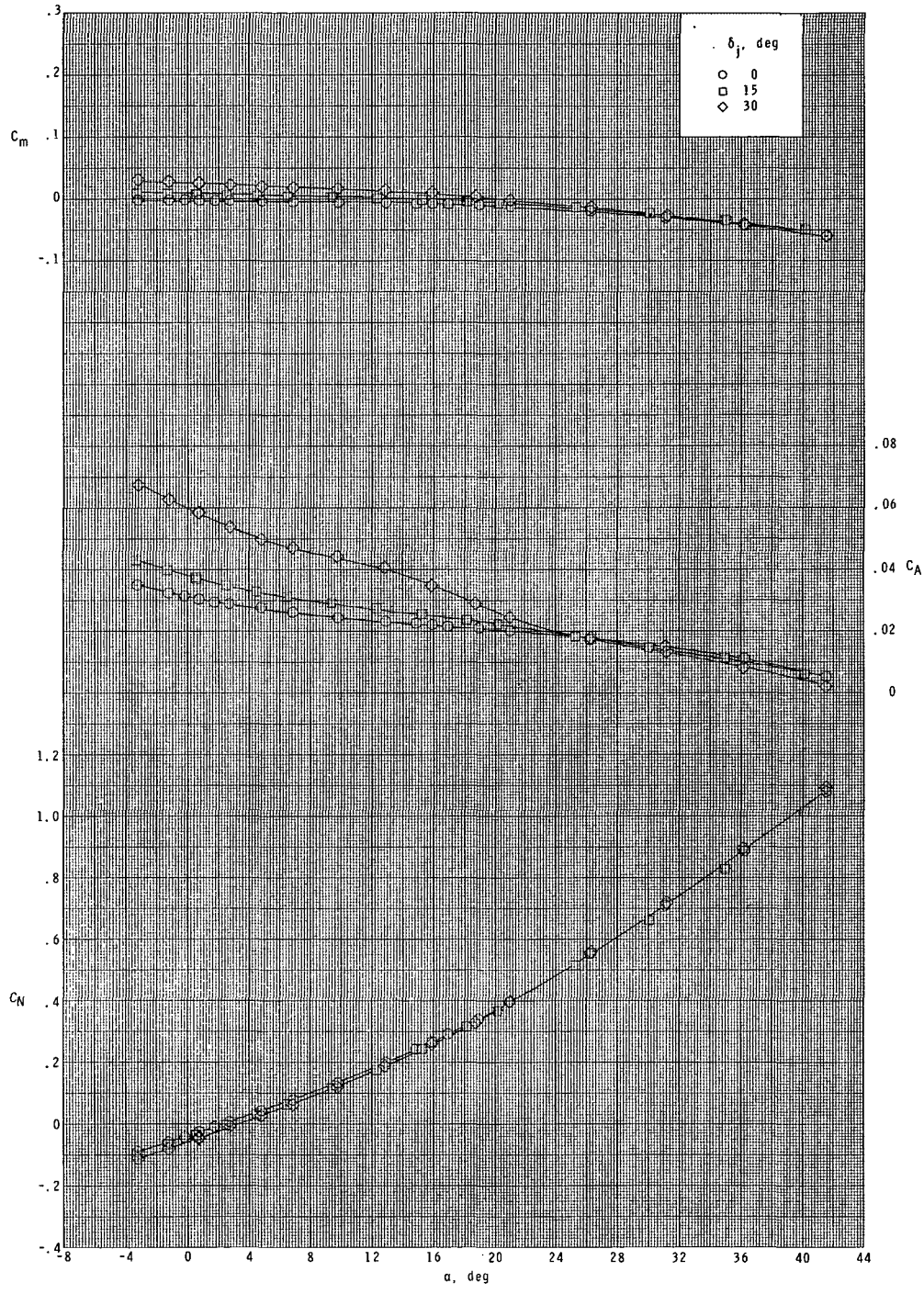

(c) M = 4.60.

Figure 9.- Continued.

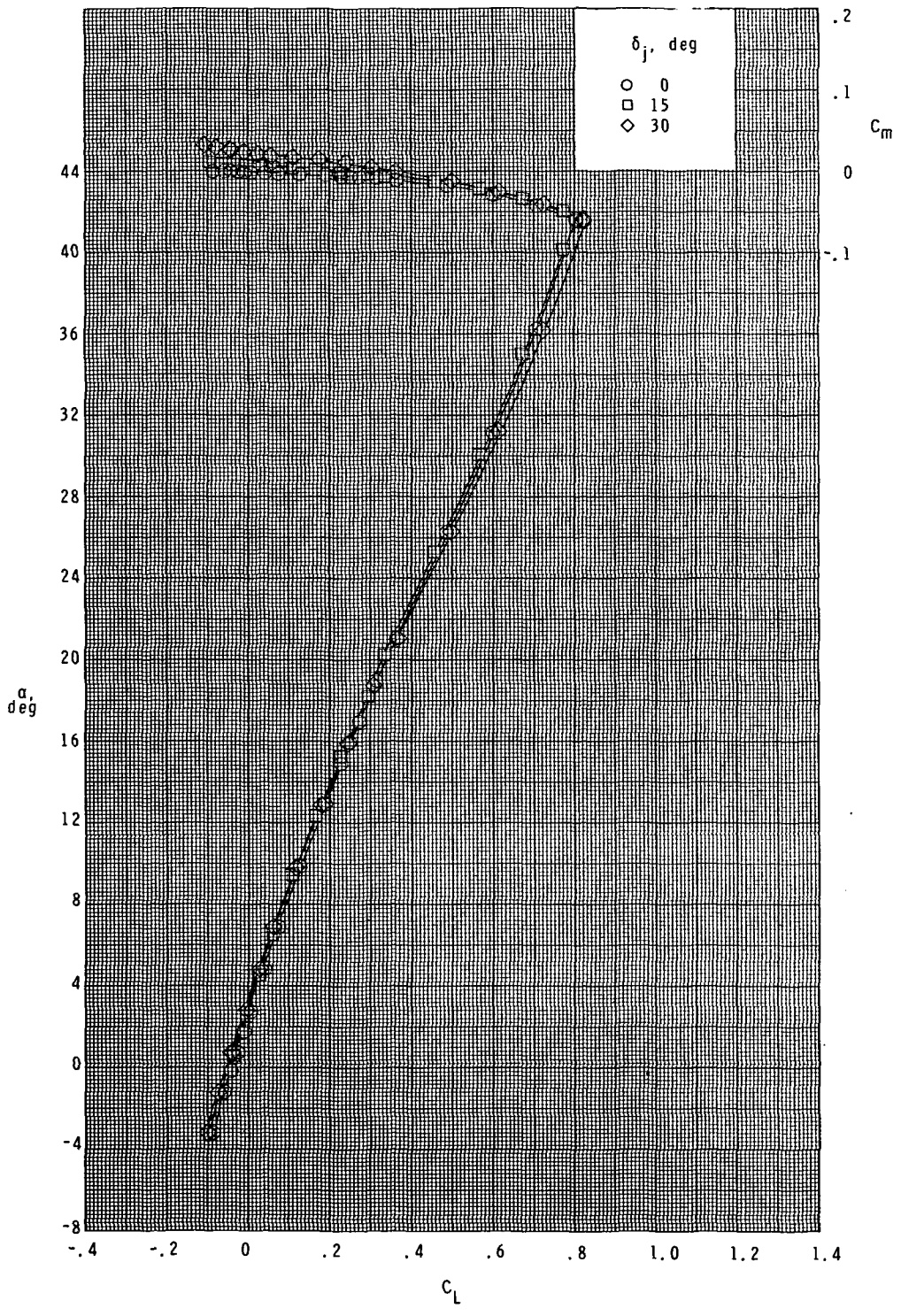

(c) Continued.

Figure 9.- Continued.

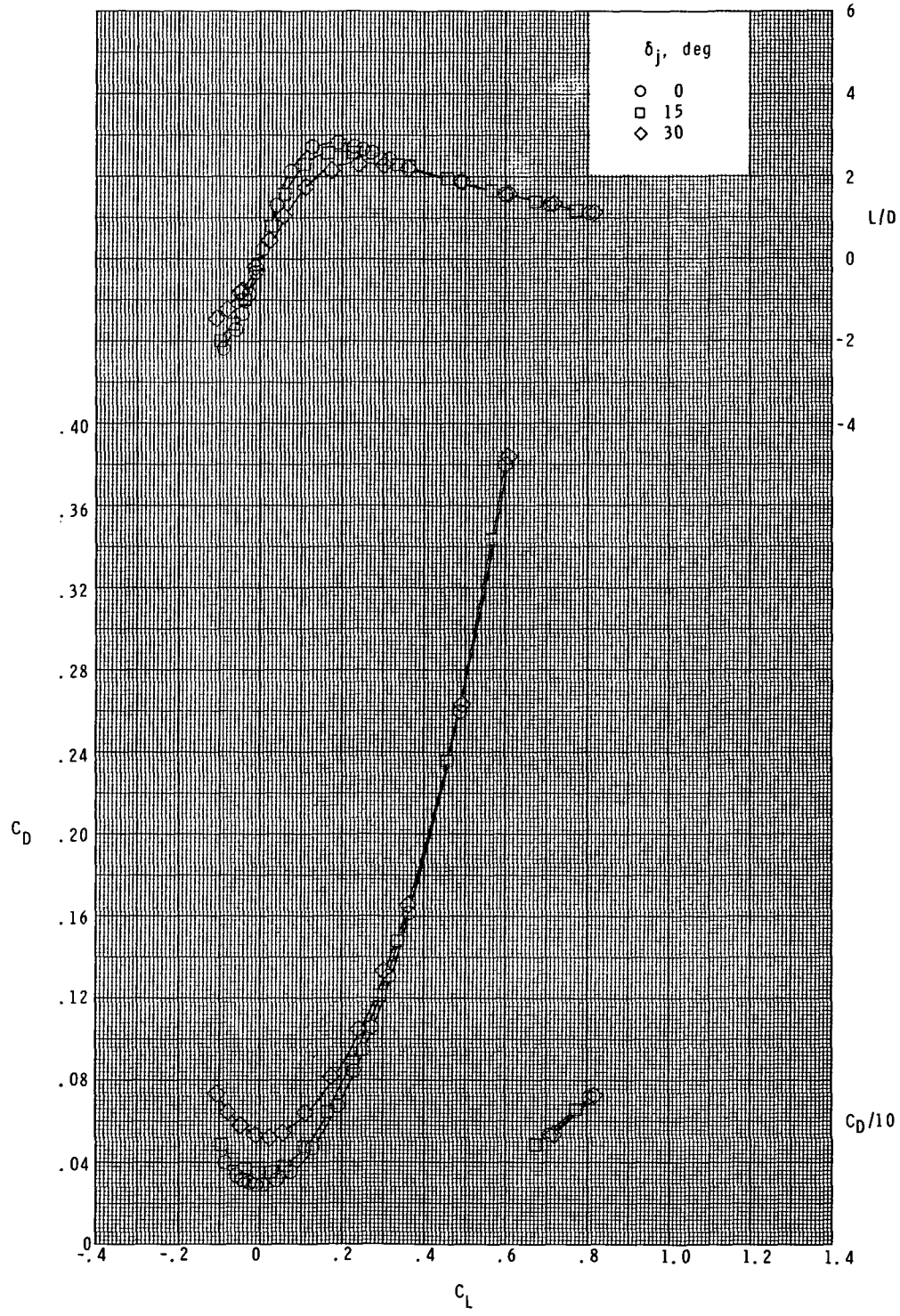

(c) Concluded.

Figure 9.- Concluded.

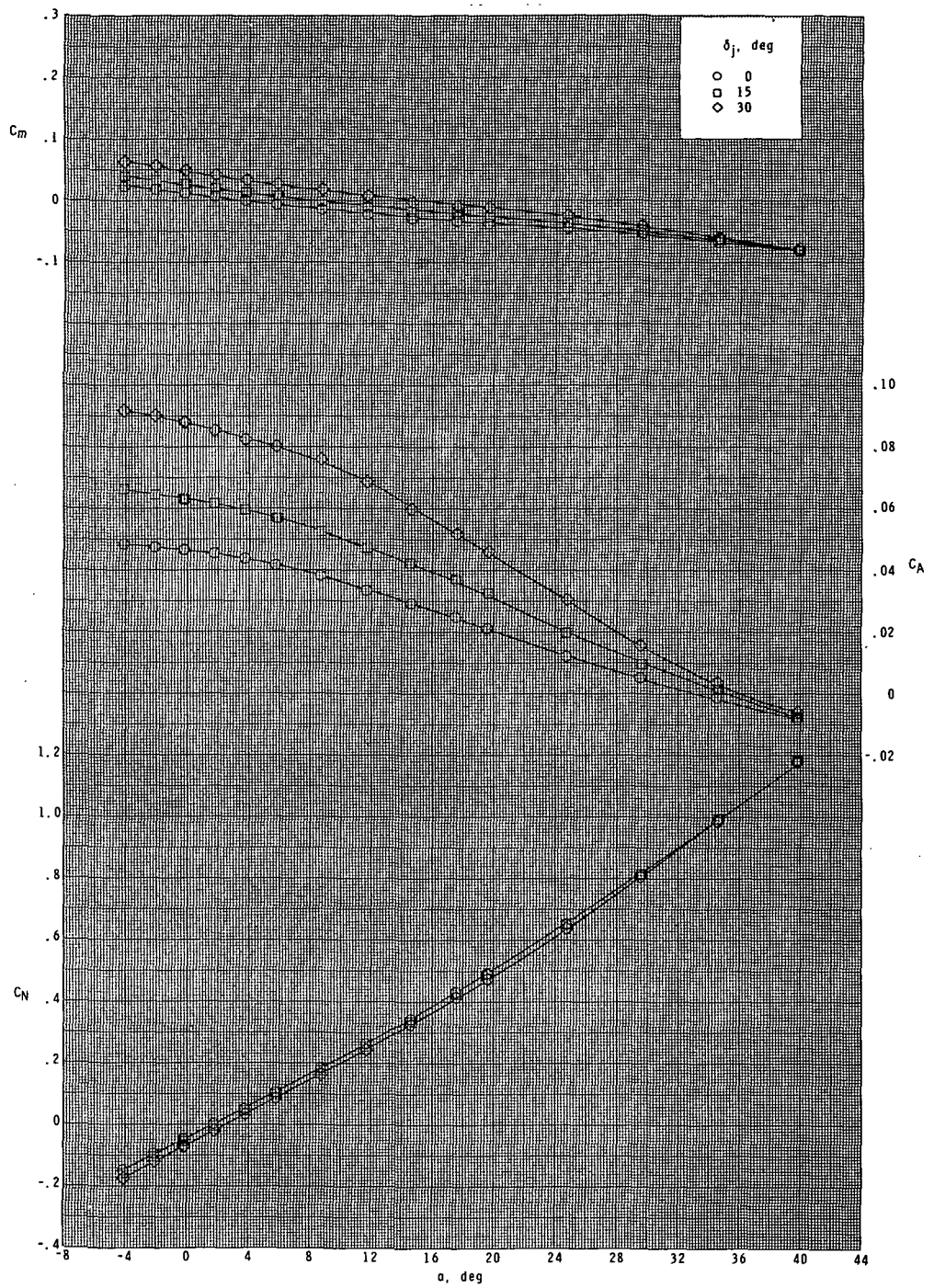

(a) M = 2.50.

Figure 10.- Effect of rudder flare deflection on longitudinal aerodynamic characteristics. $\delta_v = -20^o$.

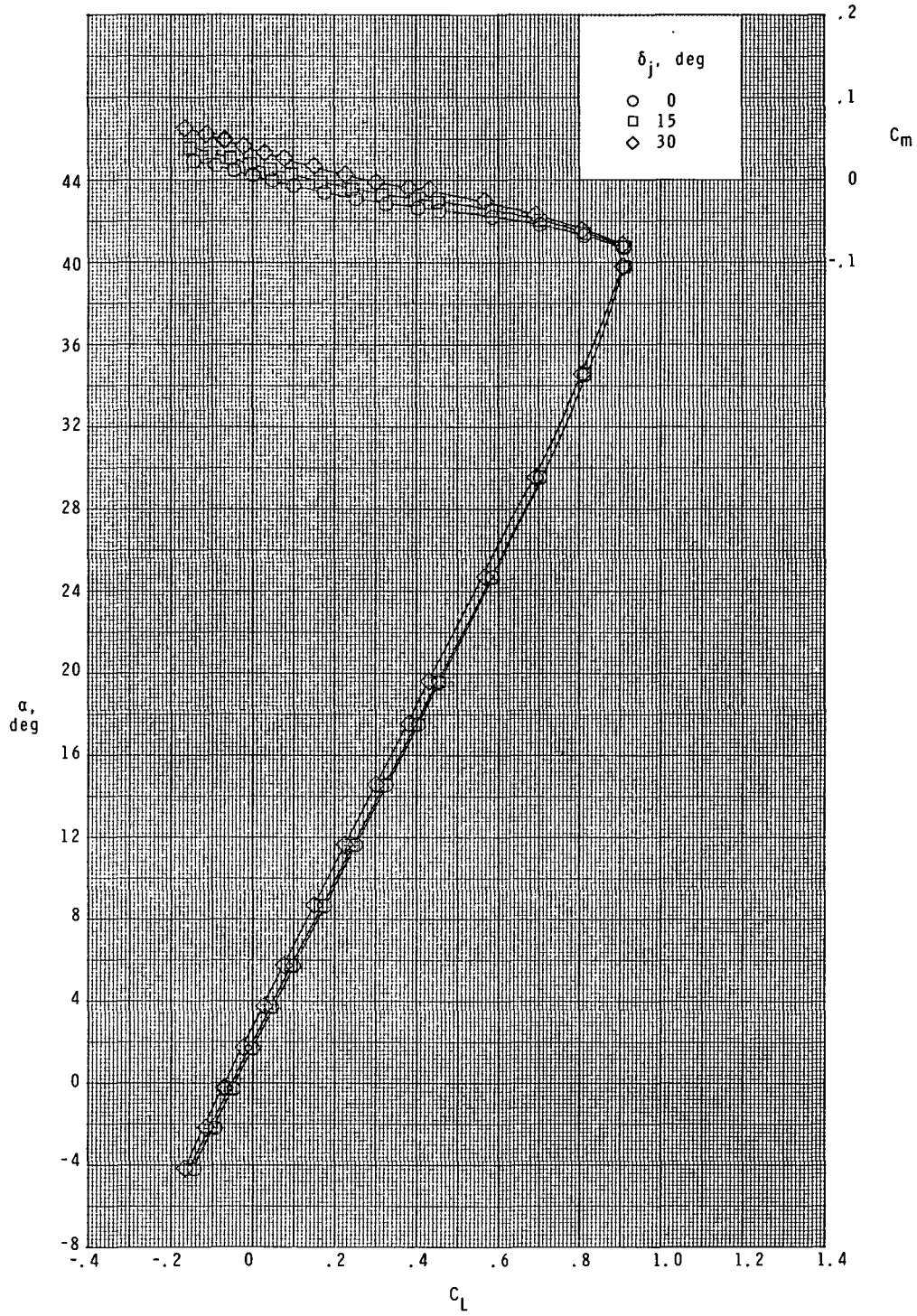

(a) Continued.

Figure 10.- Continued.

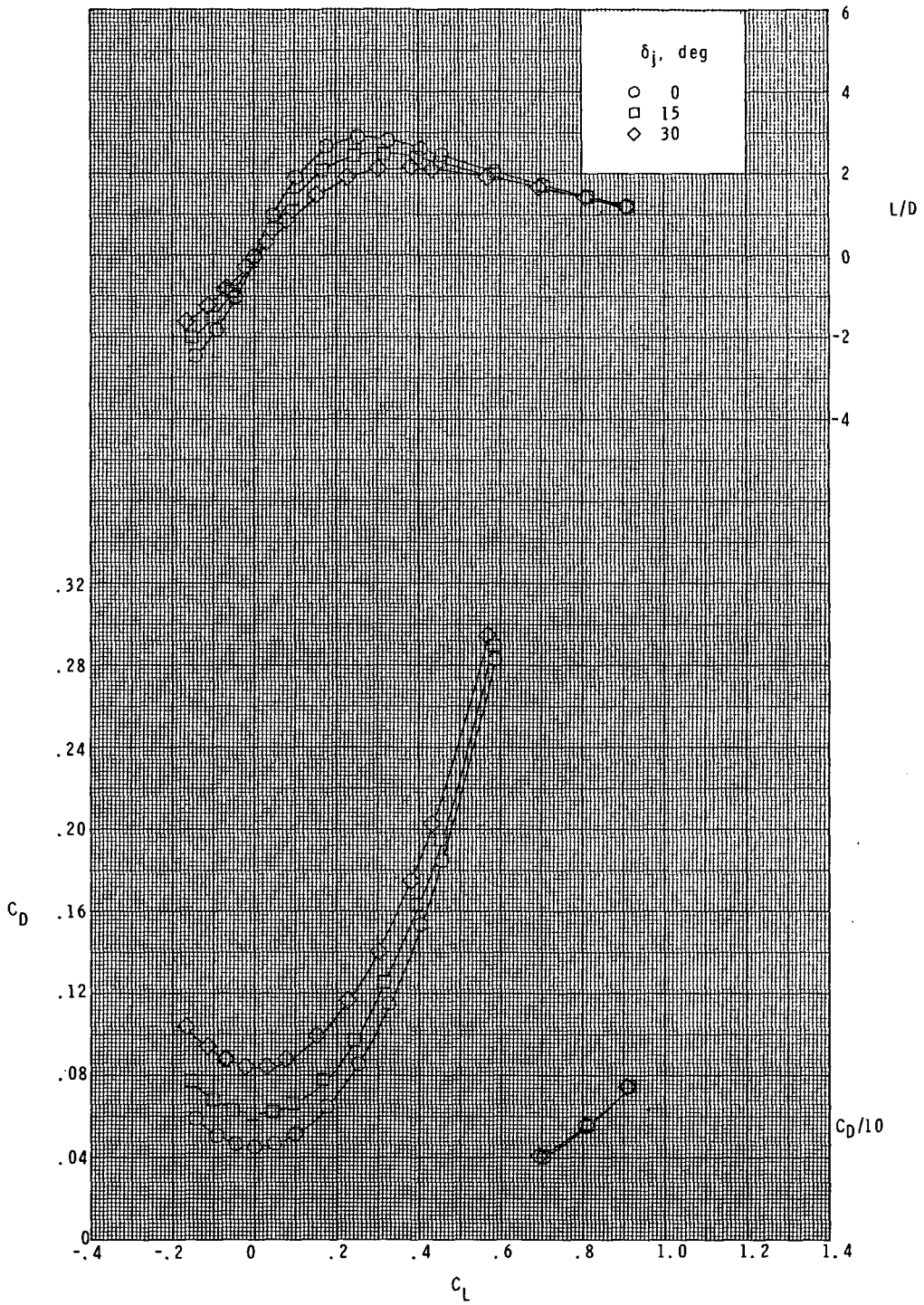

(a) Concluded.

Figure 10.- Continued.

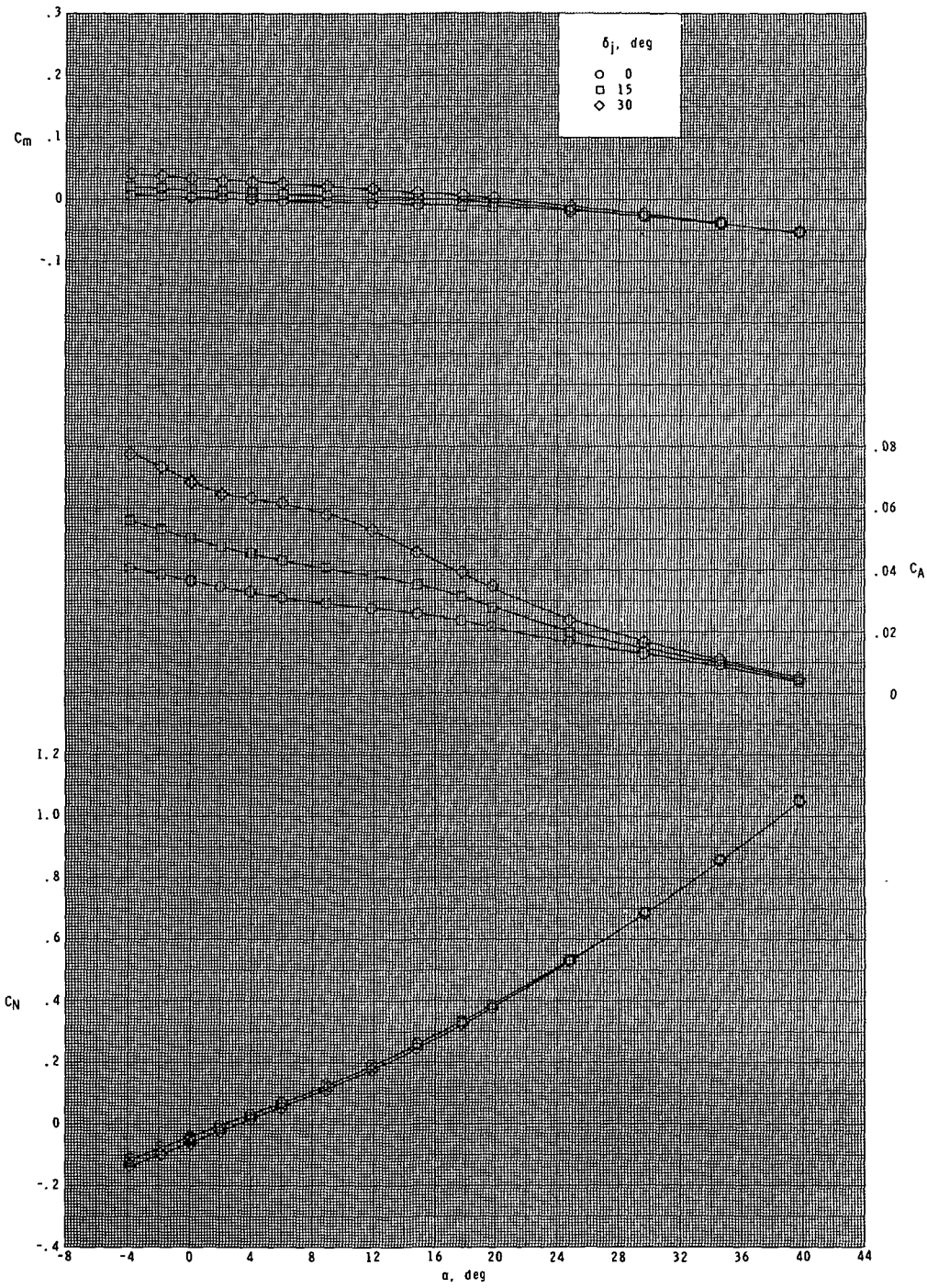

(b) M = 3.90.

Figure 10.- Continued.

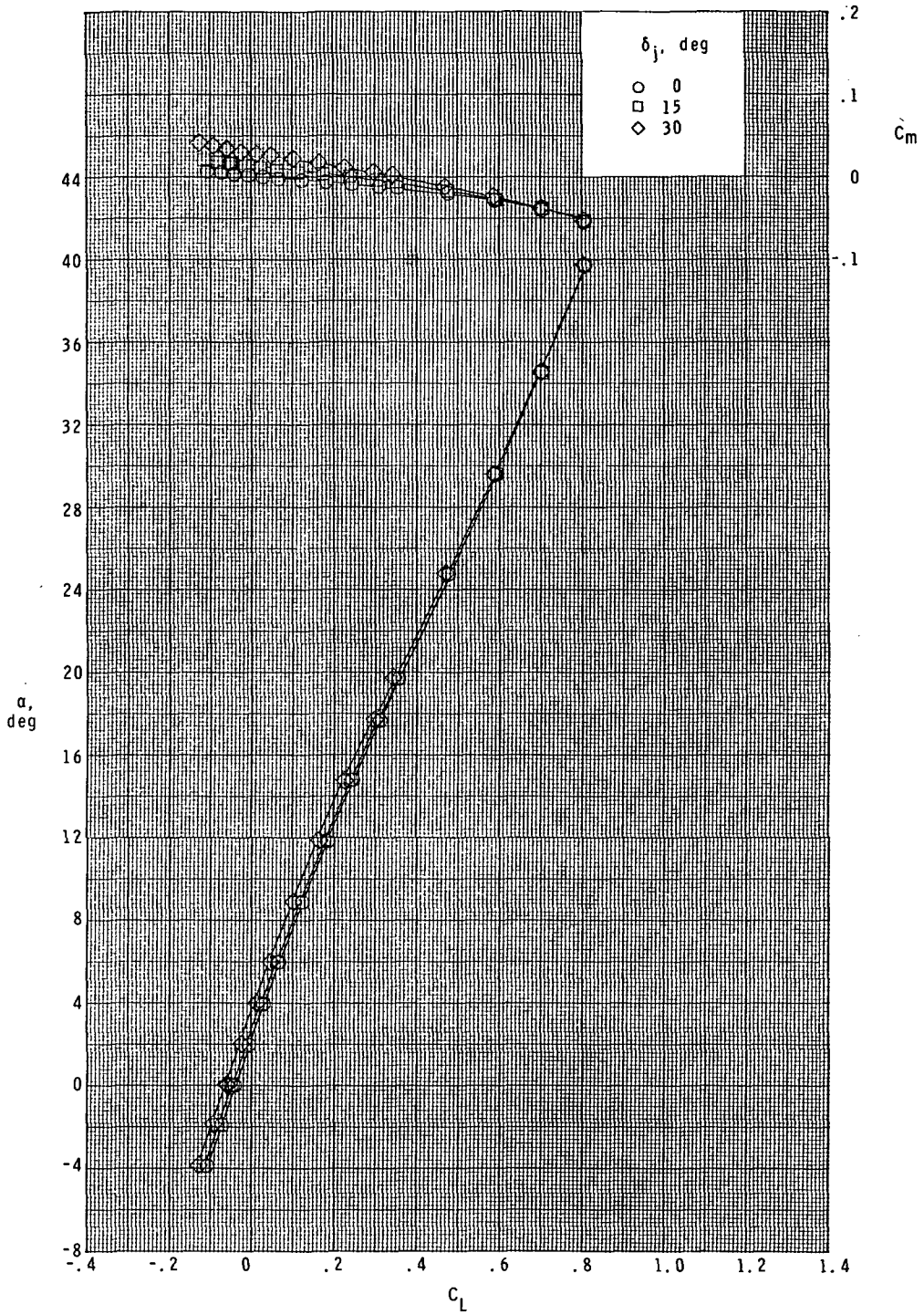

(b) Continued.

Figure 10.- Continued.

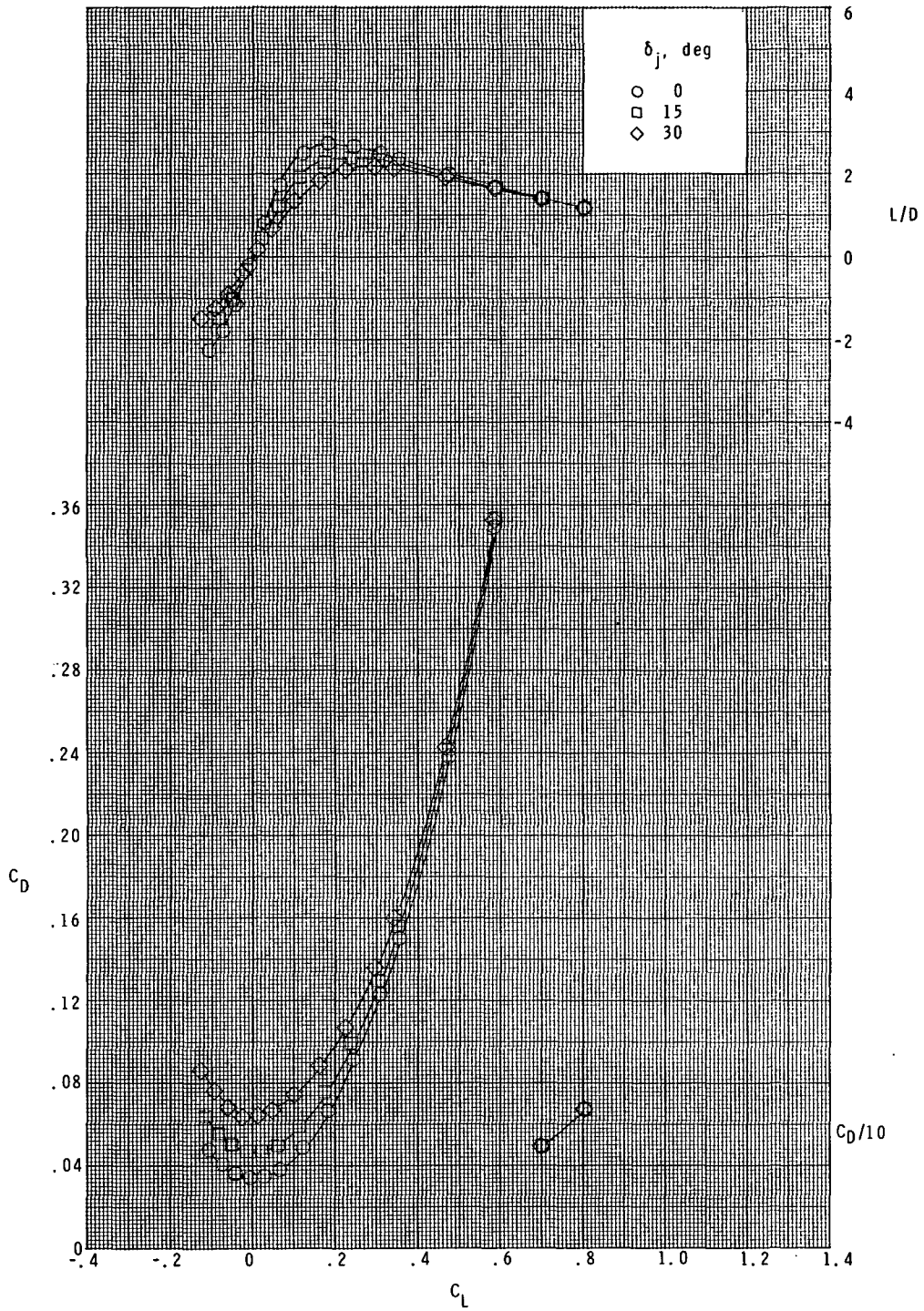

(b) Concluded.

Figure 10.- Continued.

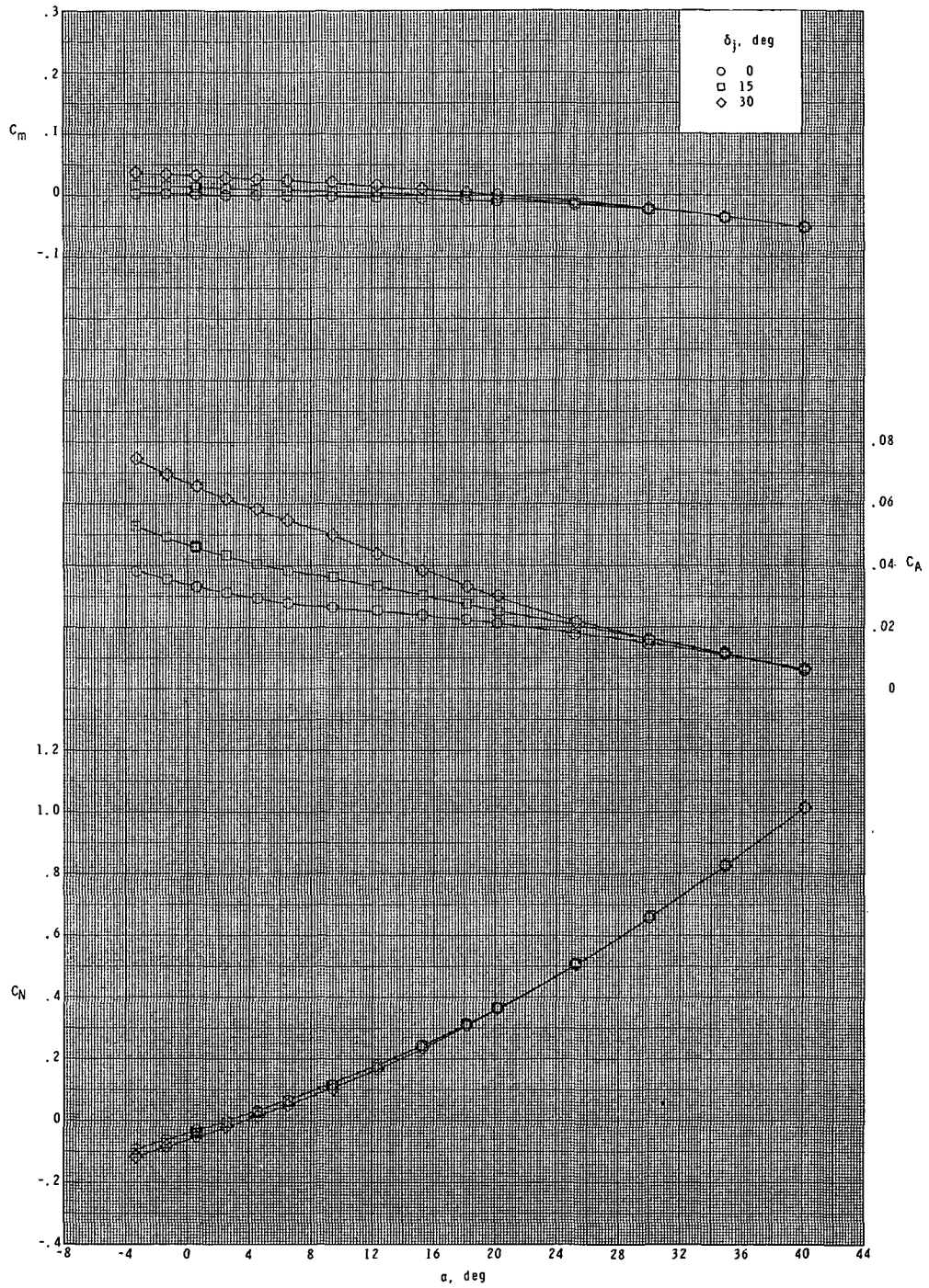

(c) M = 4.60.

Figure 10.- Continued.

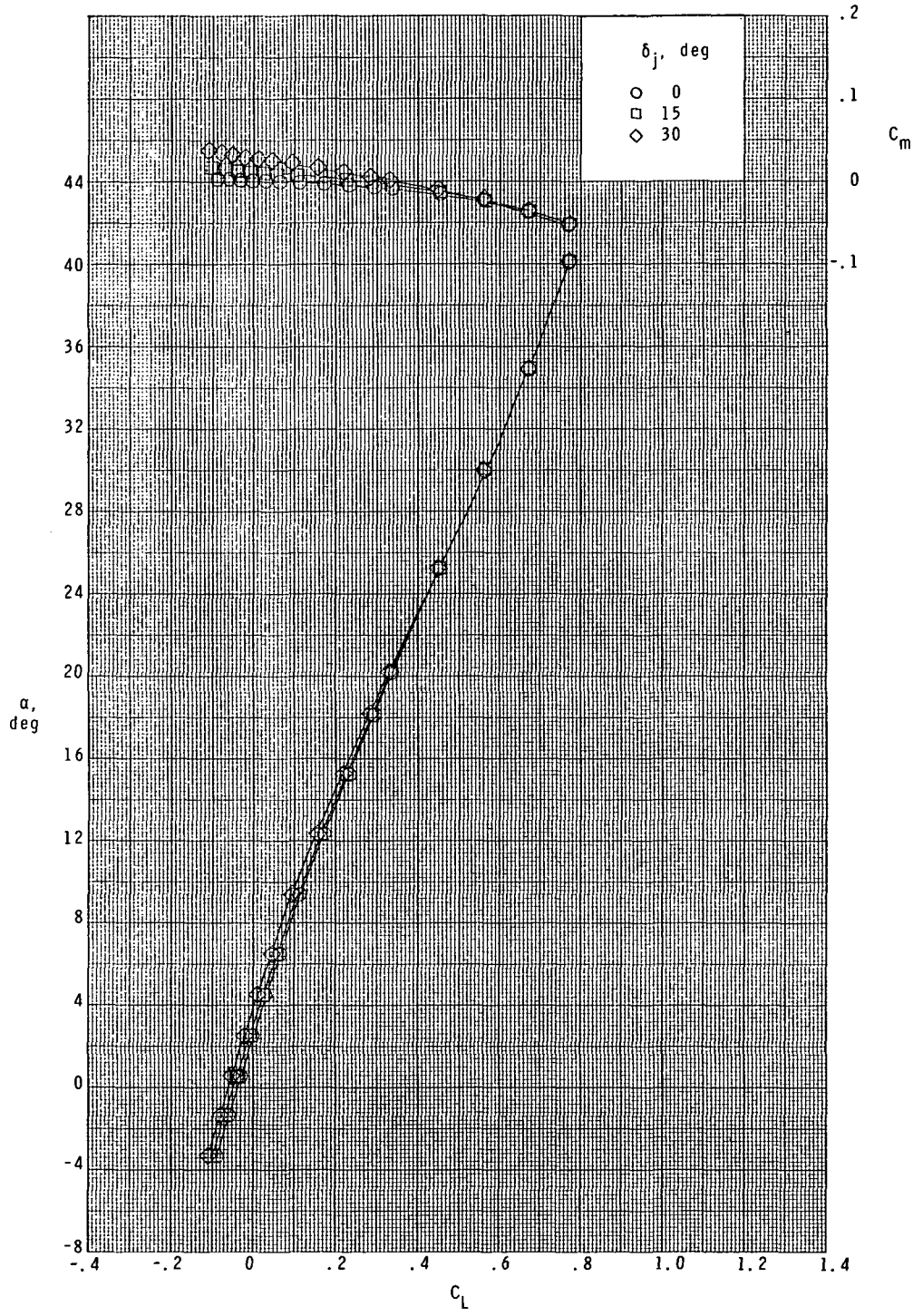

(c) Continued.

Figure 10.- Continued.

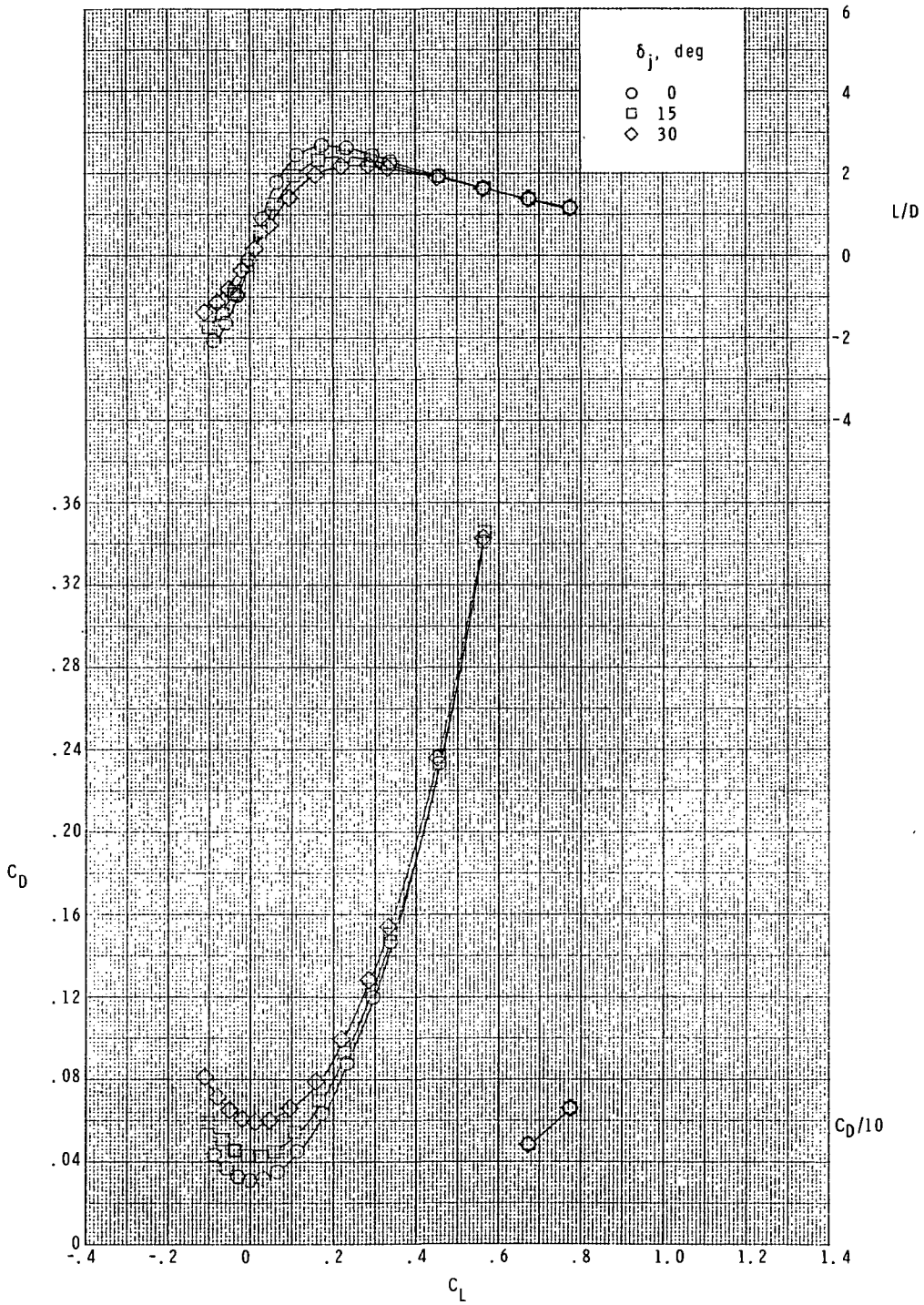

(c) Concluded.

Figure 10.- Concluded.

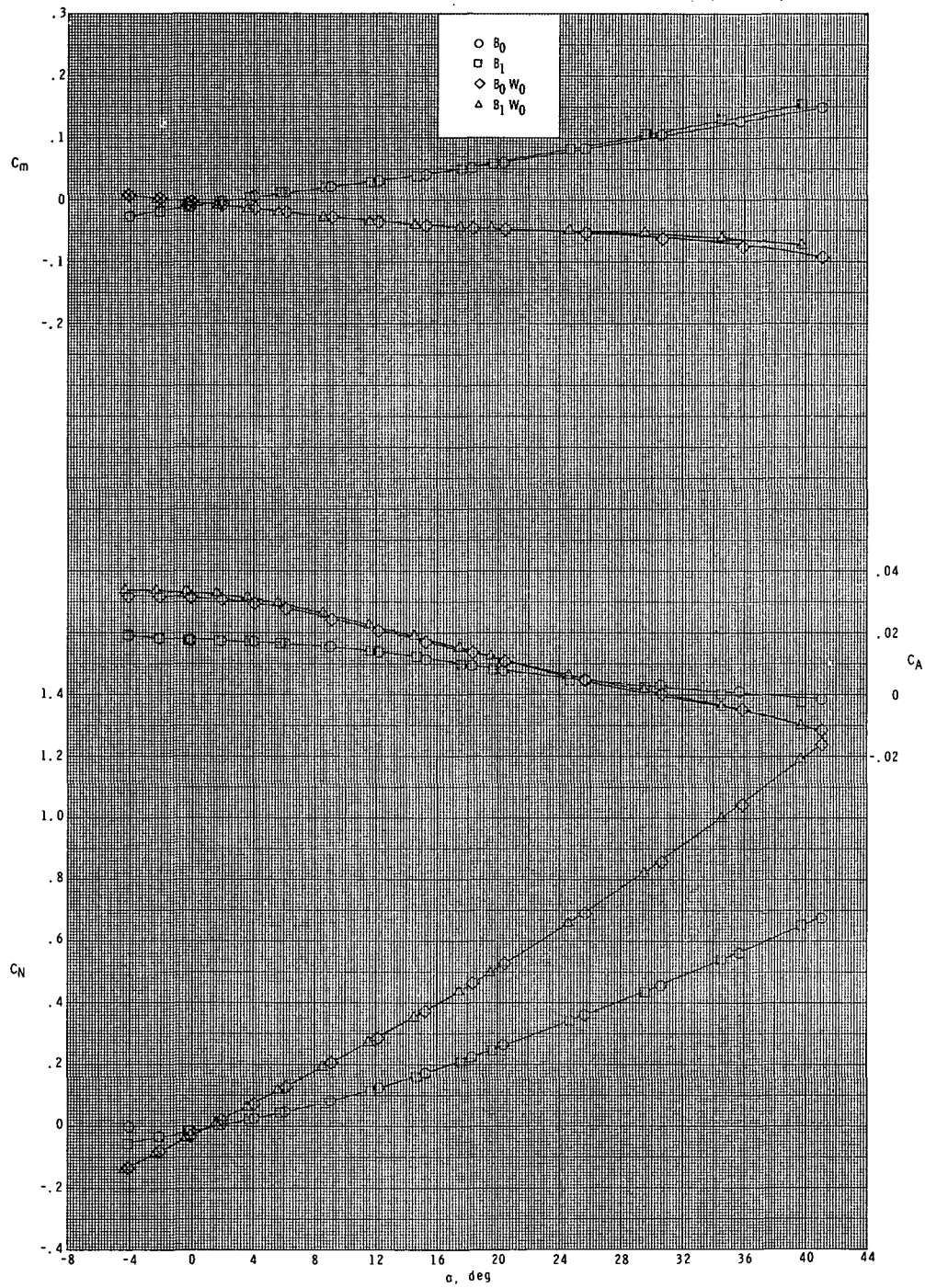

(a) M = 2.50.

Figure 11.- Effect of modified fuselage on longitudinal aerodynamic characteristics.

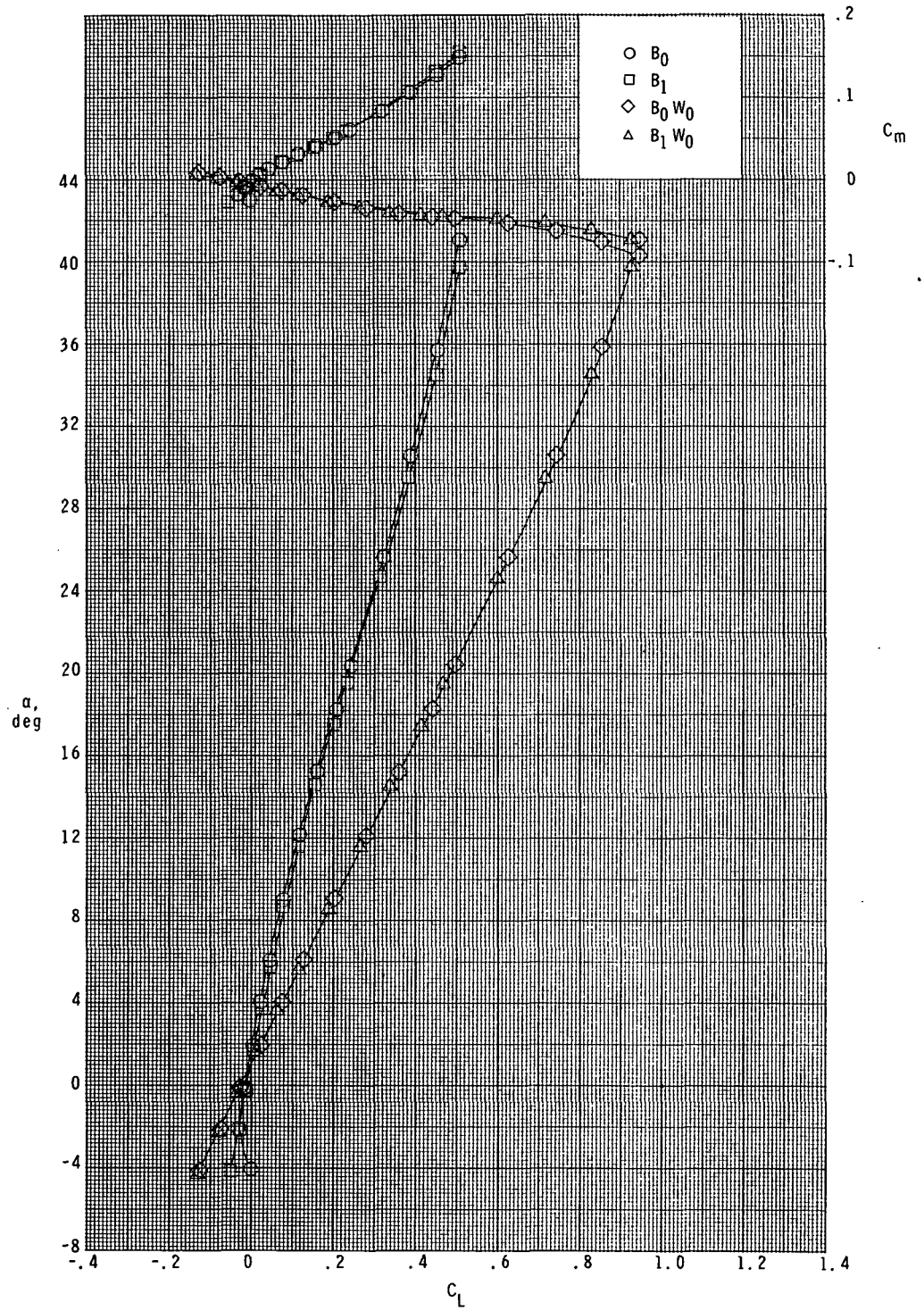

(a) Continued.

Figure 11.- Continued.

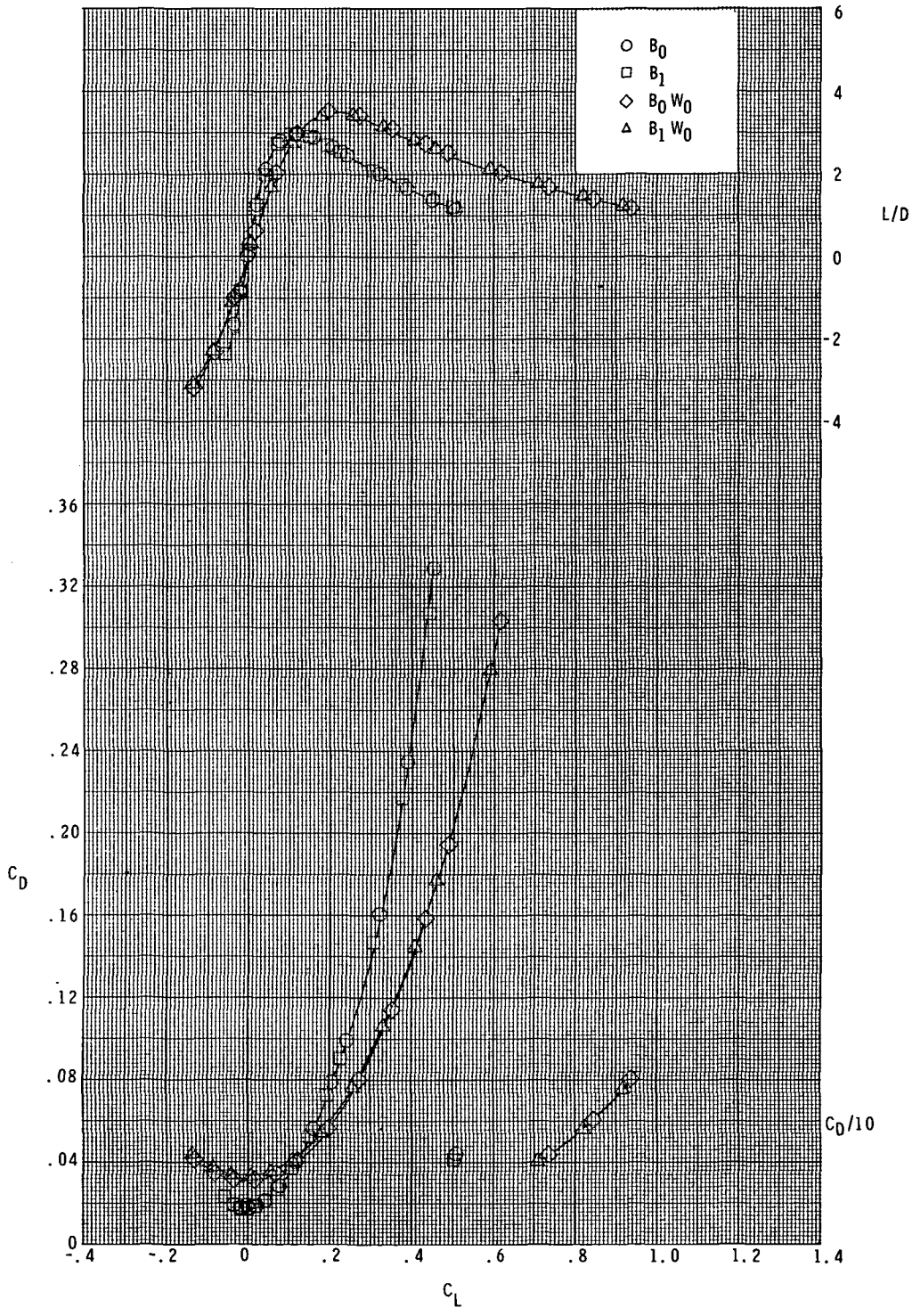

(a) Concluded.

Figure 11.- Continued.

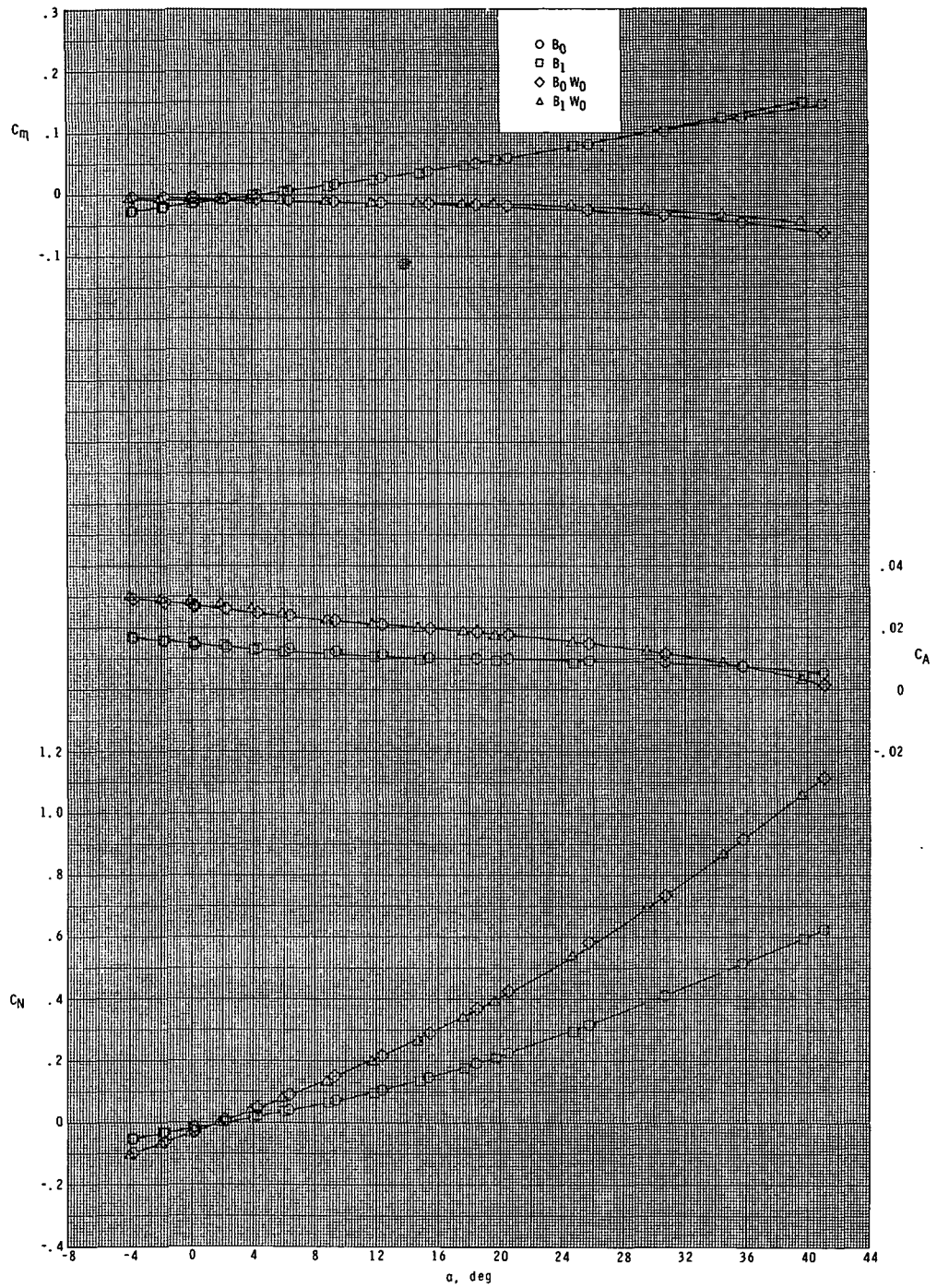

(b) M = 3.90.

Figure 11.- Continued.

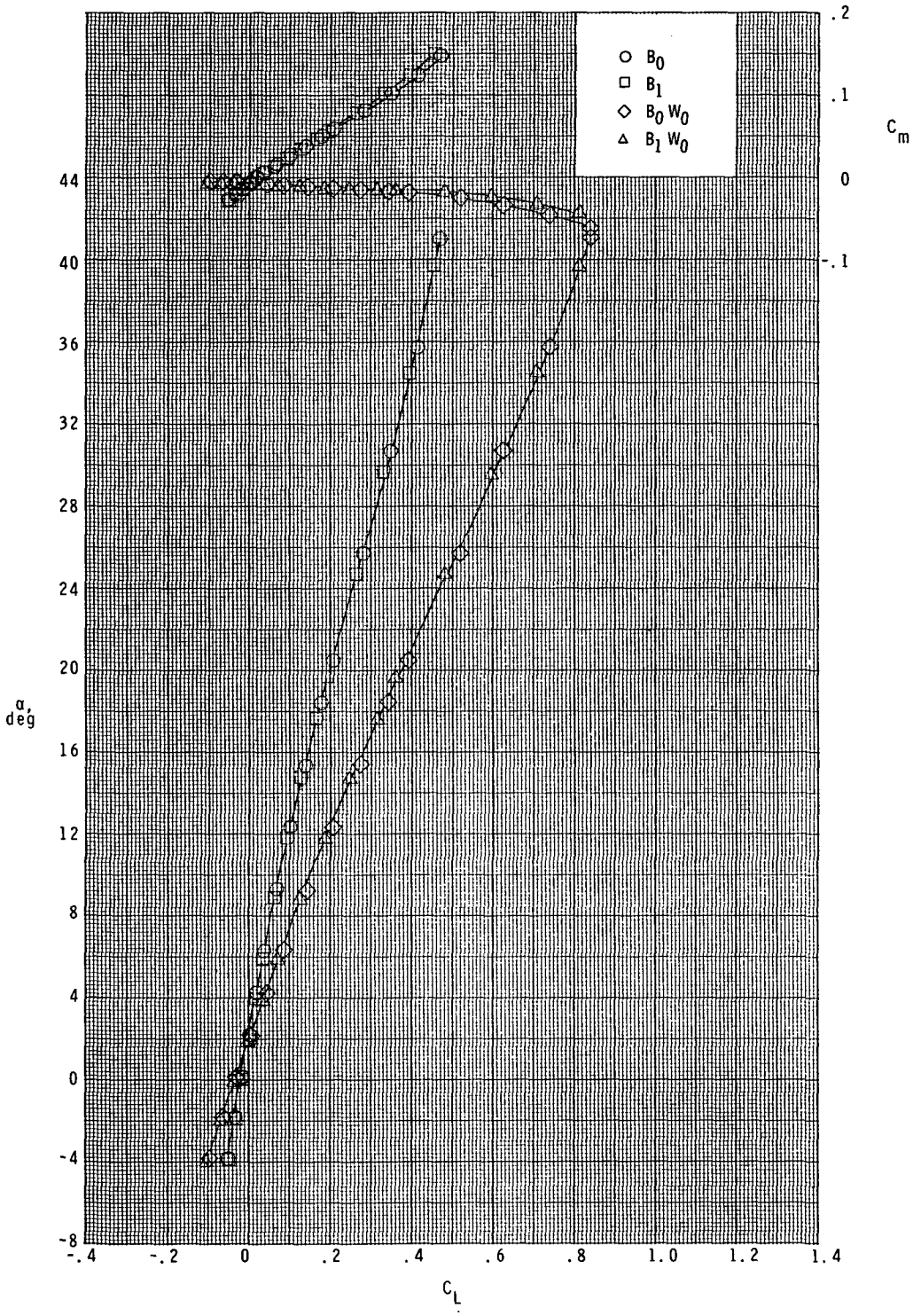

(b) Continued.

Figure 11.- Continued.

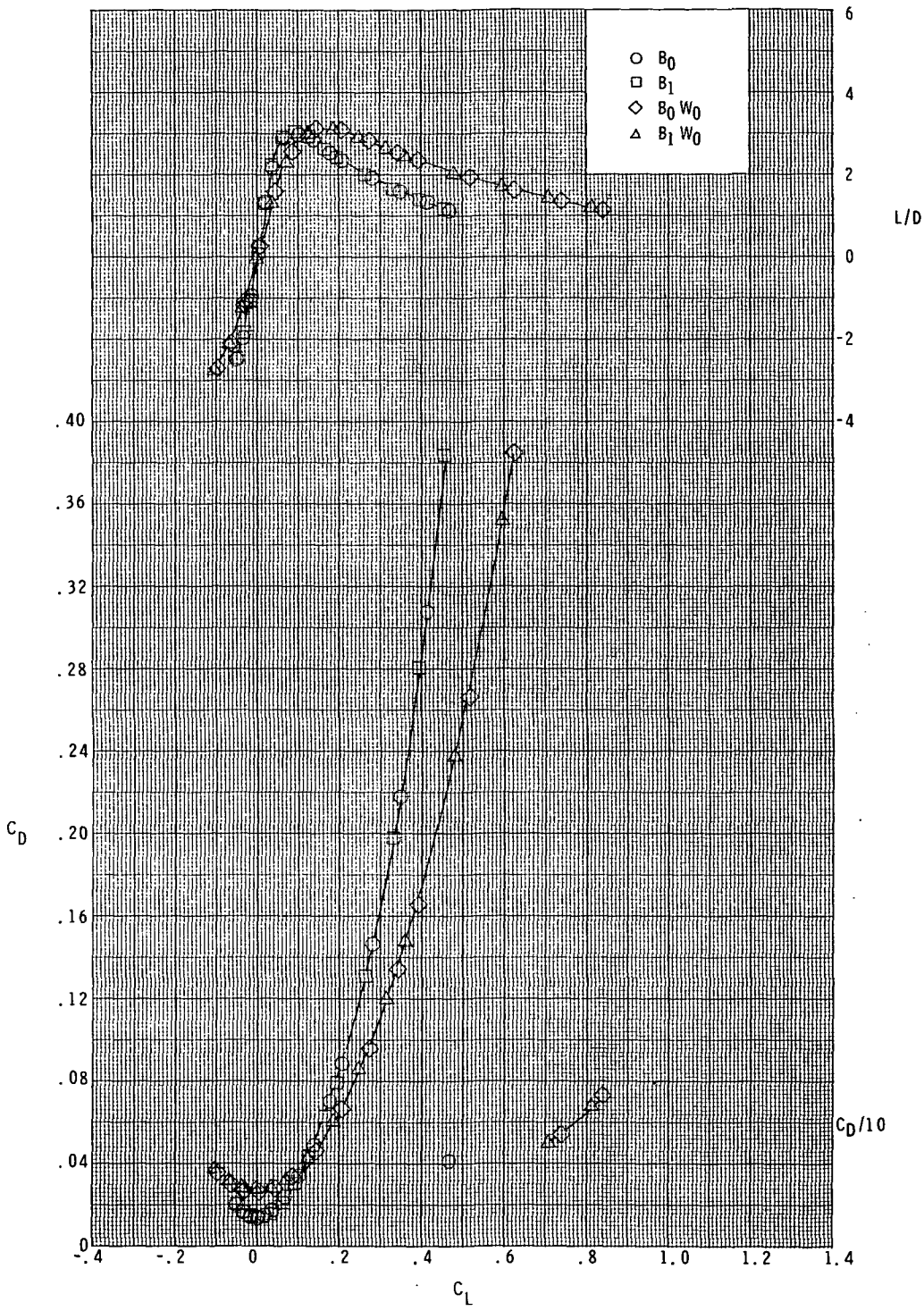

(b) Concluded.

Figure 11.- Continued.

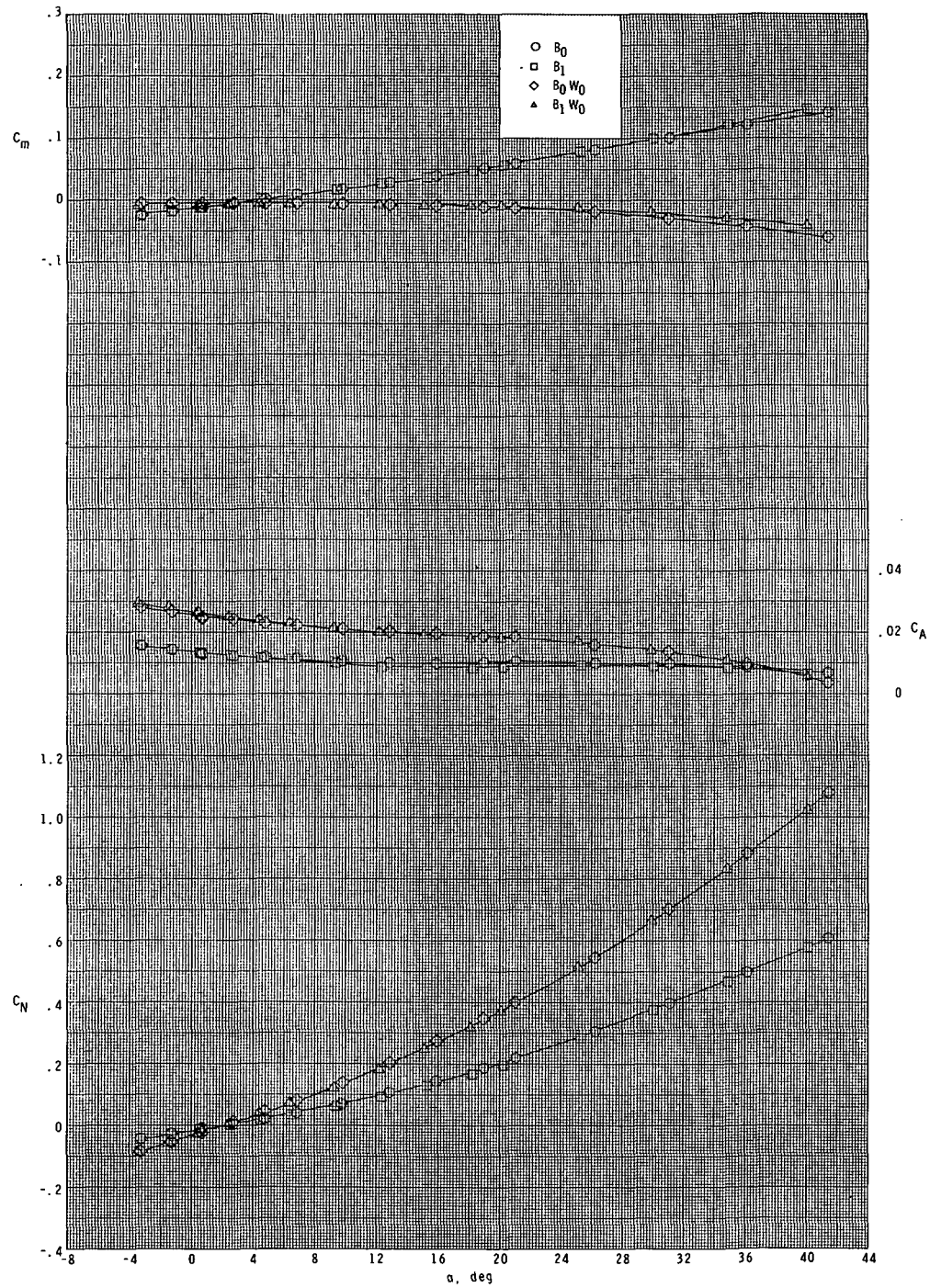

(c) M = 4.60.

Figure 11.- Continued.

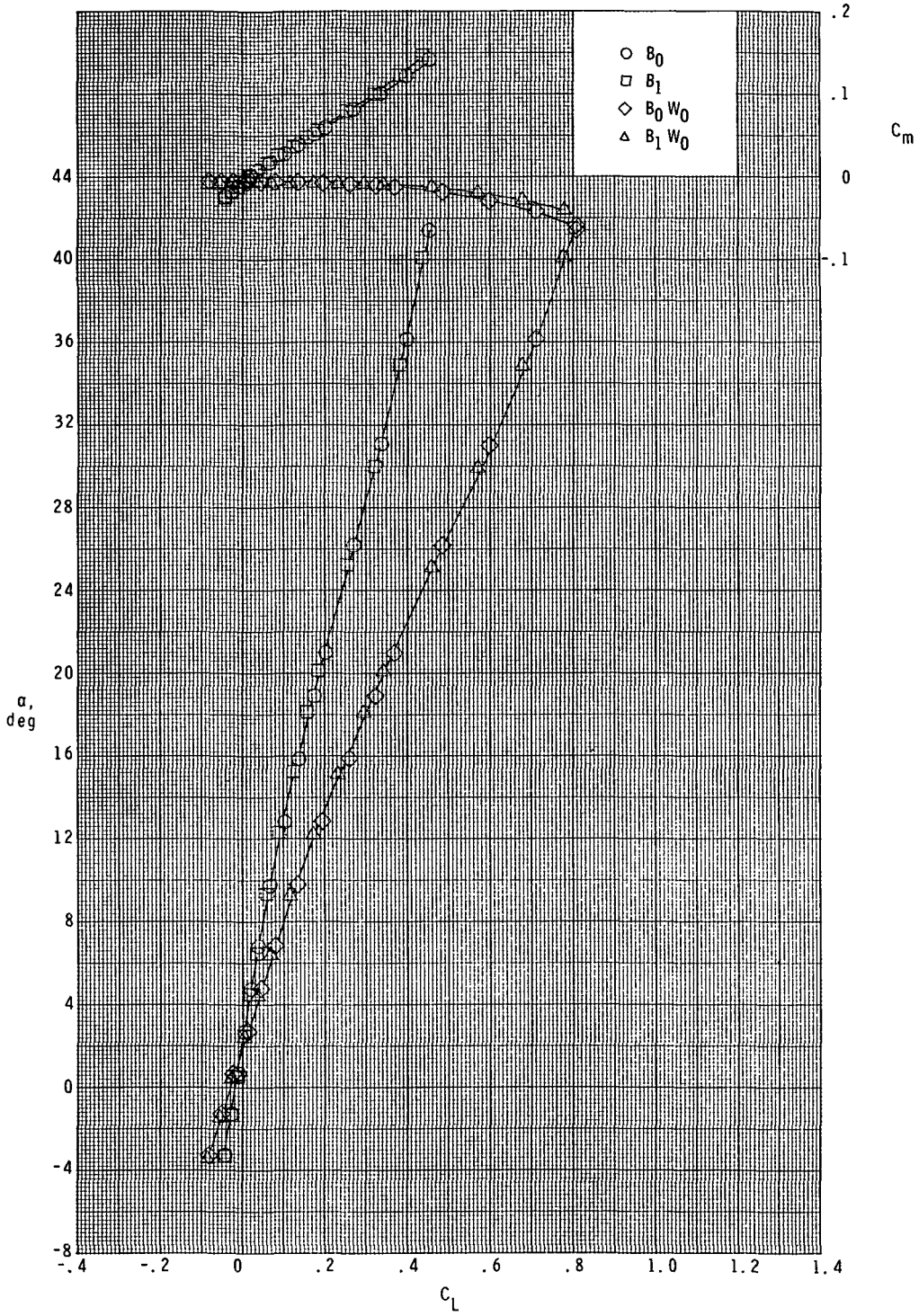

(c) Continued.

Figure 11.- Continued.

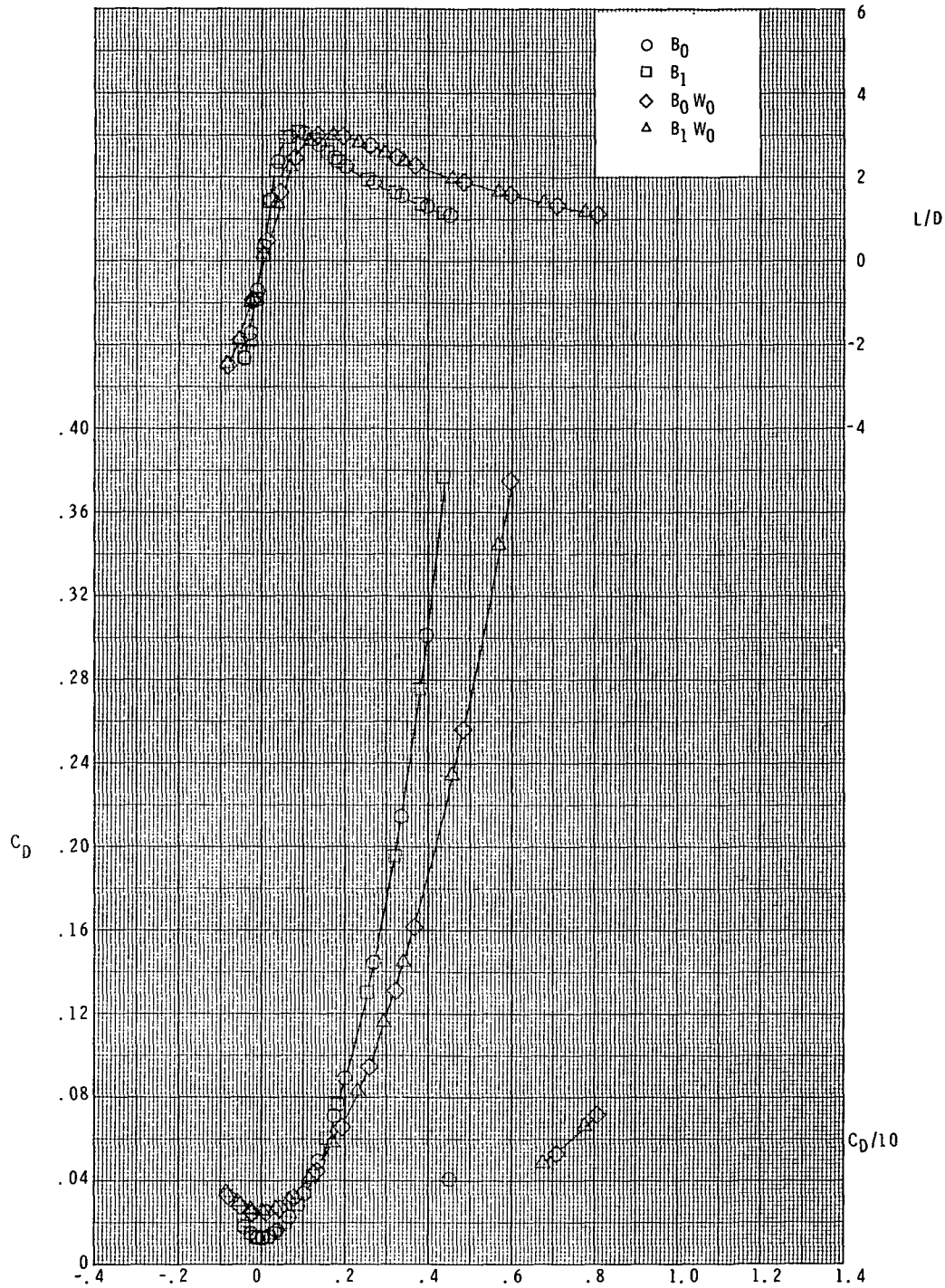

(c) Concluded.

Figure 11.- Concluded.

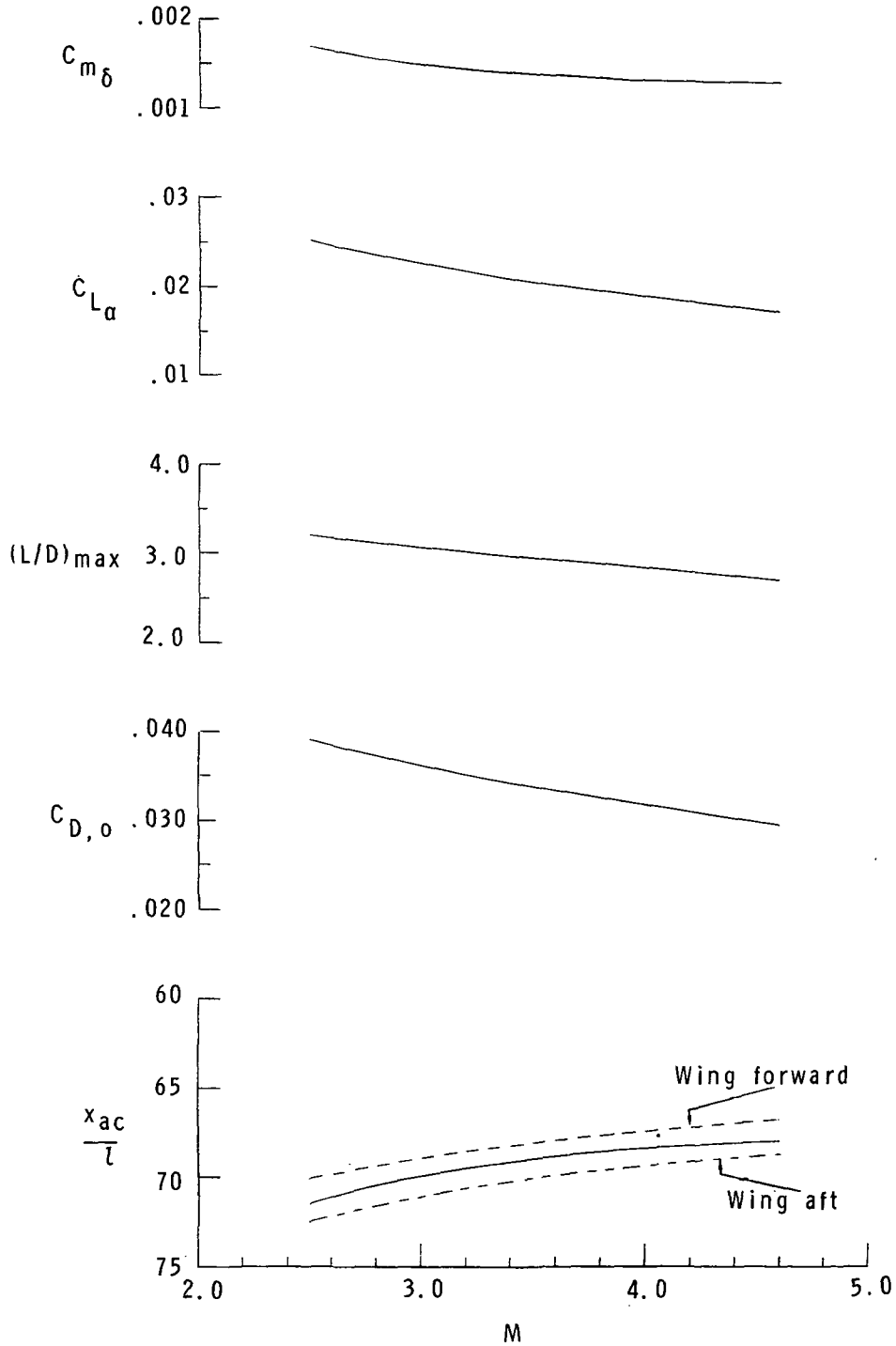

Figure 12.- Summary of longitudinal aerodynamic characteristics.

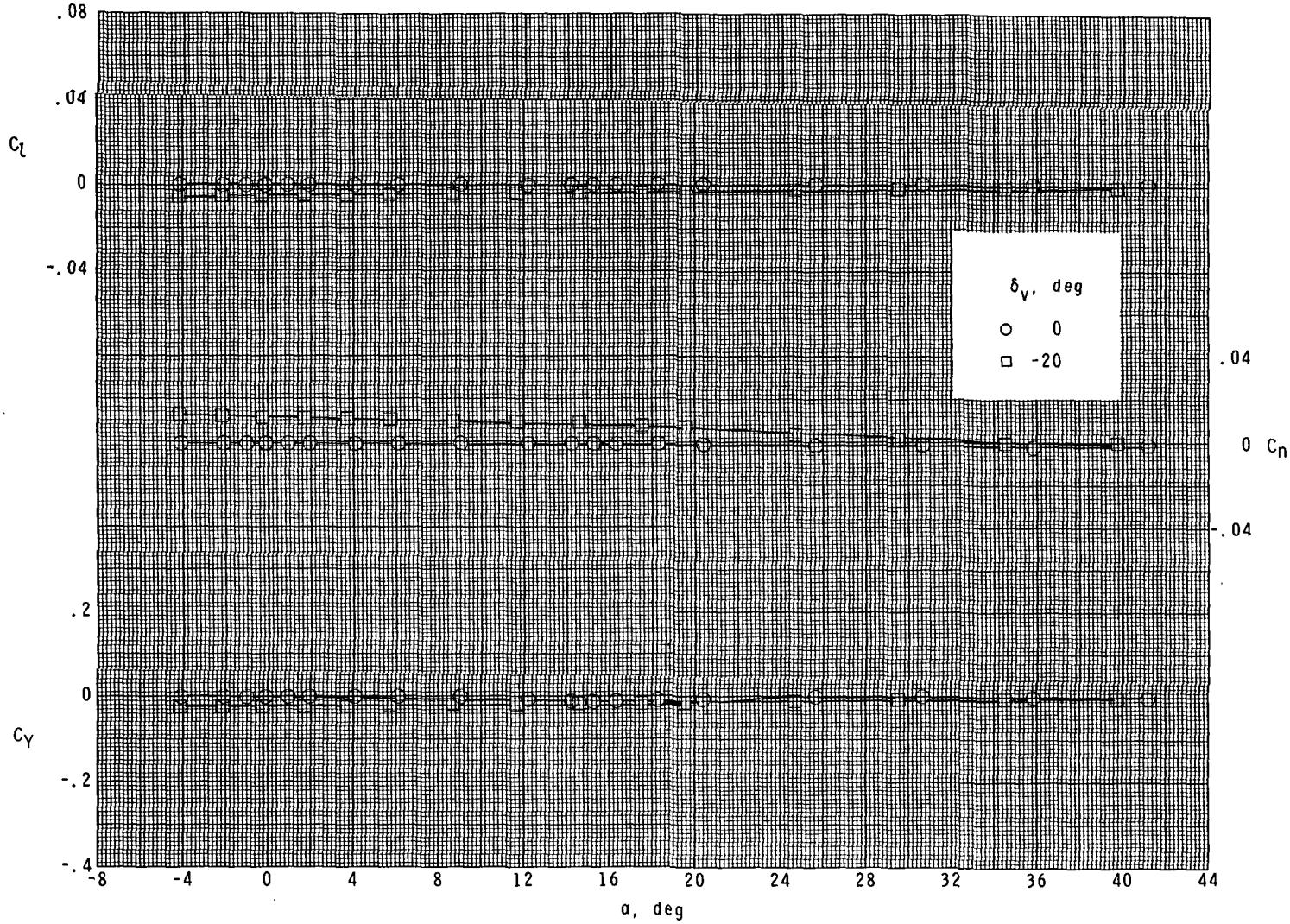

(a) M = 2.50.

Figure 13.- Rudder yaw-control effectiveness. $\beta = 0^o$.

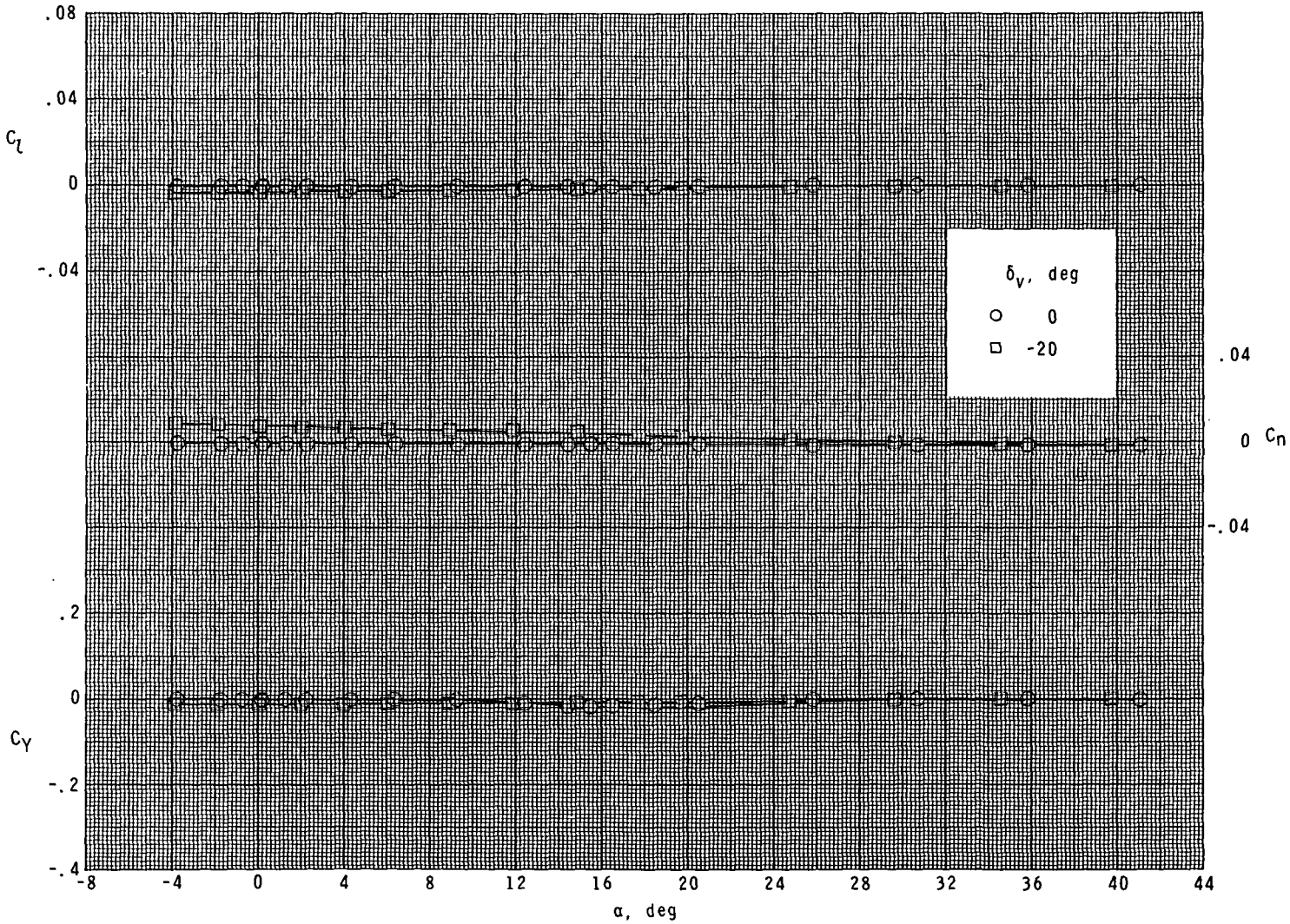

(b) M = 3.90.

Figure 13.- Continued.

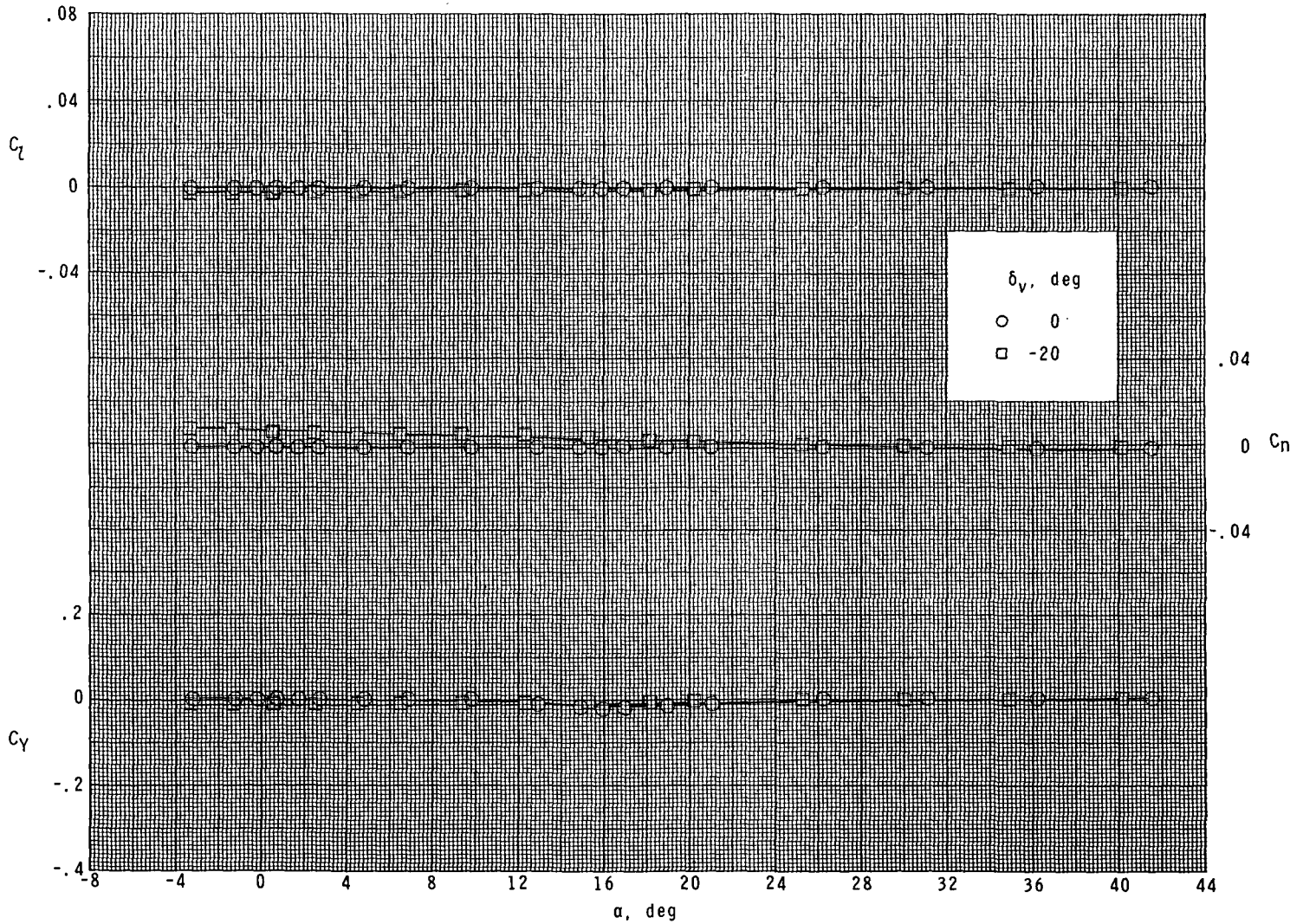

(c) M = 4.60.

Figure 13.- Concluded.

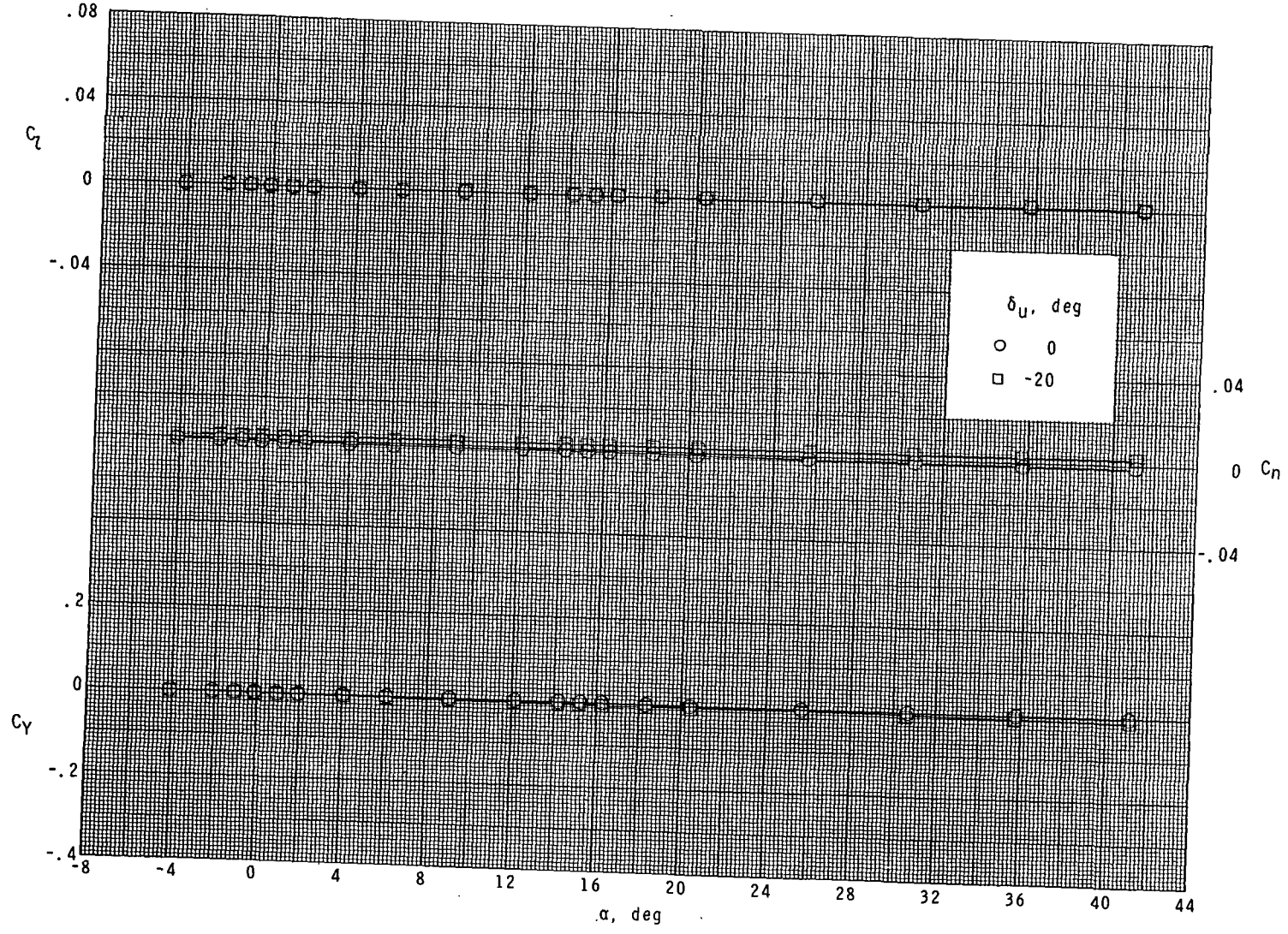

(a) M = 2.50.

Figure 14.- Ventral-fin yaw-control effectiveness. $\beta = 0^o$.

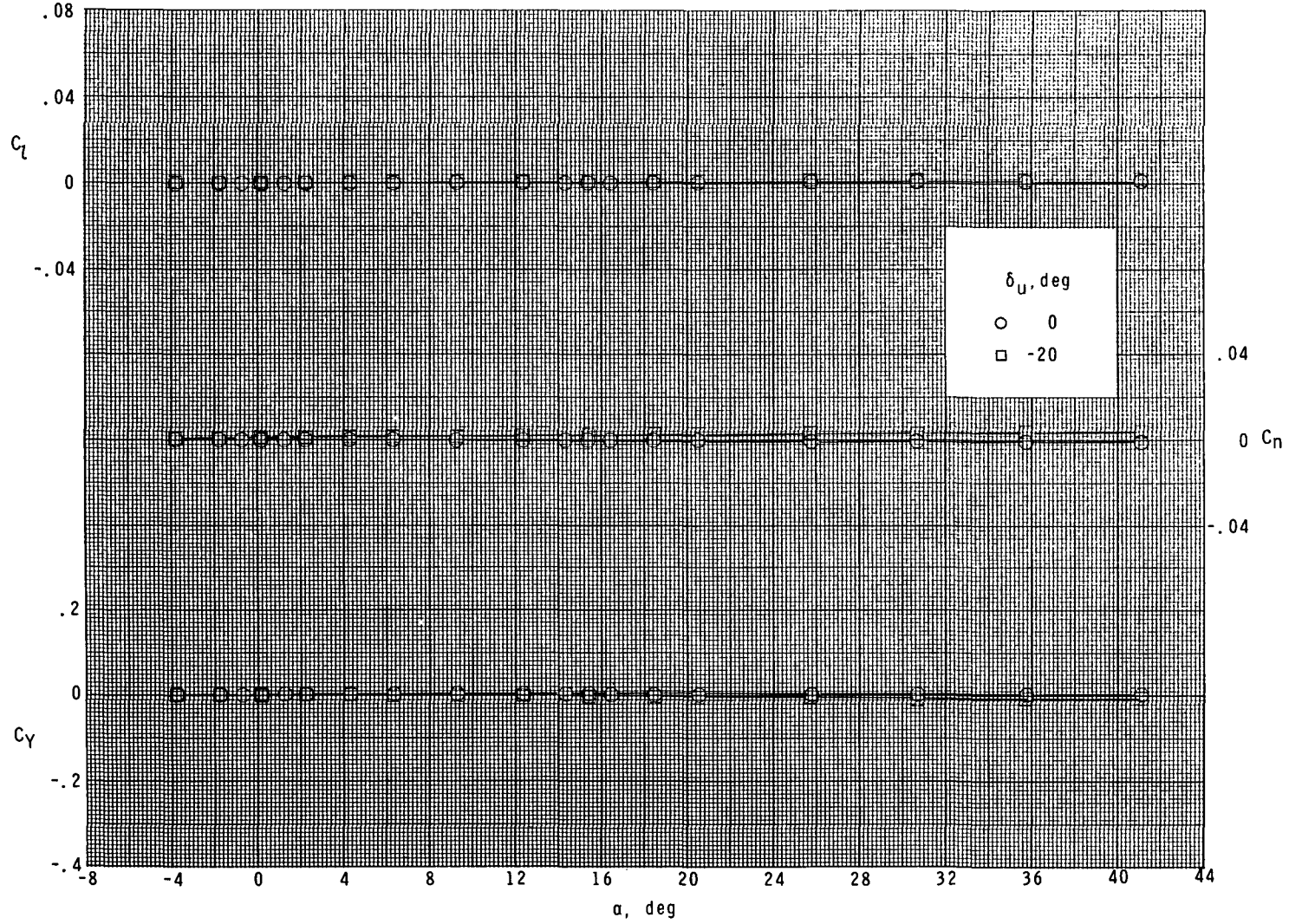

(b) M = 3.90.

Figure 14.- Continued.

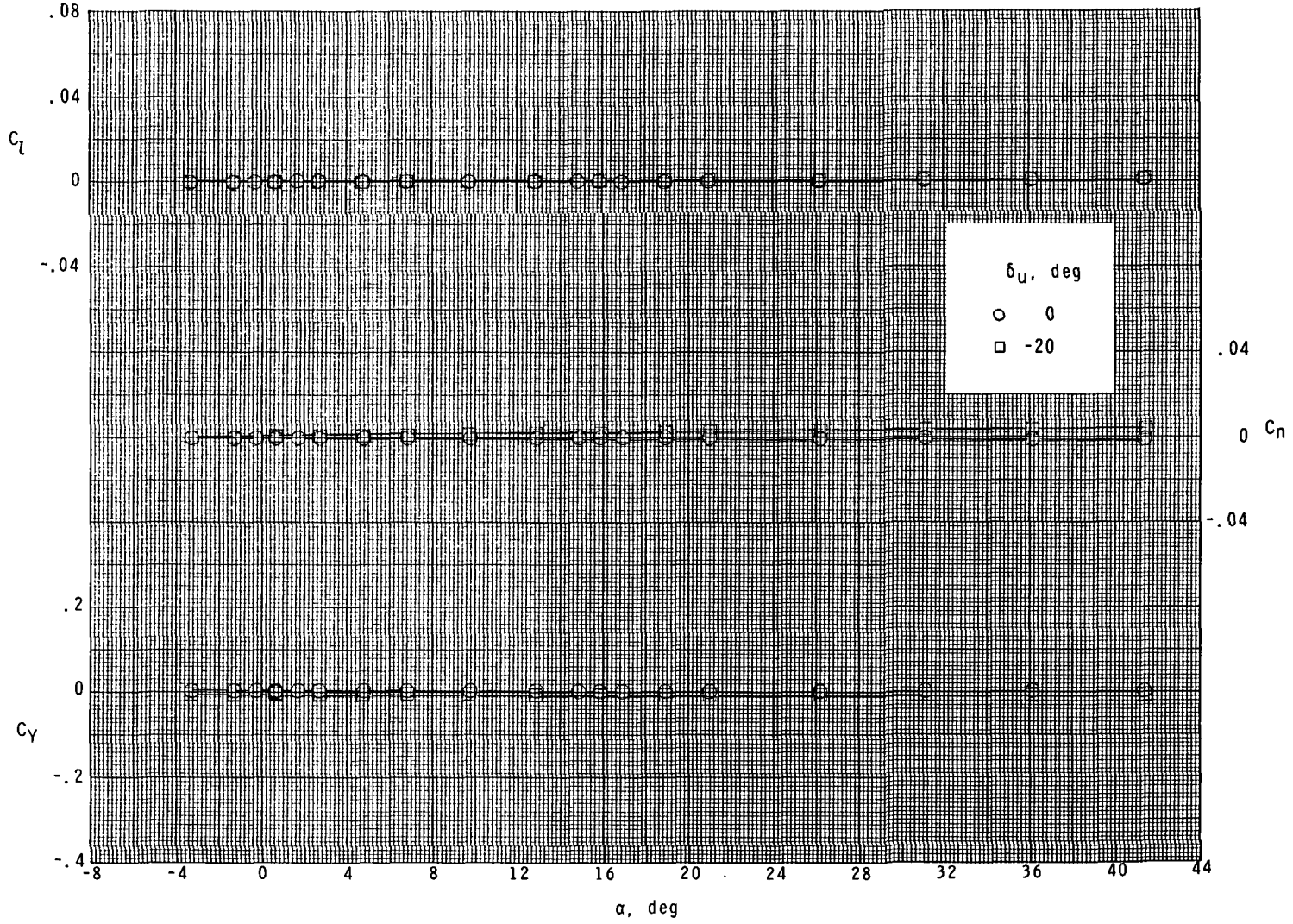

(c) M = 4.60.

Figure 14.- Concluded.

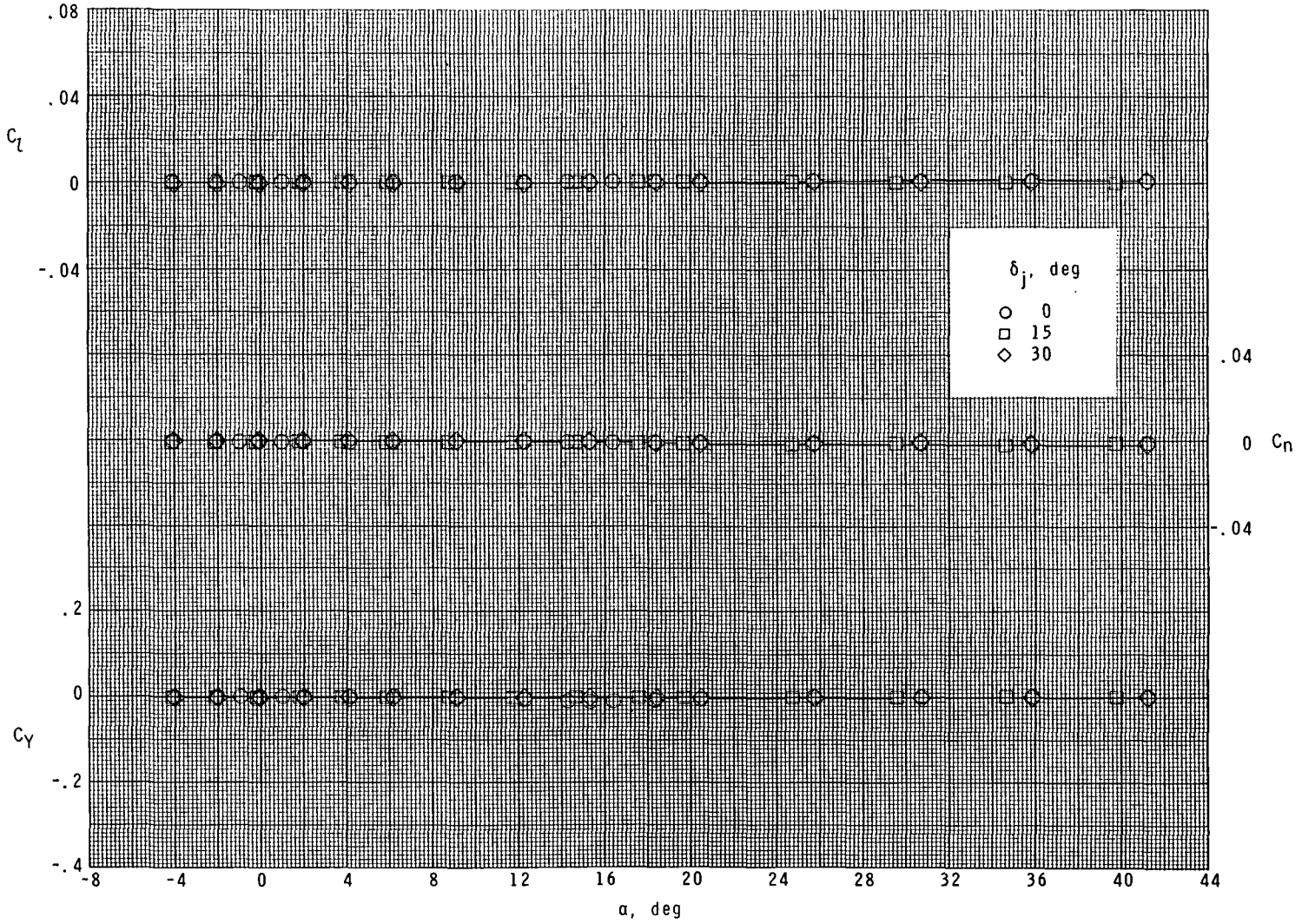

(a) M = 2.50.

Figure 15.- Effect of rudder flare deflection on lateral aerodynamic characteristics. $\delta_V = 0^o$; $\beta = 0^o$.

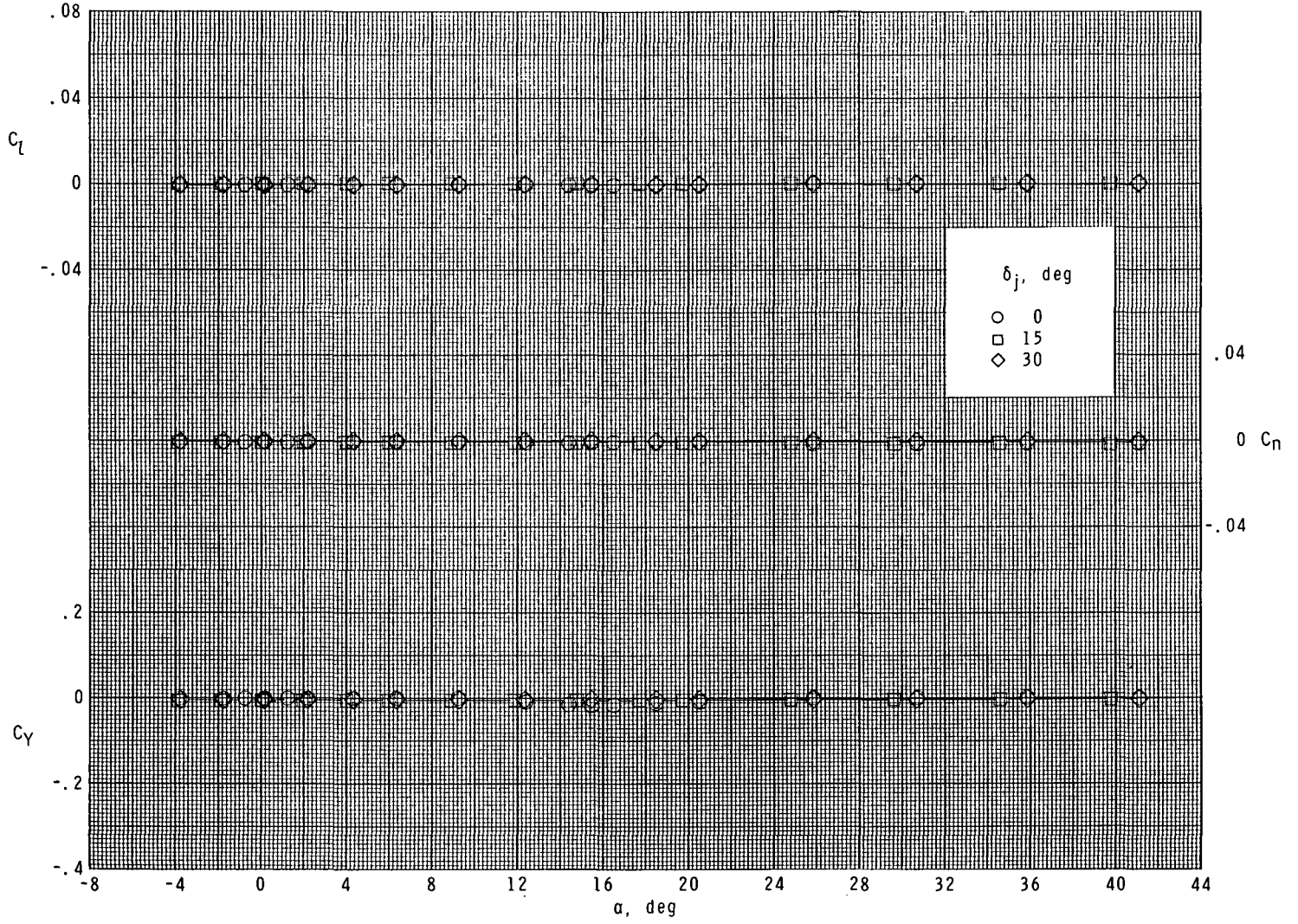

(b) M = 3.90.

Figure 15.- Continued.

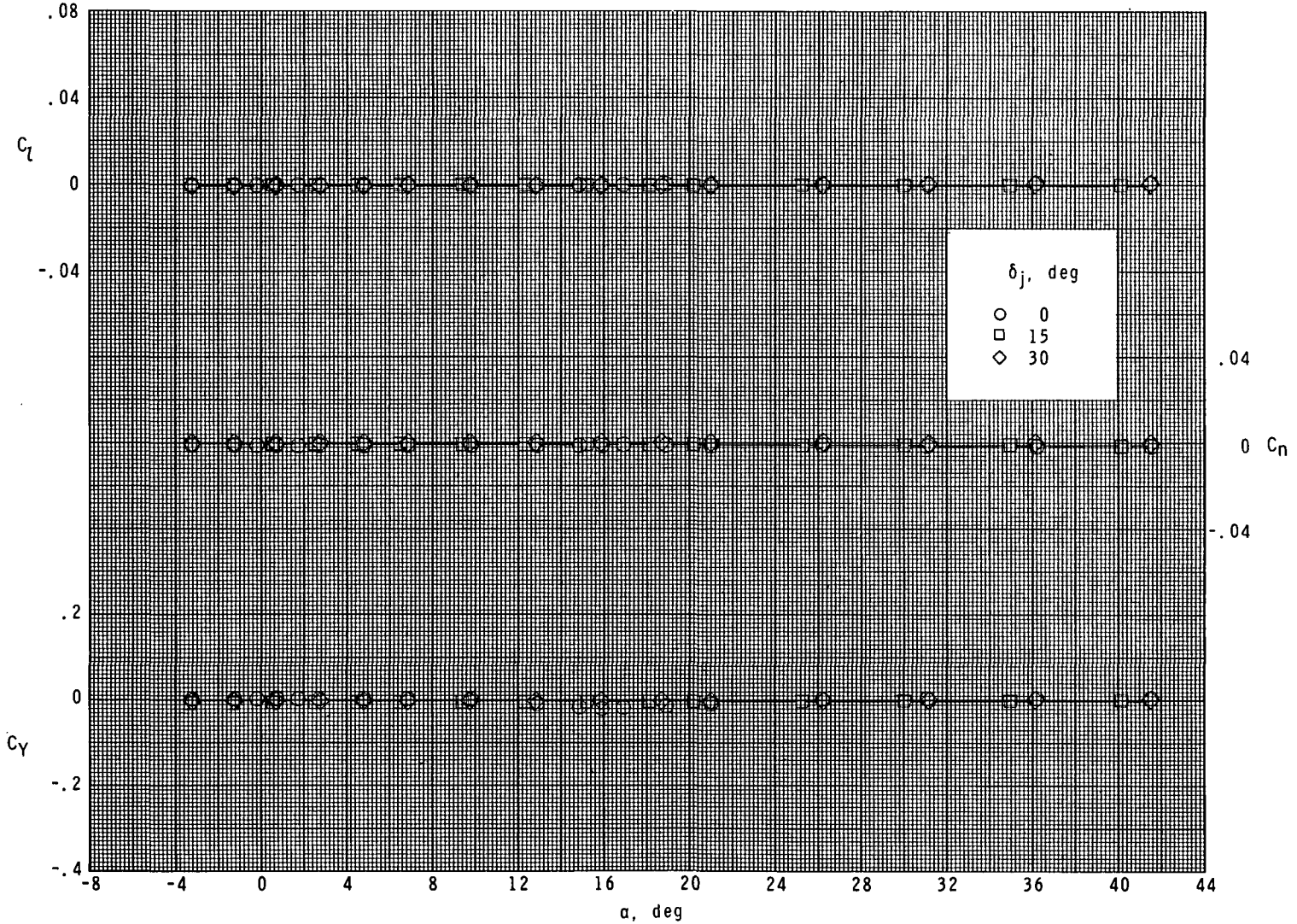

(c) M = 4.60.

Figure 15.- Concluded.

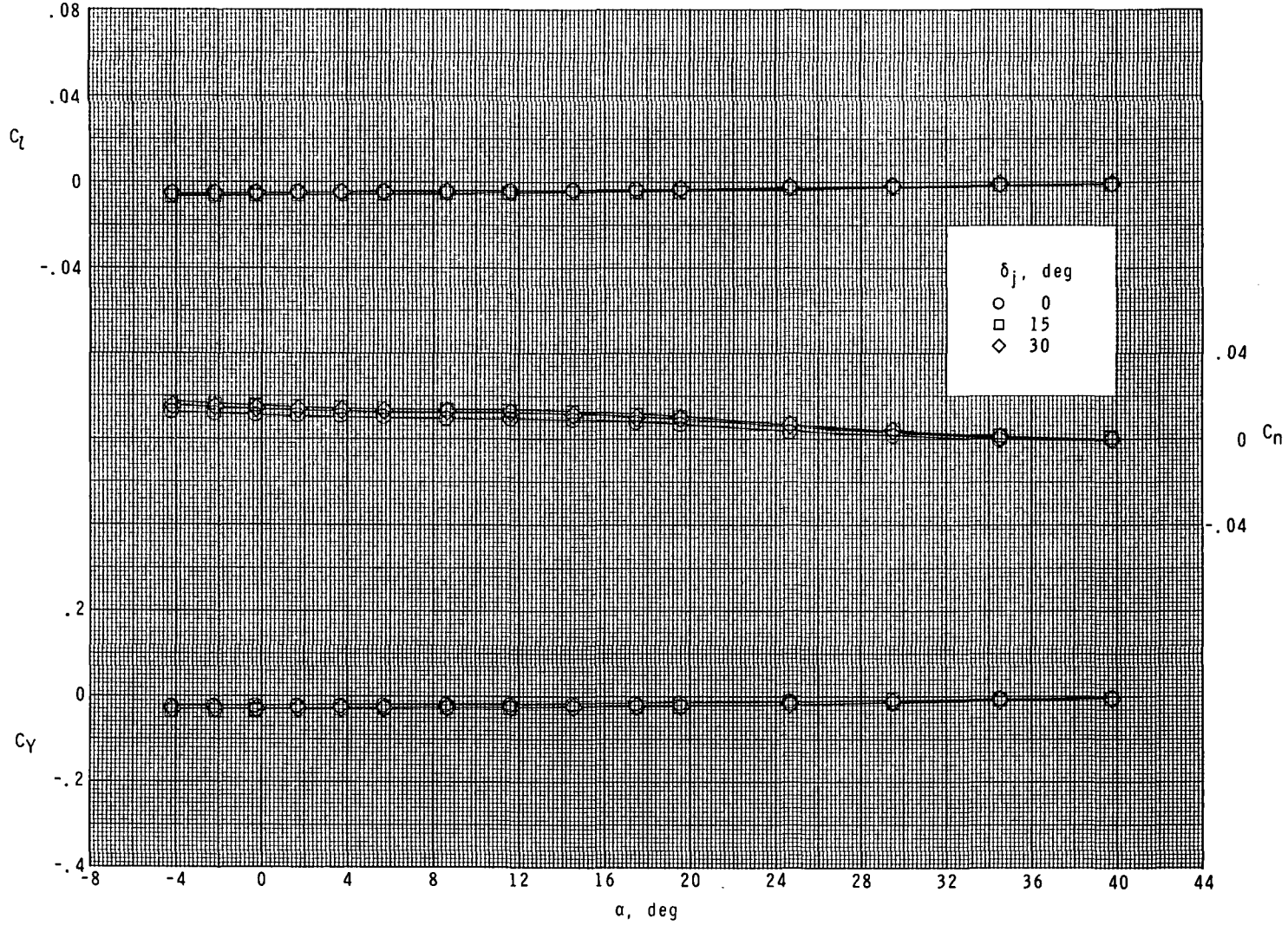

(a) M = 2.50.

Figure 16.- Effect of rudder flare deflection on rudder yaw-control effectiveness. $\delta_v = -20^o$; $\beta = 0^o$.

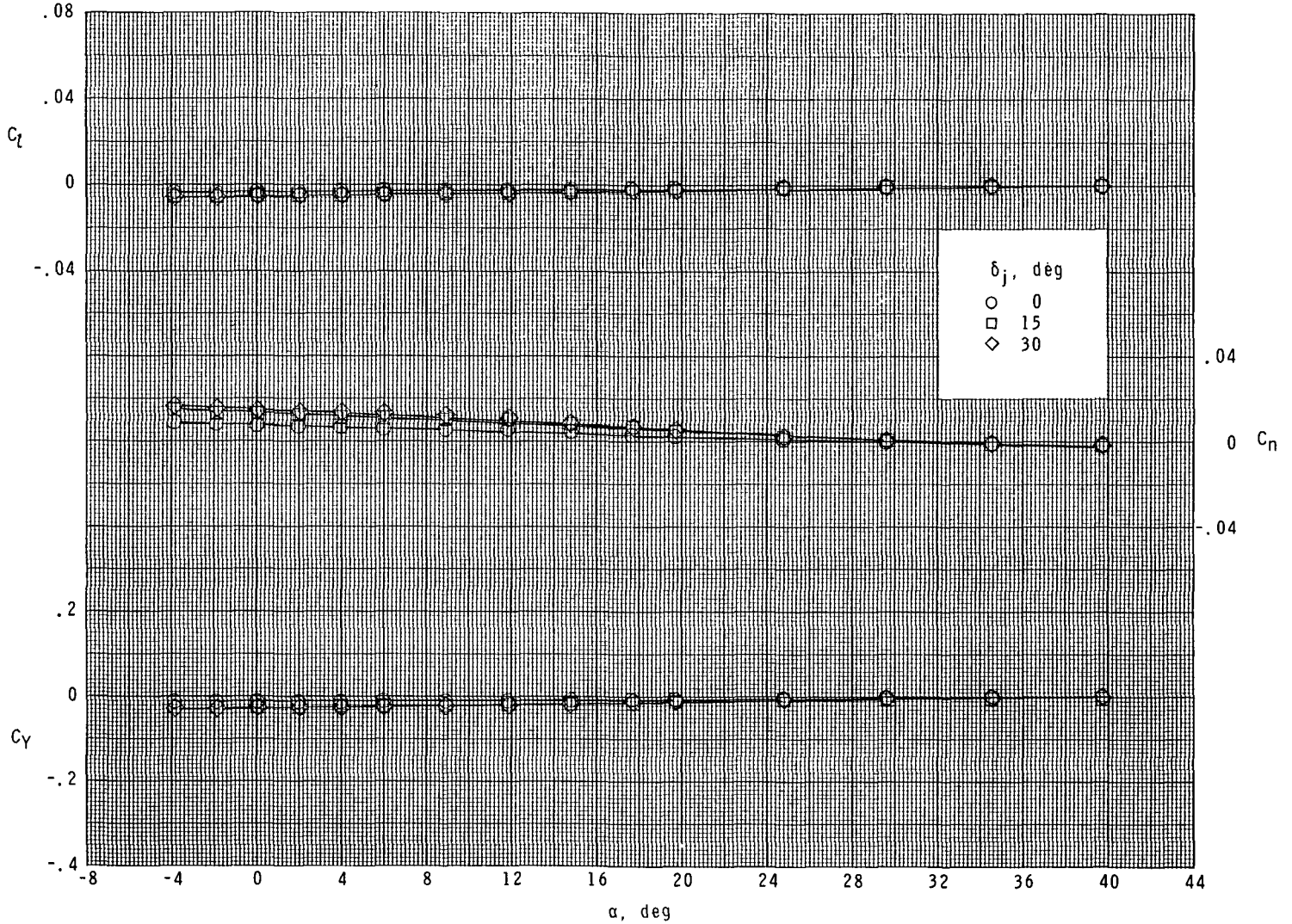

(b) M = 3.90.

Figure 16.- Continued.

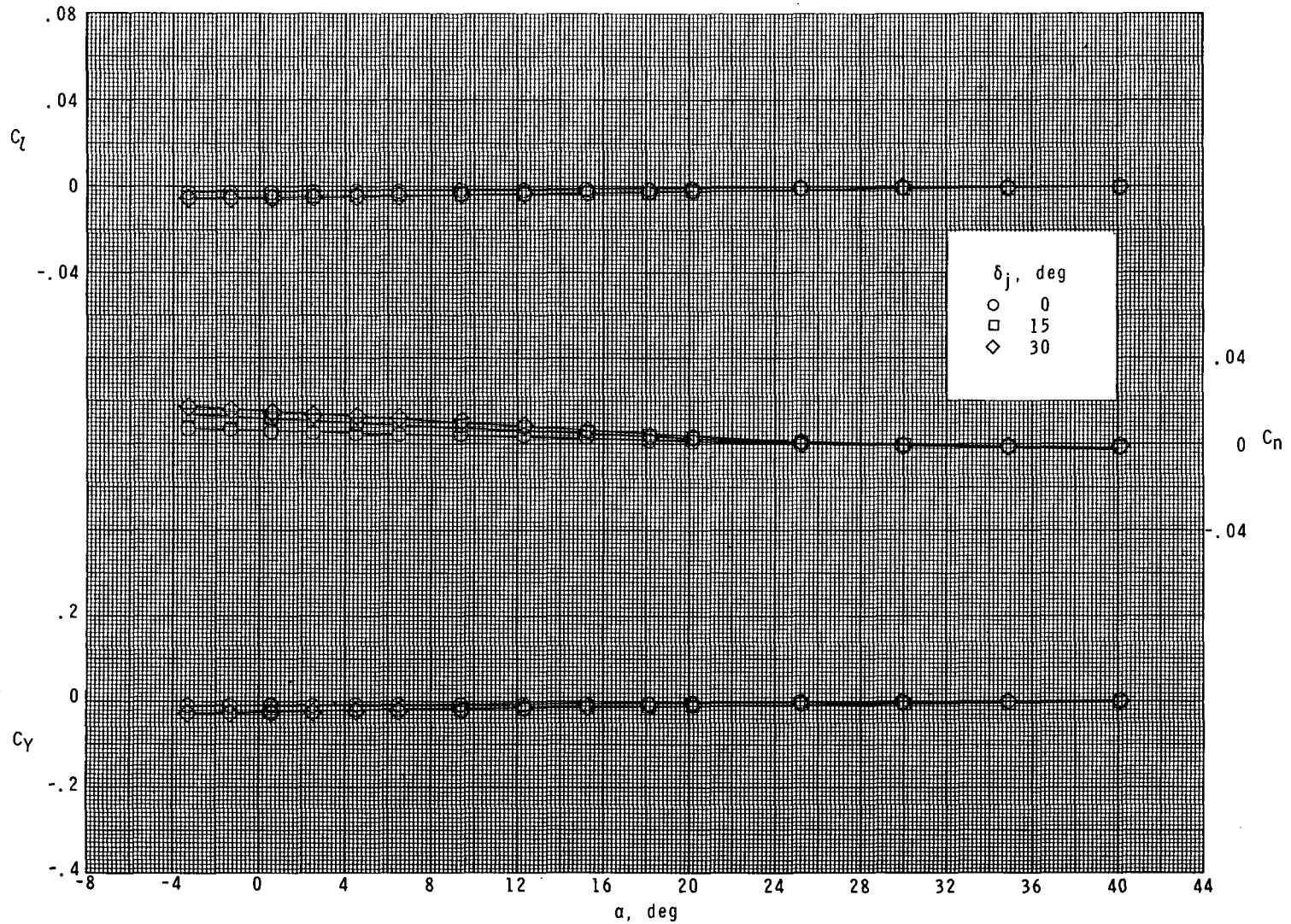

(c) M = 4.60.

Figure 16.- Concluded.

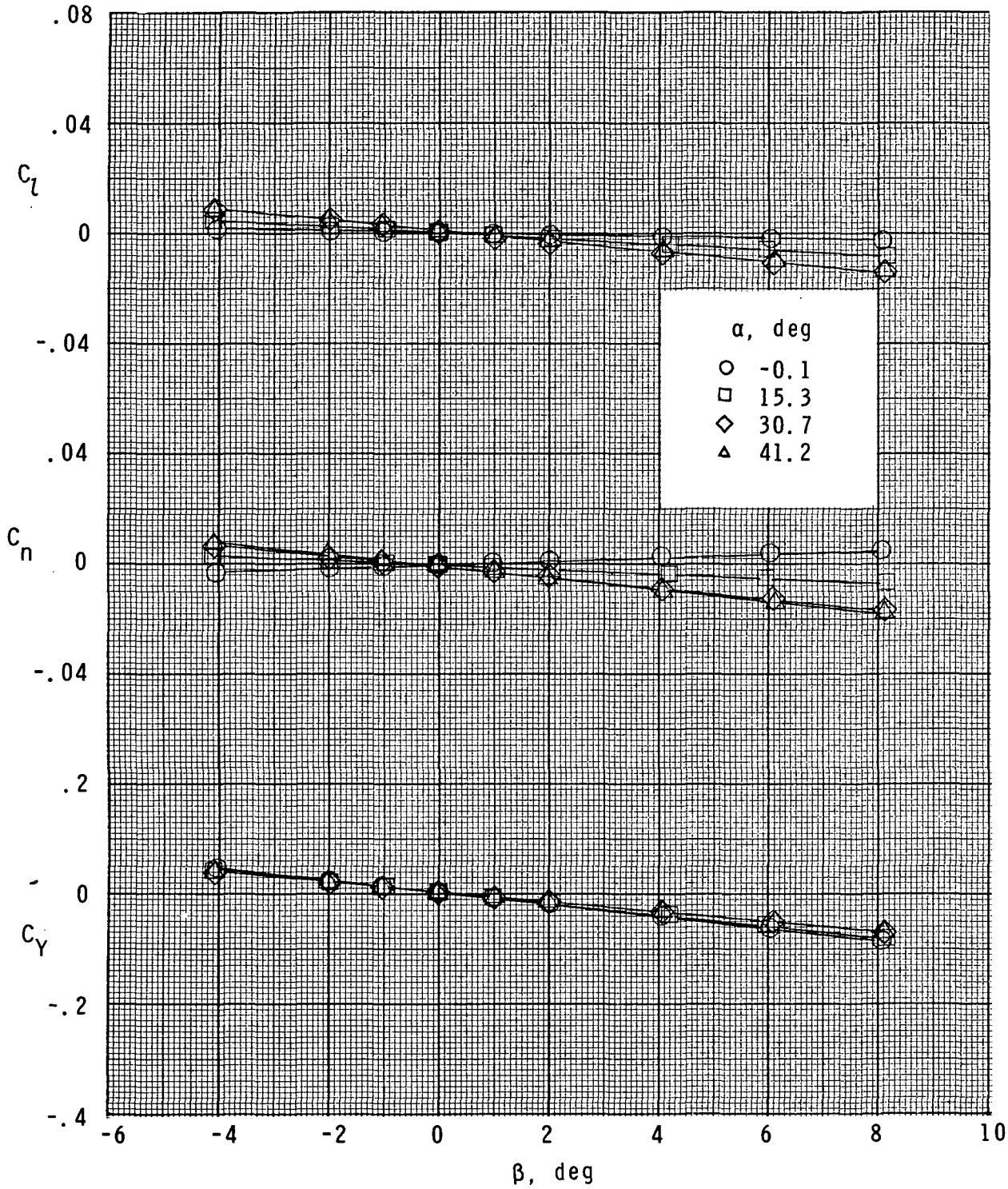

(a) M = 2.50.

Figure 17.- Lateral aerodynamic characteristics of model in sideslip.

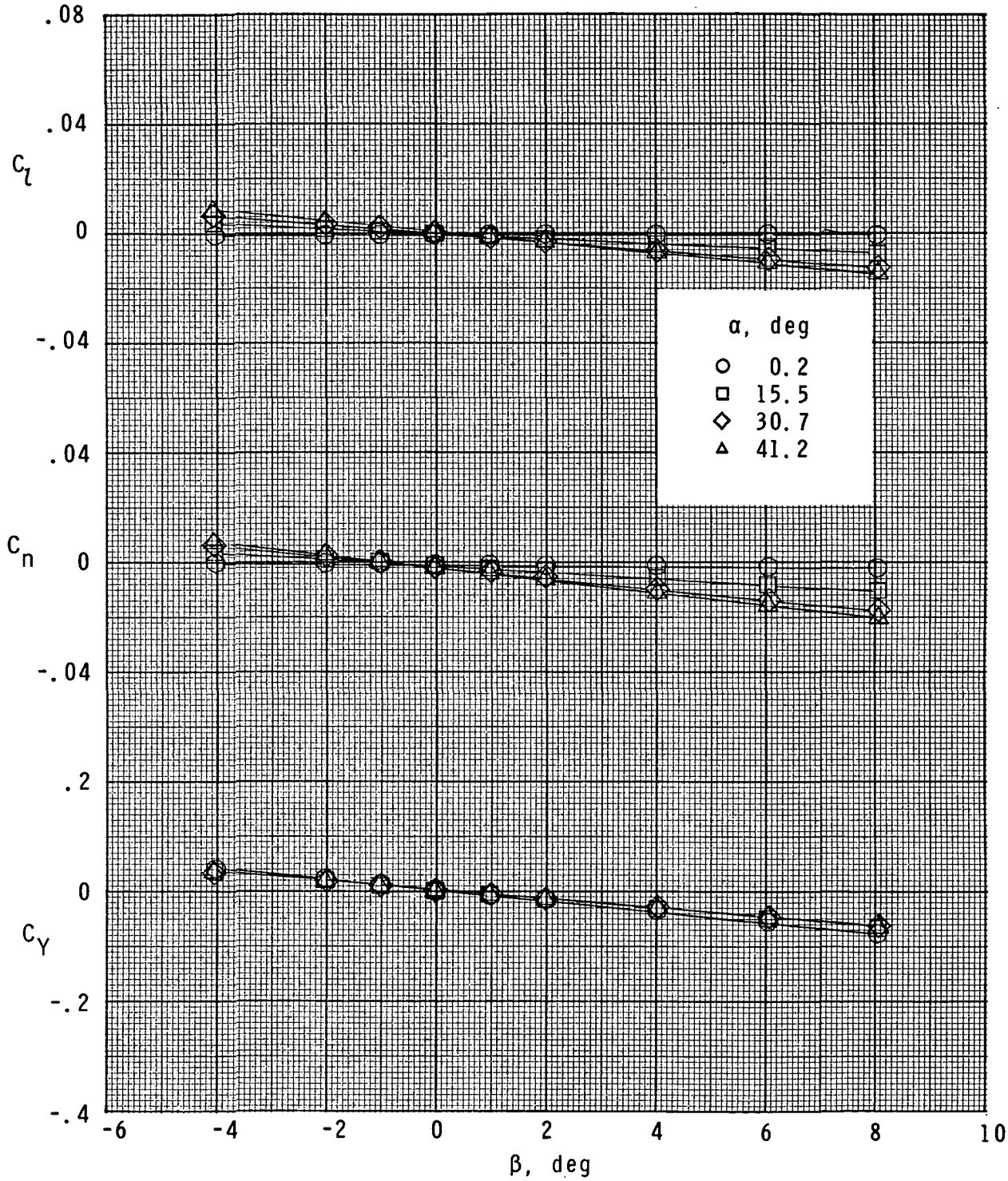

(b) M = 3.90.

Figure 17.- Continued.

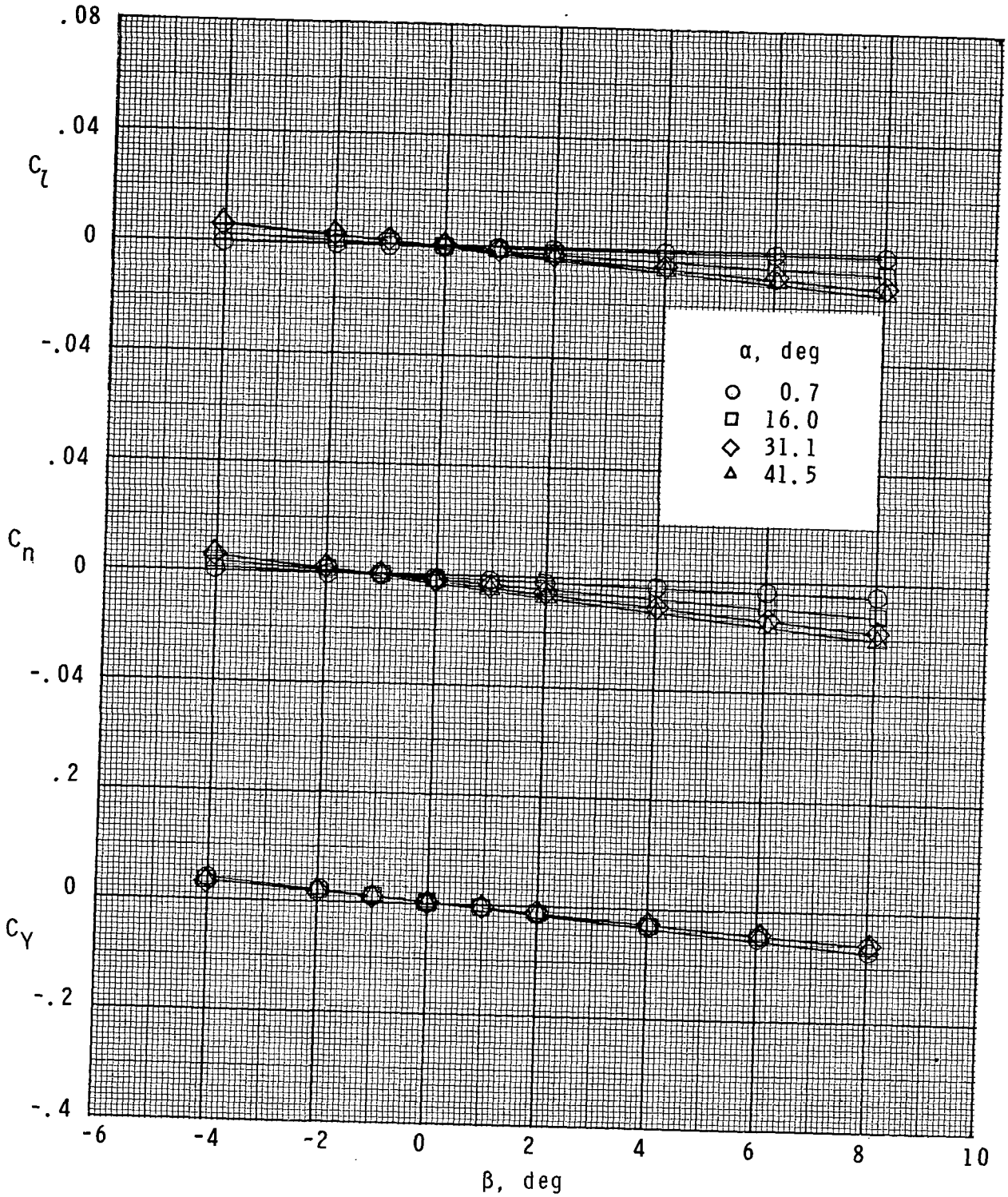

(c) M = 4.60.

Figure 17.- Concluded.

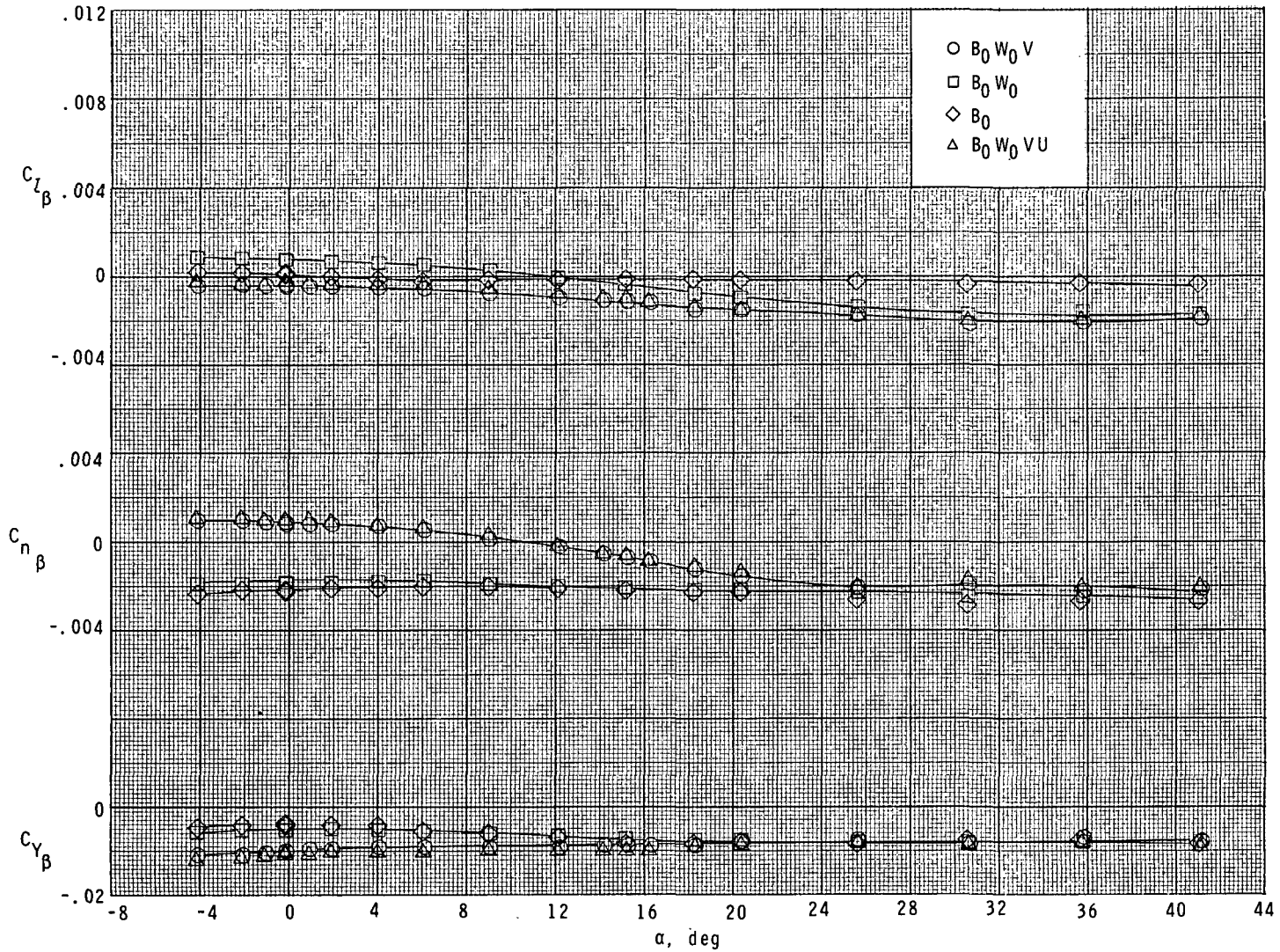

(a) M = 2.50.

Figure 18.- Effect of model components on lateral stability parameters.

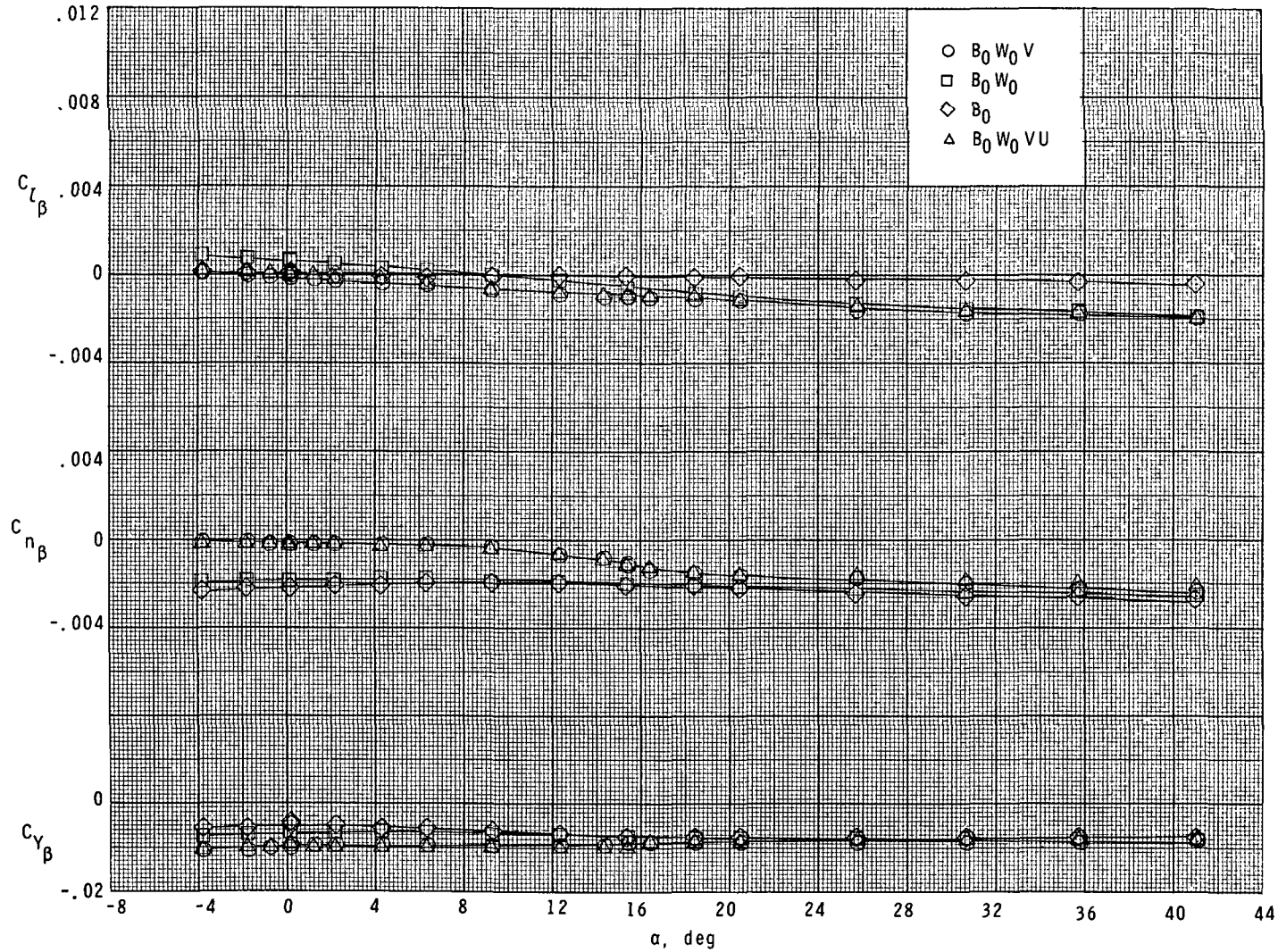

(b) M = 3.90.

Figure 18.- Continued.

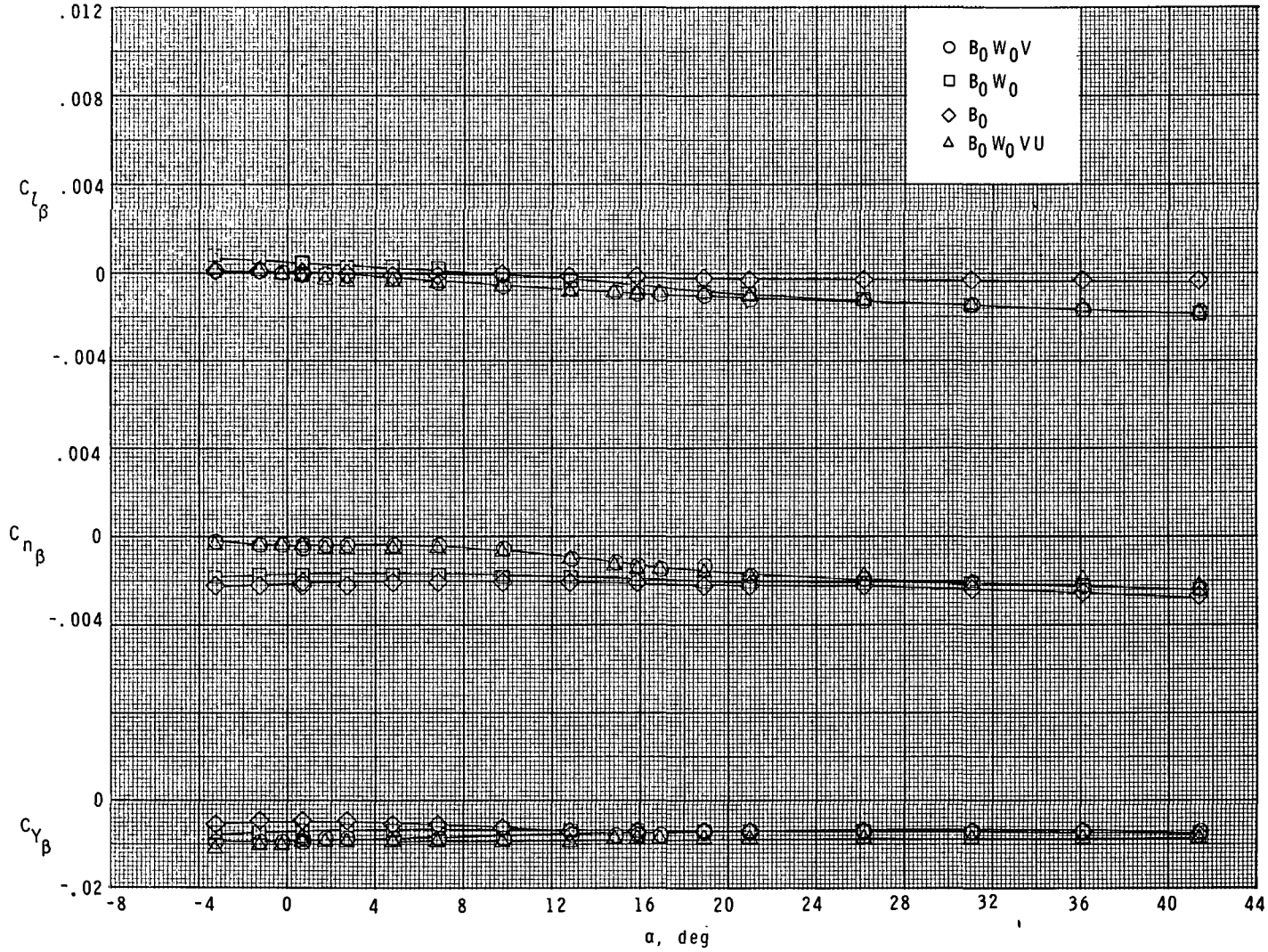

(c) M = 4.60.

Figure 18.- Concluded.

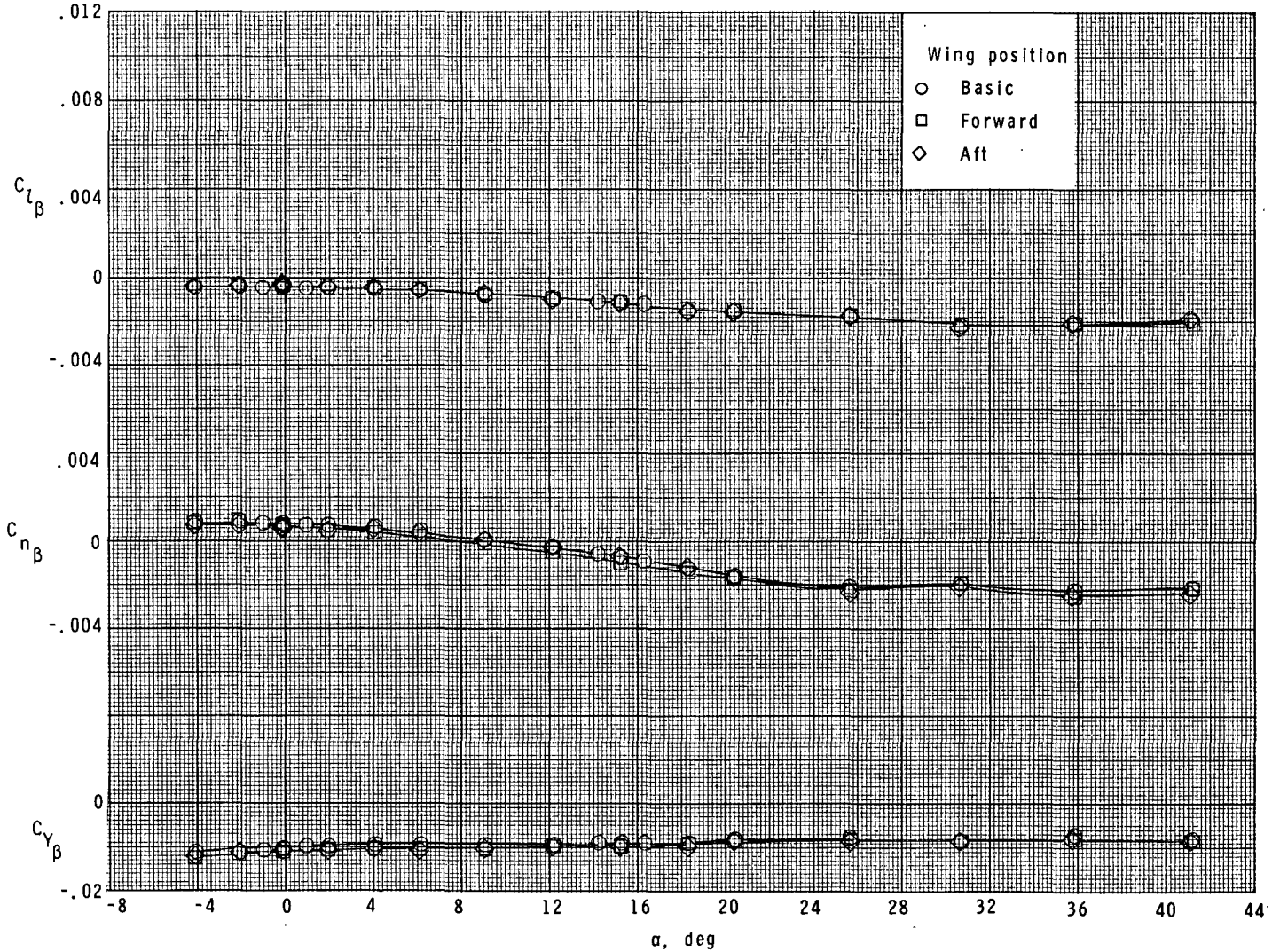

(a) M = 2.50.

Figure 19.- Effect of wing position on lateral stability parameters.

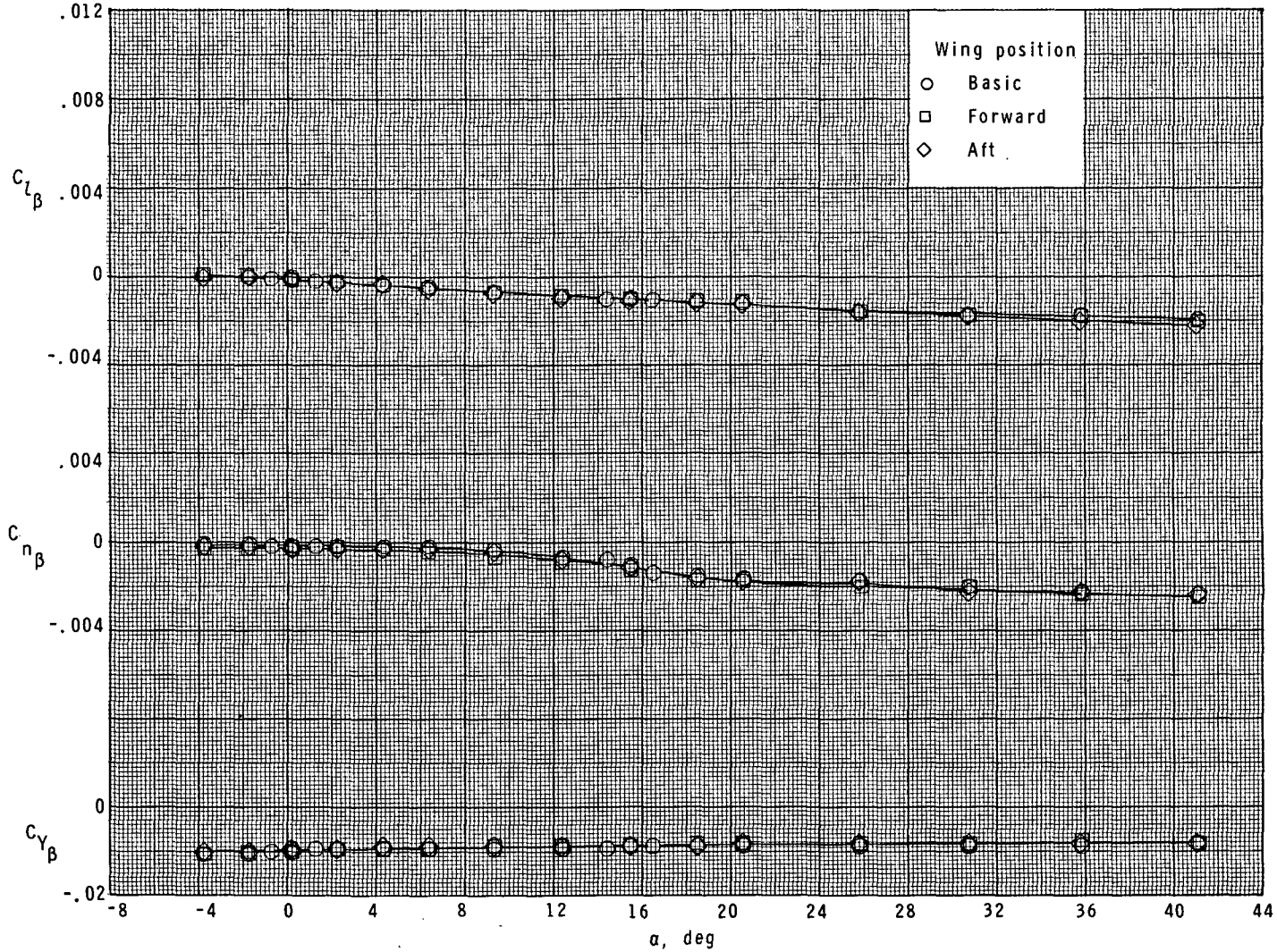

(b) M = 3.90.

Figure 19.- Continued.

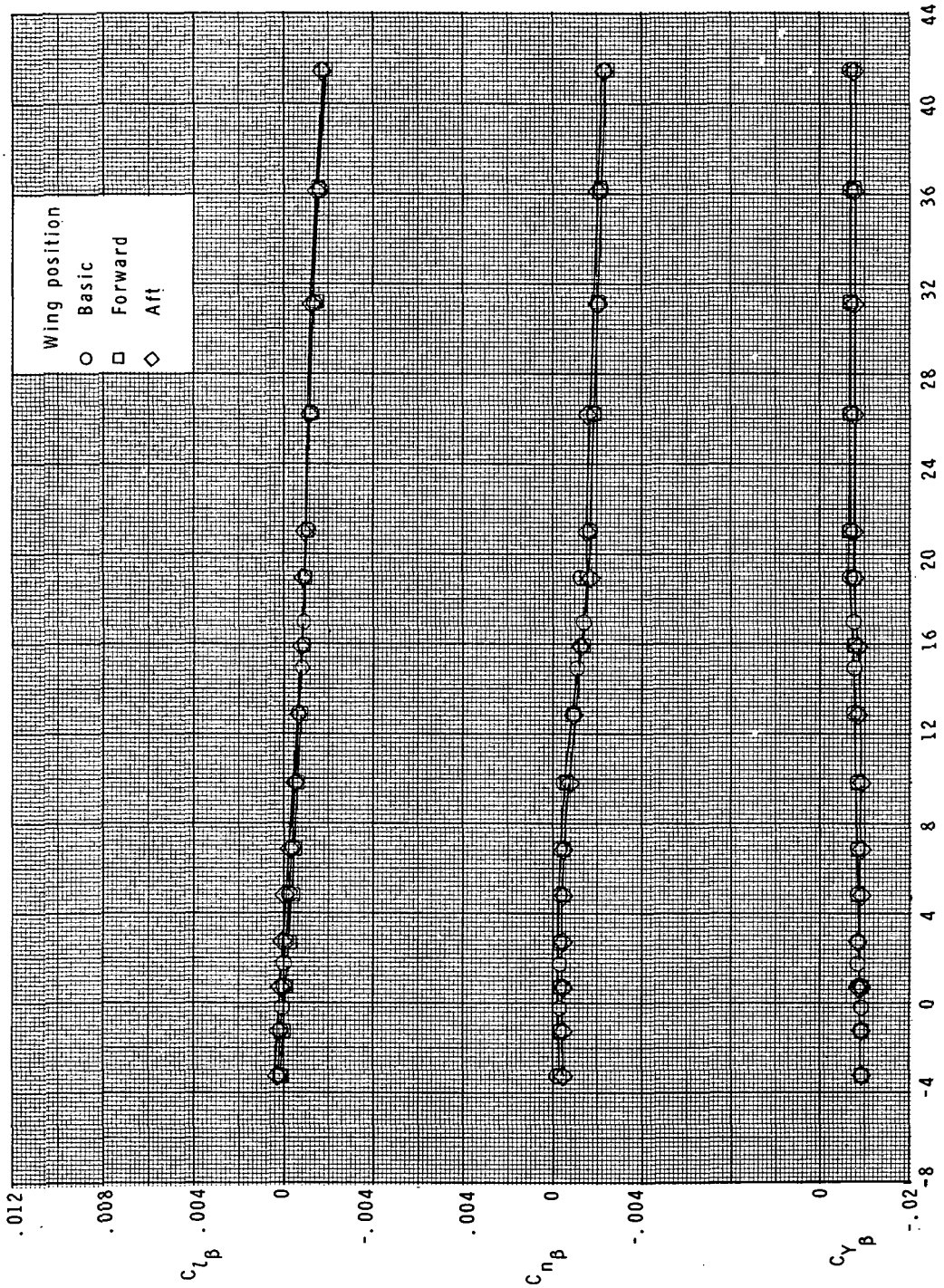

(c) M = 4.60.

Figure 19.- Concluded.

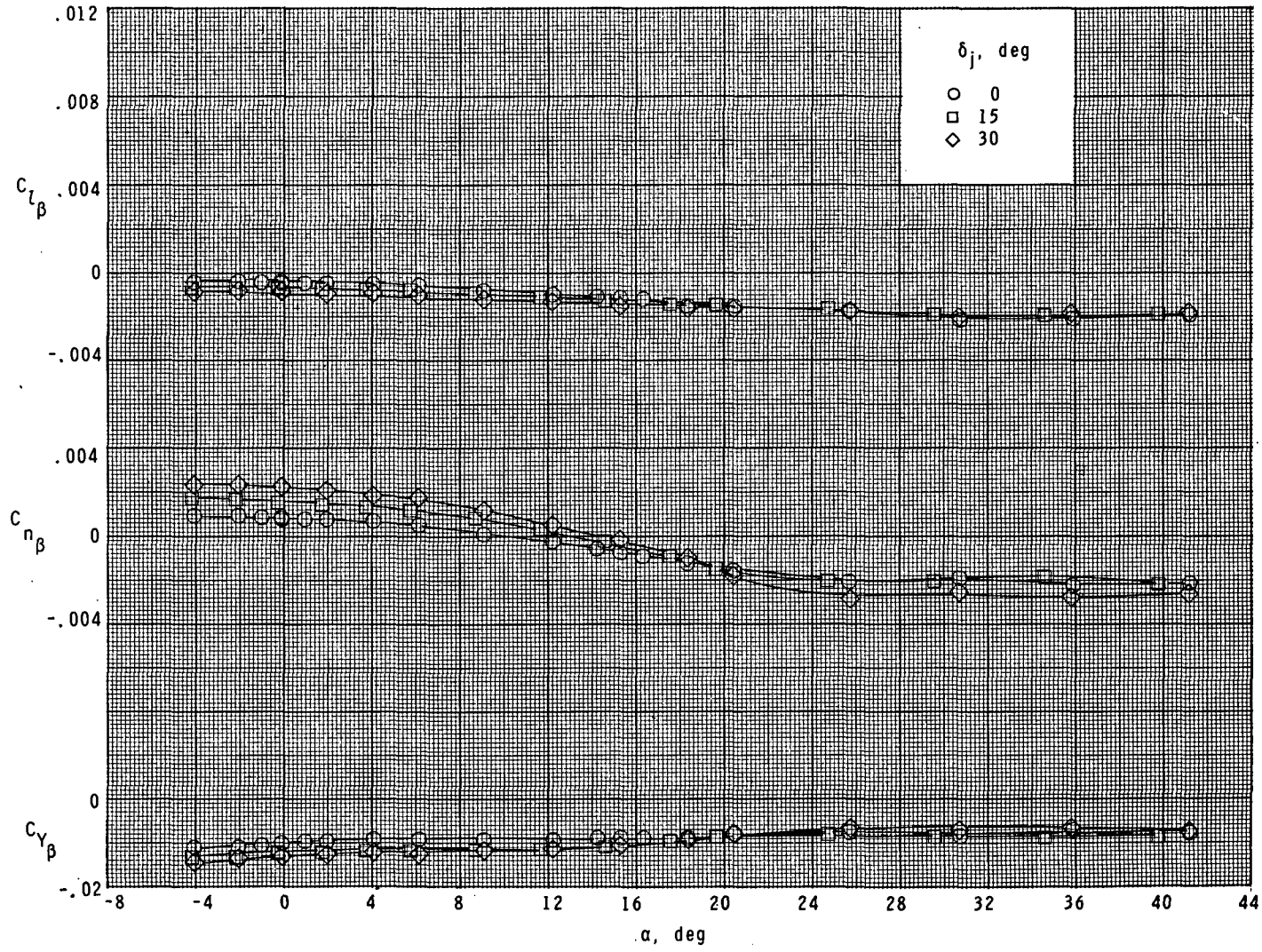

(a) M = 2.50.

Figure 20.- Effect of rudder flare deflection on lateral stability parameters. $\delta_v = 0^o$.

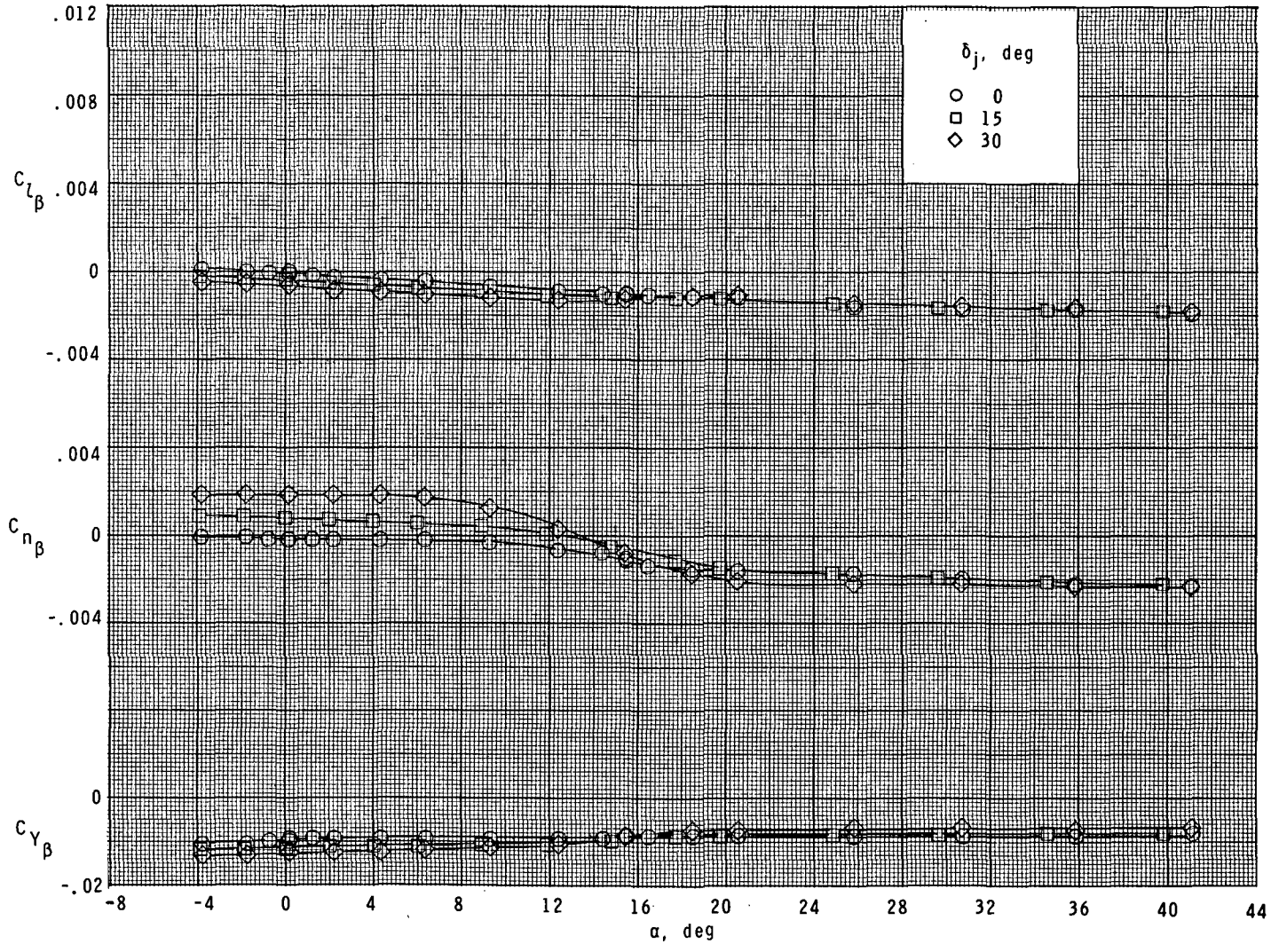

(b) M = 3.90.

Figure 20.- Continued.

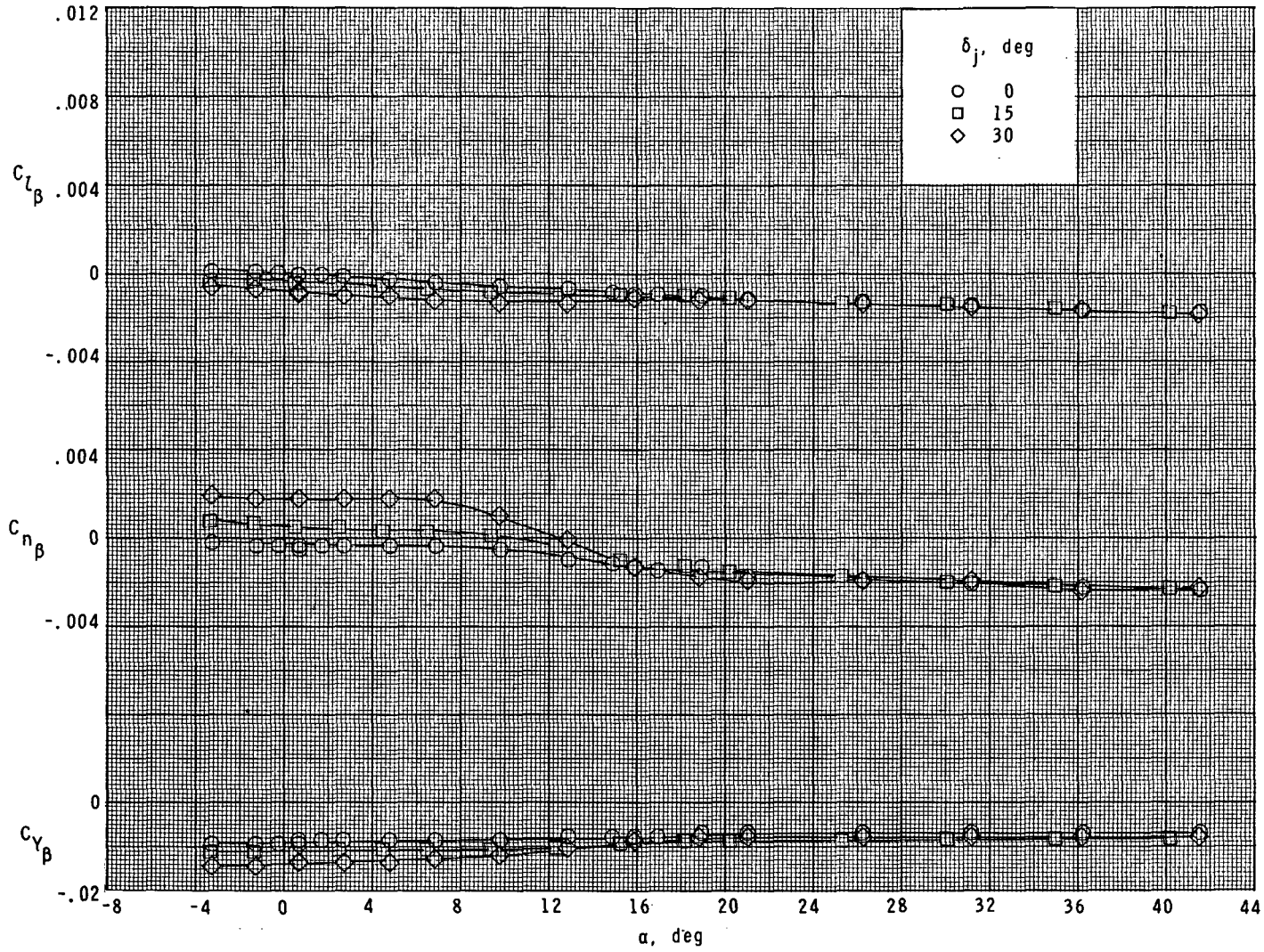

(c) M = 4.60.

Figure 20.- Concluded.

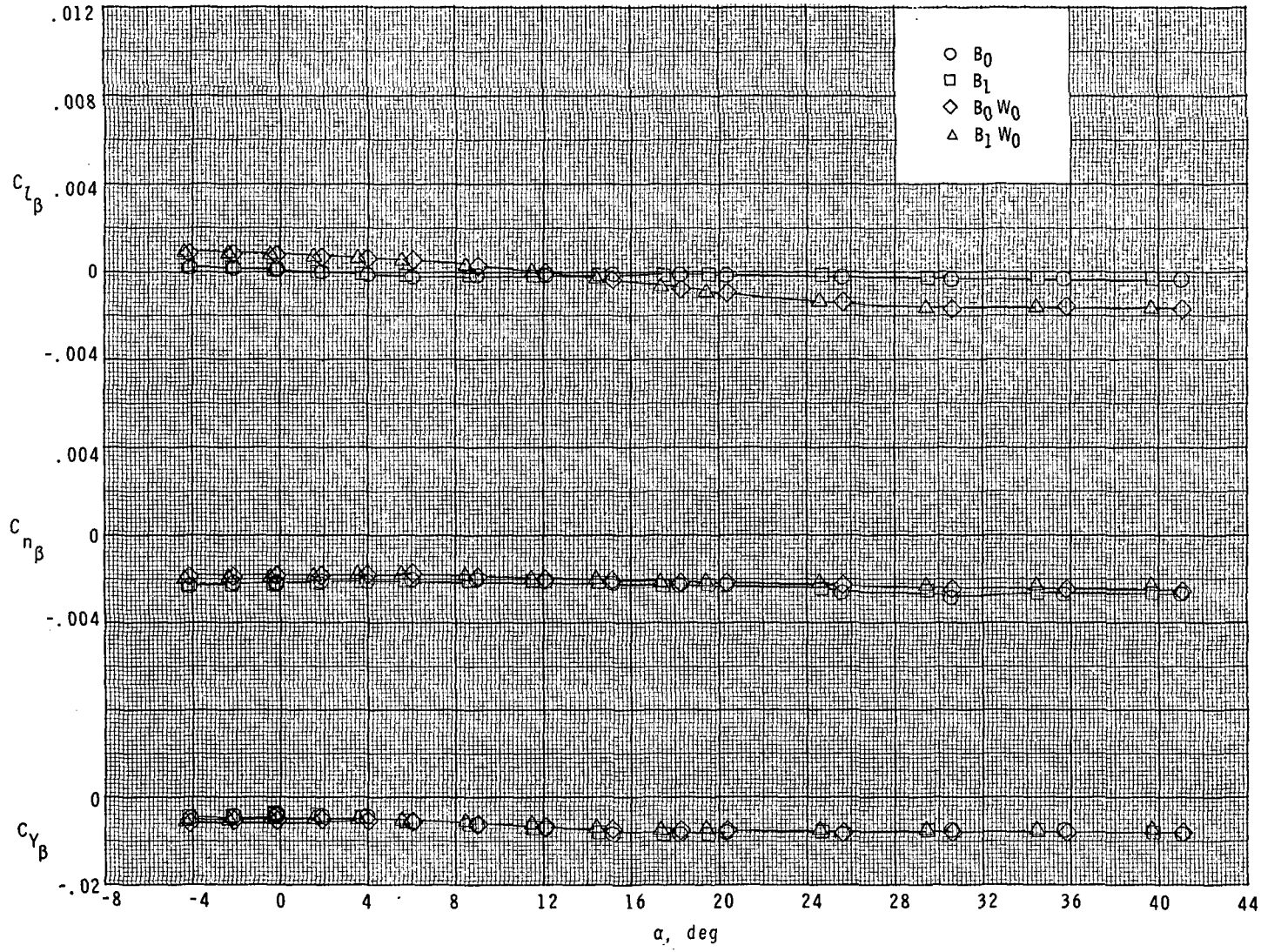

(a) M = 2.50.

Figure 21.- Effect of modified fuselage on lateral stability parameters.

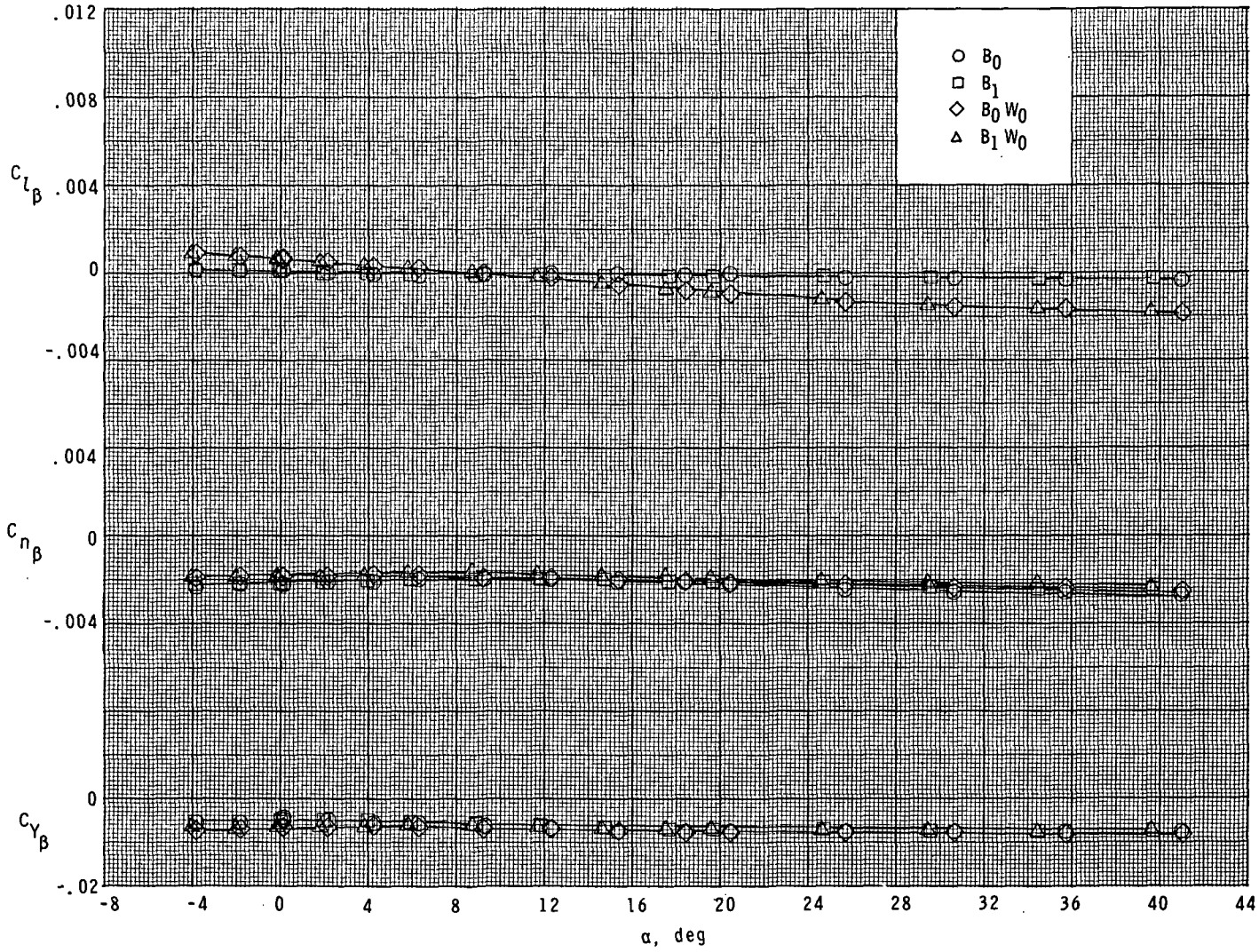

(b) M = 3.90.

Figure 21.- Continued.

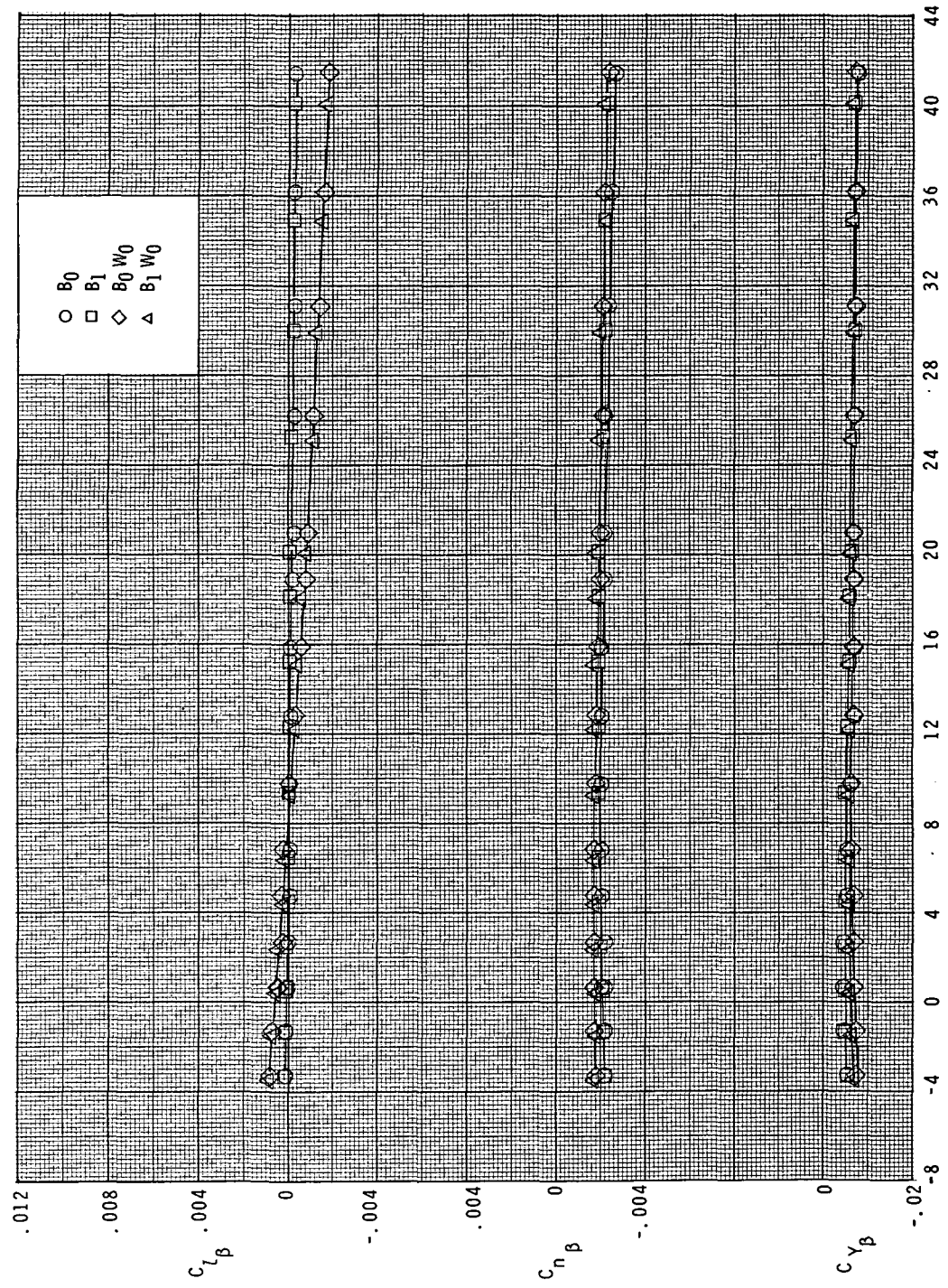

(c) M = 4.60.

Figure 21.- Concluded.

NASA-Langley, 1972 — 1 L-8243

NATIONAL AERONAUTICS AND SPACE ADMISTRATION
WASHINGTON, D.C. 20546

OFFICIAL BUSINESS
PENALTY FOR PRIVATE USE $300

FIRST CLASS MAIL

POSTAGE AND FEES PAID
NATIONAL AERONAUTICS AND
SPACE ADMINISTRATION

U.S.MAIL

POSTMASTER: If Undeliverable (Section 158 Postal Manual) Do Not Return

"The aeronautical and space activities of the United States shall be conducted so as to contribute . . . to the expansion of human knowledge of phenomena in the atmosphere and space. The Administration shall provide for the widest practicable and appropriate dissemination of information concerning its activities and the results thereof."

—NATIONAL AERONAUTICS AND SPACE ACT OF 1958

NASA SCIENTIFIC AND TECHNICAL PUBLICATIONS

TECHNICAL REPORTS: Scientific and technical information considered important, complete, and a lasting contribution to existing knowledge.

TECHNICAL NOTES: Information less broad in scope but nevertheless of importance as a contribution to existing knowledge.

TECHNICAL MEMORANDUMS: Information receiving limited distribution because of preliminary data, security classification, or other reasons.

CONTRACTOR REPORTS: Scientific and technical information generated under a NASA contract or grant and considered an important contribution to existing knowledge.

TECHNICAL TRANSLATIONS: Information published in a foreign language considered to merit NASA distribution in English.

SPECIAL PUBLICATIONS: Information derived from or of value to NASA activities. Publications include conference proceedings, monographs, data compilations, handbooks, sourcebooks, and special bibliographies.

TECHNOLOGY UTILIZATION PUBLICATIONS: Information on technology used by NASA that may be of particular interest in commercial and other non-aerospace applications. Publications include Tech Briefs, Technology Utilization Reports and Technology Surveys.

Details on the availability of these publications may be obtained from:

SCIENTIFIC AND TECHNICAL INFORMATION OFFICE

NATIONAL AERONAUTICS AND SPACE ADMINISTRATION

Washington, D.C. 20546